Technical Report 1-204

FINAL REPORT

MAN-COMPUTER ROLES IN SPACE NAVIGATION AND GUIDANCE

prepared for

Electronics Research Center Cambridge
National Aeronautics and Space Administration

under contract number

NAS 12-128

THE FRANKLIN INSTITUTE RESEARCH LABORATORIES
SYSTEMS SCIENCE DEPARTMENT

Technical Report I-204

FINAL REPORT
MAN-COMPUTER ROLES IN SPACE NAVIGATION AND GUIDANCE

by

Eugene Farber
The Franklin Institute Research Laboratories

and

Lloyd P. Crumley and Leo Spiegel
General Electric Company

February 19, 1968

prepared for

Electronics Research Center Cambridge
National Aeronautics and Space Administration

under contract number

NAS 12-128

THE FRANKLIN INSTITUTE RESEARCH LABORATORIES
SYSTEMS SCIENCE DEPARTMENT

FOREWORD

The research described in this report was sponsored by the Guidance Laboratory, NASA Electronics Research Center (ERC), Cambridge, Mass. Dr. Harold Maurer of ERC was the technical monitor. The purpose of the research was to establish crew roles in autonomous navigation in deep-space missions.

The study was performed by the System Science Department of The Franklin Institute Research Laboratories (FIRL). Dr. Carl A. Silver, now at the Drexel Institute of Technology, was Principal Investigator. Principal scientist for FIRL's subcontractor, the General Electric Re-entry Systems Division, was Dr. Lloyd Crumley.

The authors wish to acknowledge the help and interest of Dr. Harold Maurer of NASA and to express their appreciation to Bernard Epstein of FIRL for his editorial assistance.

SUMMARY

The purpose of this study was to establish the function of a human crew in autonomous navigation and guidance in future, deep-space, manned missions and to assess the implications of such functions for navigation and guidance hardware requirements. To reach this goal, a program incorporating the following seven major task areas was developed: Mission Definition, Navigation Requirements, Error Sensitivity Analysis, the Conceptualization of a Minimum Manual System for Navigation, a State-of-the-Art Review of Navigation Sensors, the Conceptualization of Automated Aids to Manual Navigation, and a Study of Navigation Display Requirements.

The mission selected for study was the Ares Mars Mission, a 630-day journey with a Venus flyby on the return leg. Navigation and guidance requirements and procedures for four mission phases were selected for detailed study: Earth Orbit Determination and Adjustment; Injection into Mars Trajectory; Post and Terminal (midcourse) Adjustments; and Entry into Mars Orbit.

To determine the sensitivity of the base trajectory to a selected group of possible errors and to determine the velocity impulse that would have to be applied to correct the error velocity as the function of errors in these variables, error sensitivity analyses were performed on the Venus flyby phase and on all the preceding phases, except earth-orbit determination. The error-sensitivity study was limited to these four phases because the analysis results are applicable to other phases. The study showed that the effect of impulse errors was moderate in all phases except Mars Orbit Entry. Orbit-Entry injection-velocity errors are relatively serious in that a 10-meter-per-second velocity error will result in an altitude error of approximately 80 kilometers at the 180-degree orbit phase point.

In studying navigation and guidance requirements, two basic approaches were considered: a fundamentally manual system with a minimum of automated equipment and a more sophisticated system requiring only a moderate amount of manual operation. Although a crew can participate in all navigation and guidance activities—obtaining basic navigation data, processing the data, and guiding the vehicle—the role of the crew was studied in detail only for

navigation data collection functions. The basic operating procedures and equipment configurations for collecting navigation data both manually and automatically were determined for the representative mission phases. In the portion of the study pertaining to navigation instrumentation, the characteristics of the sensors required to produce navigation data were discussed in detail and summarized. While the state-of-the-art of navigation sensors is based largely on automatic approaches, a review of manually operated sensors was also conducted.

To provide more insight into the functional capabilities of crew members in navigation and guidance, a detailed operational description of a minimum manual system for collecting navigational data and applying guidance impulses was developed and a timeline task analysis of the earth-orbit-determination phase was performed. These data led to the conclusion that the task load imposed by non-navigation and guidance functions becomes problemmatical only during those phases in which the navigation and guidance task loading is not heavy. At all other times, a five-man duty schedule is capable of supplying an adequate 12 man-hours per day for navigation and guidance functions.

However, data-processing requirements could not be established for reducing raw navigational data to trajectory and guidance information; therefore, crew rules in either an automated or manual data-reduction system could not be postulated and no data on the manning requirement associated with data reduction were developed.

Because information about guidance and navigation schemes, which was needed to accomplish several of the important program tasks, was not available in the form required, several program tasks were not completed. However, a number of important conclusions were reached: the program plan set forth as part of this study will lead to fulfillment of the overall program goal; astronauts are capable of using hand-held instruments such as sextants and stadimeters in the space environment and, with properly designed instruments, manual navigation with accuracy comparable to that obtained with current state-of-the-art automatic systems is possible; and additional research is required to establish in detail human capabilities and limitations in manual-navigation observation techniques, manual data-reduction schemes, and in control of thrusting.

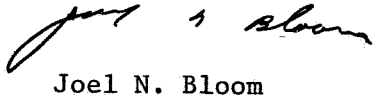

Joel N. Bloom
Technical Director
Systems Science Department

TABLE OF CONTENTS

TABLE OF CONTENTS (cont)

TABLE OF CONTENTS (cont)

LIST OF FIGURES

LIST OF FIGURES (cont)

LIST OF TABLES

SECTION 1
INTRODUCTION

1-1. PROGRAM OVERVIEW

Navigation and guidance in previous and programmed earth-vicinity manned space missions has been considered primarily a ground function. Mercury and Gemini astronauts depended almost completely on ground facilities for position and orbit determination. While autonomous navigation to the moon and back is possible in the Apollo mission by on-board navigation facilities, earth-based tracking and data-reduction facilities provide the primary navigation and control data. Navigation has been a ground-based function in these missions because the relatively short distances permit reliable communication with earth facilities. However, in the manned planetary missions now being considered for the post-Apollo period, the relative fragility of a communications link, measured in millions of miles, requires an autonomous navigation capability for manned vehicles, at least as backup.

Because such missions are very long in comparison with the near-earth missions of this decade, subsystem component reliability will be a serious problem. A way to increase reliability is to minimize the complexity of all systems, including navigation and guidance systems, to the extent feasible by assigning to the crew in a primary or backup mode functions which are normally handled automatically by hardware systems. Thus a simple, autonomous navigation system is strongly needed in future manned planetary missions.

The purpose of this project was to evaluate the role that a human crew can play in autonomous navigation and guidance in such missions and to assess the implications of such crew functions on navigation and hardware requirements. To the extent that crew members assume various navigation and guidance functions — whether primary or backup — the

need for certain types of hardware is reduced or eliminated and a requirement for interface hardware is generated. Strong human participation in navigation and guidance may be expected to have an effect on navigation-error likelihood and crew size. Thus, while allocating major navigation and guidance functions to the crew will eliminate some complex hardware, the ultimate effect on fuel consumption, vehicle weight, and hardware complexity must be carefully determined.

The overall goal of this program was to analyze these problems and provide the data necessary for future tradeoff studies between such factors as crew size, navigational accuracy, hardware complexity, and reliability for future deep-space missions. The specific program objectives were as follows:

1. To determine man and machine interface requirements for navigation and guidance;
2. To determine the velocity-error costs and savings associated with various levels of crew participation in navigation and guidance functions;
3. To determine on-board navigation and guidance computer requirements associated with different crew roles in navigation and guidance; and
4. To determine future research requirements pertaining to crew capabilities and limitations in space navigation.

1-2. METHODS AND APPROACH

The approach adopted by The Franklin Institute in pursuance of the preceding goals is illustrated in Figure 1-1. In the figure, the sequence and relationship of numbered program activities leading to program goals are shown; the tasks are described in a numbered key (Table 1-1). Many of the tasks were not completed, for the reasons described under the following heading; however, the flow chart of the complete planned program is presented because it may be of use to subsequent researchers in this area in developing future programs.

The program is divided into seven task areas. The specific tasks which they encompass are indicated on the flow chart by dashed boxes.

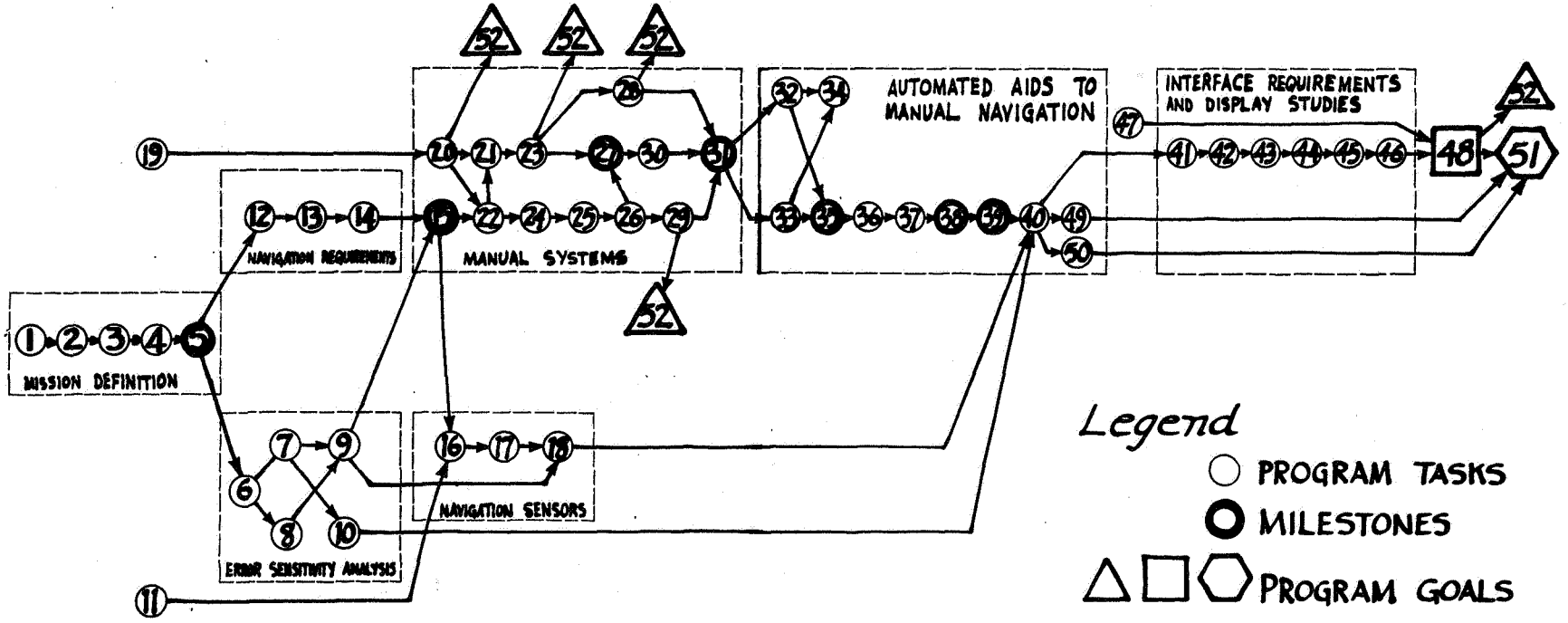

Figure 1-1. Program Flow Chart

Table 1-1. Program Events

1. Start.
2. Select mission for study.
3. Break mission down into phases.
4. Determine N & G events in each phase.
5. Specify orbits and/or reference trajectories for each phase.
6. For each phase estimate terminal velocity error as a function of initial velocity errors (pointing and burn time).
7. For each phase estimate terminal velocity error as a function of position determination errors.
8. For each phase estimate terminal velocity errors as a function of present velocity determination errors.
9. For each guidance event estimate maximum acceptable present position and velocity determination errors.
10. Indicate points of maximum sensitivity to position velocity determination and pointing errors.
11. Perform review of state-of-the-art in autonomous-automated space navigation sensor systems.
12. Indicate time of occurrence of each guidance event.
13. Specify navigation information required for each guidance event.
14. Determine measurements required to obtain the navigation information.
15. Determine measurement accuracy requirements.
16. Indicate type of sensor required in each phase.
17. Determine accuracy limitations of sensors.
18. Estimate in each phase the guidance errors probable with an automatic-autonomous navigation system.

Table 1-1. Program Events (cont)

19. Perform a review of minimal manual navigation techniques.

20. Determine for each type of measurement the expected accuracy available with manual techniques.

21. For each phase indicate the instruments and procedures required to perform navigation measurements.

22. Determine the number of observations required for each measurement to obtain acceptable accuracy.

23. Define measurement procedures in detail.

24. Determine data processing requirements associated with each observation.

25. Define minimum data processing equipment requirements.

26. Determine data processing steps in detail.

27. Summarize previous steps in detailed narrative description of minimal manual navigation and guidance system.

28. Estimate time required to perform measurement tasks.

29. Estimate time required to perform data processing tasks.

30. Establish time based N & G system information flow.

31. Perform a time line task analysis of all N & G system functions.

32. Identify peak work load periods.

33. Determine peak work load values.

34. Determine minimum crew required to perform N & G functions.

35. Determine which tasks are most costly in man hours.

36. Automate those tasks which account for the work load peaks.

Table 1-1. Program Events (cont)

37. Determine new crew functions.

38. Determine man hour savings realized.

39. Estimate savings in $\triangle V$ error (if any) attributable to automation over manual system.

40. Allocate to more sophisticated devices those tasks which man performs least accurately and/or which occur at peak error sensitivity points.

41. State the man/machine task allocation.

42. Establish man/machine interface requirements on a preliminary basis.

43. Draw a functional block diagram of semi automatic N & G system.

44. Establish semi-automatic N & G system information flow on a time base.

45. Perform a time-like task analysis of semi-automatic N & G system.

46. Specify man/machine interface requirements in detail.

47. Perform a review of the state-of-the-art in spacecraft displays.

48. Specify display, control and work station requirements.

49. Indicate work load savings.

50. Estimate velocity error savings.

51. Perform a phase by phase comparison of the different configurations on the basis of man hour requirements, velocity error costs and equipment costs.

52. Indicate future research requirements.

The first task area is mission definition. In this phase a mission is selected for consideration, divided into functional navigation and guidance phases and the trajectories for each phase defined.

In the second task area, the navigation information needed in each phase is established and the observations and measurements required to obtain the navigation information are determined.

In a parallel activity, an error-sensitivity analysis is performed on each navigation and guidance phase. In each case, the cost of an error in position, velocity, or angular displacement is expressed in terms of a velocity correction required.

The fourth study area is an investigation of navigation sensory requirements. In this area, the type of sensor required on each phase and the accuracy limitations of various types of sensors are determined. A review of the accuracy and other characteristics of state-of-the-art navigation sensors is performed. Included in the review is an assessment of the accuracy limitations of navigation observation performed manually with hand-held instruments.

In the fifth task area, a conceptualization of a minimum manual navigation system is developed. Equipment requirements and procedures are developed in some detail and summarized in the form of an operational description of crew navigation and guidance tasks in each phase. In addition, a time-line task analysis of crew navigation and guidance tasks in each phase is developed to determine the operational feasibility of the minimum manual system and to determine the cost in crew-workload manning requirements.

Using the minimum manual system as a base, two additional navigation systems are developed: the first is an "aided-manual system", in which support hardware is added to the system in those areas where manual techniques seem weakest in terms of crew time requirements and velocity expenditures; the second system is a sophisticated, state-of-the-art navigation system with maximum crew participation. In each system

the computation, interface, display, and other electronic requirements are determined. Primary consideration is given to the determination of the computation requirements associated with each level of automaticity. The time-line task analysis is updated to reflect the changes of operational procedures and the crew workload associated with the increased sophistication.

In the final task area, a comparative analysis of the three navigation and guidance systems is performed to establish relative advantages and disadvantages in navigation accuracy, fuel expenditure, the cost of equipment and weight, power requirements, complexity and reliability of hardware, and crew workload and manning requirements.

In the flow chart (Figure 1-1), the specific tasks and interrelationships between tasks needed to accomplish the objective of each task area are defined. The major outcome of the study is a definition of the interrelationship between levels of crew participation, hardware requirements, and system weight and complexity.

1-3. ACCOMPLISHMENTS AND PROBLEMS ENCOUNTERED

The program outlined in Figure 1-1 was not completed because the scope of the program was too ambitious for the number of man-hours available, and because information about guidance and navigation schemes, which was needed to accomplish several of the important program tasks, was not available in the form required. At the beginning of the program it was thought that the necessary navigation and guidance equations and schemes would be available as part of the information developed in support of unmanned planatary probe programs. However, Mars and Venus probes have been dependent on earth-based tracking and computation facilities for navigation and guidance. Thus, navigation and guidance schemes for autonomous navigation were not developed as part of these programs. Autonomous navigation and guidance schemes were not available "off the shelf" and investigation showed that many man-months would be required to develop them in the form required for this program.

In addition to specifying trajectories, development of a navigation and guidance scheme for an interplanetary mission requires that the number and type of observations made, and data-reduction procedures be specified. The latter is complicated by the requirement for treating and smoothing multiple observations. Hence, failure to obtain the required navigation and guidance data precluded a definitive analysis of observation requirements and made it impossible to perform a systematic analysis of the on-board data-processing requirements associated with navigation and guidance. In the absence of the specific guidance scheme, it was assumed that all navigation would be based on near-body observations, that is, a series of observations of the angles between selected stars and the near-body horizon, or center. However, the information needed to determine the required frequency of observation was not available and this precluded a systematic conceptualization of autonomous navigation systems.

To determine on-board data-processing requirements it is necessary to have specific equations and a scheme for weighting and smoothing multiple observations. When it was discovered that guidance equations based on autonomous navigation observations were not available, an attempt was made to generate them. Equations for several mission phases were developed (described in Appendix B), but a weighting and smoothing scheme could not be developed. Without this information, computation requirements could not be established in useful detail, and thus on-board computer hardware requirements or manual data-processing requirements could not be established. No work of this nature can be performed until at least one, and preferably several, alternative guidance schemes based on on-board navigational observations are developed; in fact, the navigation and guidance systems factors depend on the particular navigation and guidance schemes selected. For this reason, alternative navigation and guidance schemes should be considered as input variables in any future tradeoff studies of autonomous navigation and guidance requirements in manned space missions.

Despite these limitations, many tasks delineated in Figure 1-1 were completed and substantial useful information was produced. Several task areas were completed and, in other task areas, specific steps leading to the task-area objectives were completed. Not all the steps that were accomplished are specifically documented, since in many cases these were preliminary steps necessary for the completion of a subsequent step, and not of themselves significant. The completed material presented in this report is divided into the following six sections: Mission Description (Section 2); Navigation and Guidance Phase Description (Section 3); Error Sensitivity Analysis (Section 4); Navigation Systems (Section 5); Navigation Sensors (Section 6); Manual Navigation (Section 7); and Guidance Equations (Section 8). The content of these sections is described briefly in the following paragraphs:

Mission Description. The mission selected for study is described and mission constraints are discussed.

Navigation and Guidance Phase Description. In this section the base mission is divided into a series of phases, each of which contains discrete navigation and guidance requirements. Each phase is described briefly; these descriptions will help reclassify the phases into a series of more basic functions which are the basis for the balance of the study.

Error Sensitivity Analysis. This section presents the results of an overt sensitivity analysis on selected representative navigational phases, and each phase studied; the cost of an error in position, velocity, or angular displacement is expressed in terms of the required velocity correction.

Navigation Systems. This section represents a preliminary step in the development of two of the complete navigation systems described in the program plan, manual and semiautomatic. For each of several representative phases, generic systems are described to meet the navigation and guidance requirements in each phase.

Navigation Sensors. A review of the state-of-the-art in navigation sensors is presented. Included is a discussion of the advantages and limitations of hand-held navigational instruments and a review of the critical literature in this area.

Manual Navigation. A detailed description of a minimum manual navigation and guidance system is described. A time-line activity chart covering certain critical portions of the manual navigational procedure is included. Also included is a general

discussion of considerations that affect the minimum crew size required to carry out navigation and guidance functions.

Guidance Equations. The guidance equations for a number of the navigation phases selected for study are presented.

Because the work summarized above represents the accomplishments on intermediate steps on a program, the material is not highly integrated.

1-4. CONCLUSIONS AND RECOMMENDATIONS

1. *The program as set forth in Figure 1-1 can, if properly executed, lead logically and effectively to the four program goals described above.* An estimated 4 to 6 man-years would be required to complete the program described previously. It is recommended that the material generated in this report be used as the basis for additional research to complete the program.

2. *Conduct additional research in the following three areas before undertaking the completion of the program outlined:*

   a. research to establish at least one, and preferably several, alternative navigation and guidance schemes;

   b. research to determine in greater detail human capabilities and limitations in manual navigation observation techniques; and

   c. research to determine human capabilities and limitations in manual data reduction schemes.

   A complete navigation and guidance scheme is important for the type of research outlined above. A given navigation and guidance scheme indicates what observations are necessary, the required frequency of observation, and establishes the on-board data-reduction requirements. The navigation and guidance equations should be in the form that explicitly relates to specific navigational measurements to orbit trajectory and guidance parameters.

   The other two research requirements will be discussed more fully in the appropriate context in the recommedations that follow.

3. *Future studies in this area need not consider all different phases.* From the point of view of navigation and guidance many of the phases have identical requirements. If the navigation and guidance requirements of vehicle submodules such as the planetary-excursion vehicle are ignored, only

five basic navigation and guidance phases remain: planetary orbit determination; planetary orbit correction; injection into an interplanetary orbit; midcourse corrections; and injection into planetary orbit.

4. *In most of the phases studied, sensitivity to guidance errors is moderate.* In injection into Mars trajectory from an earth-orbit, 10-kilometer position and altitude errors, a 1-miliradian path-angle error, and a 10-meter-per-second injection-velocity error will produce normal and axial velocity errors of less than 12 and 17 meters per second, respectively, at the completion of the injection.

   In near-body midcourse correction phases, measurement accuracies of 20 arc-seconds will hold the subsequent velocity correction error to less than 1 meter per second. Navigation errors are most serious in injection into planetary orbit. For example, a 10-meter-per-second velocity error will result in an approximately 80-kilometer altitude error at a 180-degree orbit phase point. This phase imposes the most serious navigation accuracy requirement of the mission.

5. *With currently available hand-held sextants, astronauts are capable of making star-horizon angle measurements to within about 30 seconds of arc.* Moderate spacecraft motions produce consistent but slight degradation in sextant reading accuracies. A gimbaled sextant will produce more accurate readings than an ungimbaled sextant when sextant magnification is high.

6. *Sextant accuracies are largely a function of the magnification of the device.* However, as magnification is increased the limiting factor on reading accuracy becomes spacecraft motion and vibration. Research is required to determine the motion noise environment in free fall, and to determine the effect on sextant reading accuracy of various levels of magnification.

7. *A problem with high-magnification sextants is that the resulting small field of view may not be large enough to encompass the two target objects.* This problem can be eliminated by designing a sextant which incorporates high- and low-power telescopes.

8. *The accuracy of a series of manual navigation observations can be increased by giving the observer the option of eliminating what he considers to be faulty readings.*

9. *Astronauts are capable of using hand-held instruments, such as sextants and stadimeters, in a space environment.*

10. *With properly designed hand-held instruments, manual space navigation with accuracy competitive with current state-of-the-art systems is possible; this is a consequence of the fact that current planet trackers and horizon scanners cannot deal as accurately with surface irregularity and gibbous effects as a human observer.*

11. *A simple stellar background optical display of minimum complexity can provide an astronaut with all the information required to control the spacecraft during guidance maneuvers.* The accuracy with which the astronaut can control the maneuver depends on the nature of the attitudinal and translational disturbances during thrust. Research is required to determine typical disturbance environments and spacecraft thrusting, and to determine the influence of these factors on the ability of the astronaut to control the spacecraft during periods of thrusting.

12. *Empirical research is required to determine human ability to perform complex data reduction with such aids as tables, nomagraphs, and special-purpose slide rules.*

13. *For a long-duration, deep-space mission, six men is a minimum feasible crew size.* A crew of this size will provide ample manpower for navigational observations in all mission phases. However, since on-board data requirements are not known, it cannot be stated whether a crew of six can accomplish any required data reduction without the aid of a computer.

In summary, it is concluded that a human crew could successfully collect the necessary raw navigational data on a deep-space mission with relatively simple navigational instruments. The role of a human crew in on-board data reduction and control of guidance maneuvers remains unknown.

SECTION 2
MISSION DESCRIPTION

This report describes the navigation and guidance requirements of a manned, deep-space mission; these requirements will form the basis for later work to determine whether manual navigation and guidance systems are feasible for space flights beyond the moon. "Feasible" in this context means that the manual system must promise acceptable accuracy; that it must be less complex than an automatic system and, hence, more suitable for extended missions; that it must be operable within the constraints imposed by the other systems; and that it be acceptable from a crew task-load standpoint.

2-1. GENERAL MISSION CONSTRAINTS

Future design studies in this area will require that certain related information be available for possible trade-off analysis and that the navigation and guidance problem be considered in a context which permits conclusions to be drawn in terms of some particular set of constraints. Thus, it is desirable to base this study on a mission for which a nominal trajectory and tentative mission systems can be described; with such a base, the navigation and guidance system(s) under study can be evaluated against other specifically stated system factors.

It would be possible to consider a particular trajectory and to disregard the fact that no other systems, such as a life-support or communications system, were available for discussion in the same mission context. This approach, however, would preclude the opportunity to compare navigation and guidance system changes in terms of their effect on other factors.

Early in this phase of the study the Project ARES Mission (Benjamin and Hester, 1965) was suggested as a good, representative mission on which to base the study.

2-2. *Project ARES Mission*

The Project ARES report describes a manned mission to Mars. The mission, which was developed to take advantage of the highly favorable Earth-Mars-Venus positions during the 1984 opposition, involves a six-man crew and postulates both a Mars landing and a Venus flyby. Although several flyby options are described in the ARES study, it appears most logical to consider a direct Mars transfer with a Venus flyby on the return trip as a base mission; that option makes better use of the Venus flyby as an energy conservation tool.

The schedule of events for the base mission is shown in Table 2-1; Figure 2-1 shows the interplanetary trajectory in a sun-centered reference. Some events differ from ARES events as a result of factors introduced when an *autonomous* navigation and guidance system is defined for the mission.

2-3. *Equivalence of Trajectories*

To ensure adequate mission analysis, it is assumed that a nominal trajectory is determined on earth before the flight, and that on-board navigation and guidance consists of determining and correcting for deviations which may occur as the mission progresses. The reasons for this basic approach are beyond this study; however, they generally reflect the state-of-the-art in space-vehicle design and computer technology.

Weight restrictions resulting from thrust limitations impose severe constraints on space vehicles; missions, however, tend to have requirements which work to overextend the available energy. As a result, vehicle designers must know the exact mission to trade off alternatives for the optimal vehicle design. Once designed and built, a vehicle cannot easily undertake a mission which deviates substantially from the one for which

Table 2-1. Mission Events

Event	Julian Date (244-)	Calendar Date
Earth Launch	5580	Sept. 3, 1983
Injection to Mars	5581	Sept. 4, 1983
Final Velocity Corrections and Vehicle Spinup	5601	Sept. 24, 1983
Spindown and Initial Terminal Navigation Sightings	5818	April 8, 1984
Mars Orbit Arrival	5833	May 6, 1984
Station Keeping Begins	5834	May 7, 1984
Injection to Venus	5880	Oct. 8, 1984
Final Velocity Corrections and Vehicle Spinup	5895	Oct. 23, 1984
Spindown and Initial Flyby Navigational Sightings	6059	Dec. 27, 1984
Venus Flyby	6074	Jan. 10, 1985
Final Velocity Corrections and Vehicle Spinup	6089	Jan. 25, 1985
Spindown and Initial Terminal Navigation Sightings	6190	May 6, 1985
Earth Arrival	6210	May 26, 1985

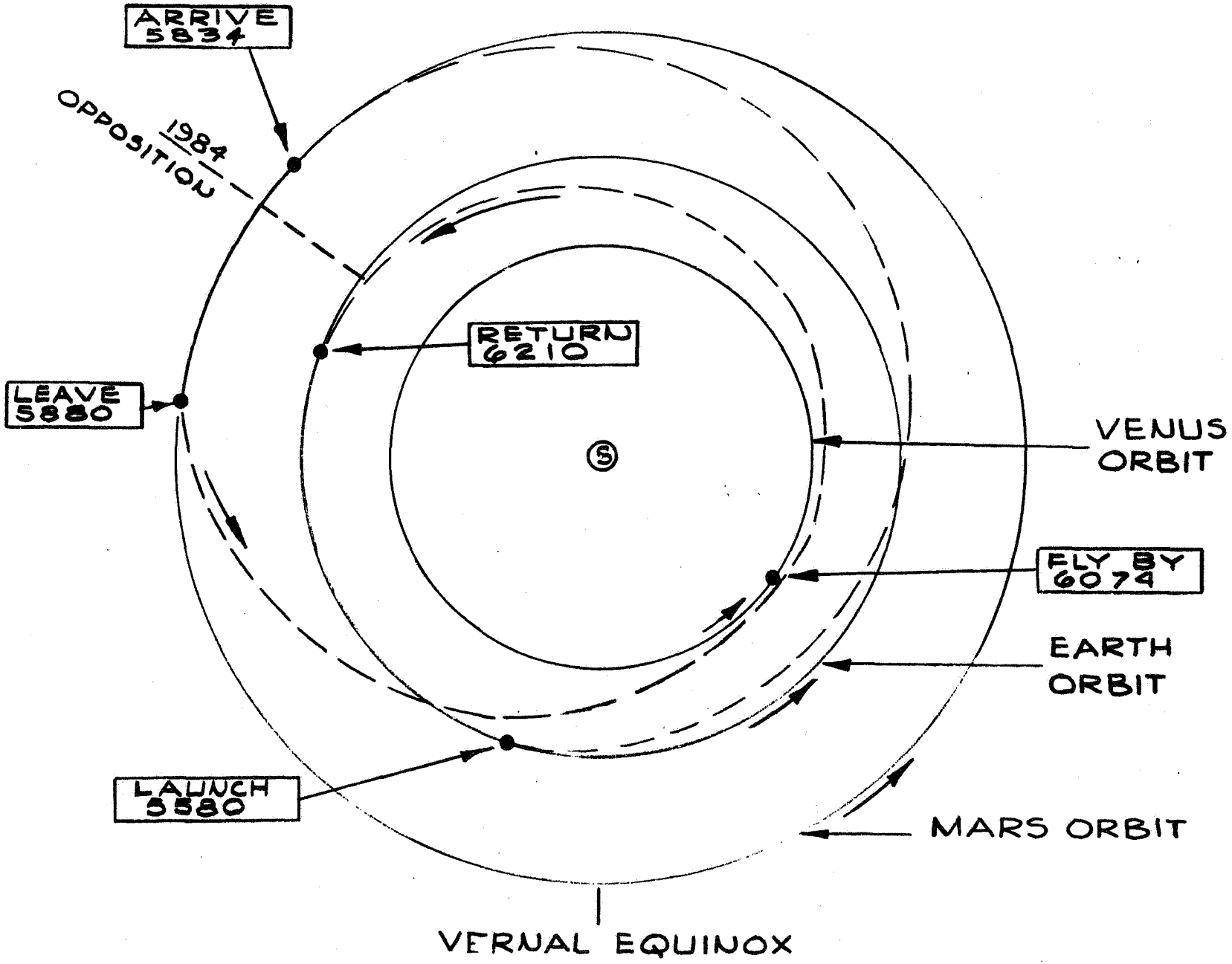

Figure 2-1. Major Mission Events in Sun-Planet Reference

it was designed; thus, once a vehicle is launched, the range of options available to it is limited.

In addition to weight restrictions, the problems of selecting between-trajectory classes and computing trajectories is significant. These activities require hardware, software, and skills that probably will not be available in space vehicles for some time. Therefore, most authorities consider that a "perturbation" approach to interplanetary navigation should be employed, in which course deviations are compensated for by determining the guidance required to put the vehicle onto the available course option which best approximates the nominal trajectory. The design of the ultimate hardware, and the success of the mission after launch, require that a mission use a trajectory "equivalent" to the one defined for the mission. The mission described for this study involves a major leg of 252 days which begins and ends at specific points in the solar system. Since no adequate trajectory data were found for this exact mission, the problem arose of determining what was an equivalent trajectory.

Trajectory analysts at the General Electric Re-Entry Systems Department indicated that time was the important parameter and that a trajectory with the same Earth-to-Mars time would be equivalent, even though the distance covered or the departure and arrival positions for the planets differed. They also indicated that all time-equivalent missions of a particular class had essentially similar error sensitivities, and that while minor differences between missions in a class could have important influences on total system development they would have no significant impact on the navigation and guidance system itself. It was therefore concluded that any 252-day mission of the "high-energy" class could be used and a trajectory from Clarke, *et al.* (1964) was selected. The trajectory data are shown in Table 2-2; the notation used in the table is defined in Appendix A.

2-4. *Autonomous Navigation and Guidance Requirement*

Another constraint on the base mission and the navigation and

Table 2-2.

Heliocentric Data for a 252-Day Earth-Mars Trajectory

Parameter*	Value	Parameter*	Value	Parameter*	Value
RL	151.96	RP	249.20	RC	163.807
LAL	0	LAP	1.80	GL	-13.81
LOL	301.00	LOP	152.57	GP	13.86
VL	32.816	VP	19.883	ZAL	156.45
GAL	-13.23	GAP	11.55	ZAP	144.31
AZL	93.44	AZP	87.07	ETS	160.58
HCA	211.62	TAL	301.52	ZAE	167.00
SMA	198.14	TAP	153.13	ETE	81.16
ECC	0.32225	RCA	134.29	ZAC	91.83
INC	3.4366	APO	261.99	ETC	266.60
V1	29.318	V2	21.975	CLP	146.77

*Defined in Appendix A.

guidance systems is that all navigation and guidance must be performed on-board by a fully autonomous manned system. The purpose of this constraint is to ensure that maximum consideration is given to man's role in space navigation and guidance.

2-5. NAVIGATION AND GUIDANCE EVENTS

An interplanetary mission consists of a complex sequence of navigational and guidance events. However, the complexity can be reduced and conceptualization simplified if the base mission is considered as a series of lesser missions, each involving its own vehicle. The base mission will therefore be considered as three discrete cycles: an earth-centered cycle, an interplanetary cycle, and a Mars-landing cycle.

Earth-centered mission operations include the launch, rendezvous, and reentry of two ferry vehicles, one of which delivers the mission crew to the previously assembled mission vehicle and then returns the checkout crew to earth, and the other of which rendezvouses with the returning mission vehicle and returns its crew to earth. The interplanetary cycle involves all other mission phases except those mission events undertaken by the vehicle that descends and returns to the interplanetary vehicle from the Martian surface.

2-6. Earth Cycle

The base mission assumes that, several weeks before the injection window, the mission vehicle is launched into a suitable parking orbit. It is then checked out and made ready by a checkout crew. Shortly before the injection date, the mission crew is launched in a six-man ferry vehicle. The vehicle then maneuvers into the proper orbit and a rendezvous is performed. The mission crew then boards the mission vehicle and the checkout crew begins its return to earth in the ferry vehicle. The landing sequence involves an adjustment into an orbit from which a ballistic reentry can be performed.

After the mission is completed, a similar set of phases occur. The returning mission vehicle enters and maneuvers into a suitable orbit. A ferry vehicle is then launched and the rendezvous-and-exchange cycle is repeated.

It is assumed that ballistic reentries are used so that the control and navigation of maneuverable vehicles need not be considered. Such an assumption avoids the requirement of an extraordinary level of space-vehicle piloting by either the checkout crew on its return to earth, or by the returning mission crew — which would certainly be out of practice after nearly two years in nonpilot roles.

It is also assumed that the ferry vehicle can use ground-based tracking data without violating the fully autonomous navigation and guidance requirement. This assumption appears permissable because ephemeris data concering the assembled vehicle and the returned vehicle would be available from ground facilities; such data are equivalent to the planetary and star-position data that will be obtained on earth but taken on the mission for use as required.

2-7. *Interplanetary Cycle*

The flight crew must ensure that the assembled vehicle is in the proper orbit for injection into an Earth-Martian trajectory. If the orbit is not suitable, it must be corrected before the injection window opens. The interplanetary mission phases then proceed as described in Section 3.

2-8. *Mars Excursion Cycle*

The Mars exploration involves essentially the same mission phases as are involved in the Earth-centered ferry portions of the mission. However, the phases are in reverse order because the Mars exploration begins with a vehicle launched from the orbiting mission vehicle, and terminates when the returning exploration module rendezvouses with the primary mission vehicle. These phases, and those in the Earth-centered mission cycle, are also described in Section 3.

SECTION 3
NAVIGATION AND GUIDANCE PHASE DESCRIPTIONS

In this section the base mission is divided into a series of phases, each of which contains discrete navigation and guidance requirements. The 27 phases of the nominal mission are shown graphically in Figure 3-1. Each phase is described briefly; these descriptions will help reclassify the phases into a series of more basic functions which are the basis for the balance of the study.

3-1. EARTH CYCLE, PART 1

3-2. Earth Launch

The earth-launch phase begins when the crew enters the ferry vehicle and terminates when the vehicle is successfully injected into earth orbit.

3-3. Earth-Orbit Correction

Ideally, the inital earth orbit should be close enough to the mission vehicle to permit immediate initiation of the rendezvous; however, the mission navigation and guidance sequences are based on the assumption that a separate orbit adjustment before rendezvous may be required. During this phase, the ferry-vehicle crew determines the orbit into which their vehicle has been placed and their position relevant to the mission vehicle. Orbital corrections are then made and the ferry vehicle is moved into position for the rendezvous attempt.

3-4. Rendezvous

After the ferry vehicle is brought into the proper position, it will rendezvous with the mission vehicle. Rendezvous and the transfer of the two crews may be accomplished with or without physical mating of

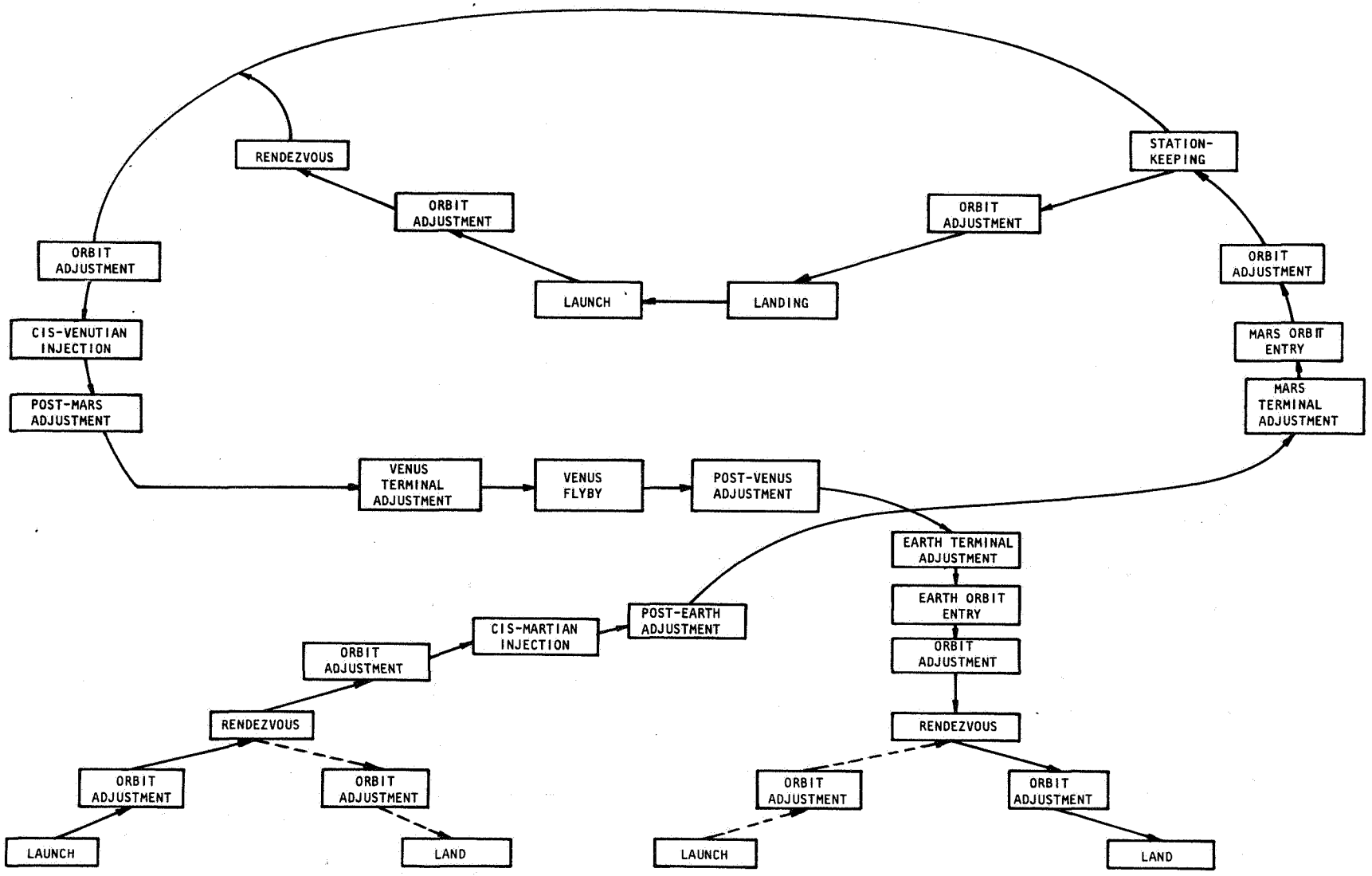

Figure 3-1. Representation of Navigation and Guidance Phases in Sequence

the vehicles; in either event, the flight crew assumes control of the mission vehicle and the checkout crew returns to earth in the ferry vehicle.

3-5. INTERPLANETARY CYCLE

3-6. Orbit Adjustment

After the mission crew has assumed command of the mission vehicle, they will check its orbit and make any adjustments necessary to ensure that the vehicle can be injected at the optimal time and place.

3-7. Cis-Martian Injection

At the proper time, the vehicle is stabilized and power applied. Sufficient velocity is imparted to inject the mission vehicle into a Mars trajectory.

3-8. Post-Earth Adjustment

After the cis-Martian injection, the crew evaluates vehicle condition and determines the trajectory. Corrections are made, as required, during a period beginning about 2 days after injection and ending a maximum of 20 days later.

3-9. Mars Terminal Adjustment

Fifteen days before arrival at Mars, terminal navigational processes begin. Corrections are made as required to ensure entry into the correct Martian orbit.

3-10. Mars-Orbit Entry

At an appropriate time, the vehicle is positioned and a negative impulse imparted to it; the slowed vehicle then enters an orbit around Mars.

3-11. Mars-Orbit Adjust

After the vehicle has entered a Martian orbit, the crew determines the orbit and makes necessary corrections so that the mission vehicle is in the planned station-keeping orbit.

3-12. Station Keeping

After the mission vehicle has been placed in the proper station orbit, its crew performs any necessary navigation and guidance functions required to remain in this orbit. They also perform the mapping tasks required to select a landing site. After a site has been selected, the required lander trajectories are determined and the Mars lander is launched. Station keeping then continues until the lander crew is recovered and the next mission vehicle phase is required. While the lander is on Mars, the station crew continually updates launch time and trajectory data for the lander crew.

3-13. Orbit Adjustment

After the Mars lander crew has been recovered, the orbit is checked and corrected if necessary for optimal cis-Venutian injection.

3-14. Cis-Venutian Injection

This phase is similar to the cis-Martian injection previously described.

3-15. Post-Mars Adjustment

The post-Mars adjustment is similar to the post-Earth adjustment, except that it must be completed by the 15th day after injection; by this time, the accuracy of the navigation system would be extended to its limit because of Mars' smaller diameter.

3-16. Venus Terminal Adjustment

This adjustment is similar to the already described Mars terminal adjustment, except that, again, the disc size of Venus would require that a closer approach (15 days) be made before adequate sightings could be obtained.

3-17. Venus Flyby

The flyby phase is a special case of orbital entry. As the vehicle passes Venus, a velocity correction may be required to correct either exit velocity or the trajectory inclination. Although these corrections do not result in an orbit around Venus, they do change the direction at which the vehicle leaves the influence of Venus.

3-18. Post-Venus Adjustment

This phase is similar to the post-Earth and post-Martian adjustment phases, but again the differing planet size varies the time by which the final adjustment must be made in order not to make corrections based on sightings where instrument error is significant.

3-19. Earth Terminal Adjustment

Similar to previously described terminal adjustments, this phase begins 20 days before scheduled earth arrival.

3-20. Earth-Orbit Entry

Initial entry for the returning spacecraft is to a relatively high orbit which will minimize the criticality of the entry maneuvers. Options for the initial orbital entry may be available.

3-21. Earth-Orbit Adjustment

After an initial earth orbit has been reached, the crew determines the orbit and calculates the necessary adjustments required to put the vehicle into the terminal orbit. The final orbit will be selected from

orbits defined prior to launch so that a ferry vehicle can be ground-launched into an orbit where it can rendezvous with the returning vehicle. After the final orbital adjustment, the crew will station-keep until the ferry vehicle arrives.

3-22. EARTH CYCLE, PART 2

3-23. Earth Ferry Rendezvous

The ferry vehicle will arrive, be maneuvered to a rendezvous position, and a rendezvous performed. After rendezvous, the returning Mars mission crew will transfer for the return to Earth.

3-24. Earth Landing-Orbit Correction

After transfer of the crew and of the material being returned to earth, with them, the ferry-vehicle orbit will be checked and corrected to the optimal reentry orbit.

3-25. Earth Landing

After the ferry vehicle has entered the final orbit, the reentry sequence will be initiated.

3-26. MARS CYCLE

3-27. Mars-Lander Orbit Correction

The orbit selected as optimal for station-keeping probably will not be optimal for terminal descent of the lander. Consequently, after leaving the main vehicle, the lander crew will have to correct the orbit to position their vehicle properly for the Mars landing.

3-28. Mars Landing

After the landing vehicle is maneuvered into a suitable initial position, it will land and preparations will be made so that an abort can

be executed if required. An updated abort plan, and nominal return plan, must be maintained during the exploration.

3-29. Mars Launch

After the exploration period, or if an abort is required, the lander vehicle will be prepared for launch and injected into orbit.

3-30. Mars-Lander Orbit Adjustment

After the lander has been successfully injected into orbit, the orbit will be determined and corrections made to position the lander vehicle for rendezvous.

3-31. Mars-Station Rendezvous

The rendezvous phase may involve docking, or it may require only a close approach, during which time the exploration crew and their collected material may be transferred to the main vehicle. In either case, the lander is jettisoned after the transfer is completed.

3-32. CLASSIFICATION OF PHASES BY FUNCTION

Although the base mission involves 27 sequential phases, a separate navigation-and-guidance approach is not required for each phase. Many phases are repetitions of earlier phases, and others are essentially similar. In Table 3-1, the various mission phases are grouped by basic function. It is apparent from Table 3-1 that the navigation and guidance requirements for the base mission can be considered in terms of eight general functions, rather than the 27 phases described earlier.

3-33. FUNCTIONS DELETED FROM CONSIDERATION

To constrain the total study effort within the implicit bounds set by the interplanetary aspect of the base mission, it is desirable to omit some functions noted in Table 3-1 from further consideration; launch, rendezvous, and landing have, therefore, been excluded. Also, no

Table 3-1. Mission-Cycle Phases Classified by Function

Function	Phase of Mission Cycle*			No. of Phases in Functional Group
	Earth	Interplanetary	Mars	
Launch	3-2	-	3-29	2
Orbit adjustment	3-3, 3-24	3-6, 3-4, 3-13, 3-21	3-27, 3-30	8
Rendezvous	3-4, 3-23	-	3-31	3
Injection	-	3-6, 3-14	-	2
Post and terminal adjustments	-	3-8, 3-9, 3-15, 3-16, 3-18, 3-19	-	6
Orbit study	-	3-10, (3-17), 3-20	-	3
Station keeping	-	3-12	-	1
Landing	3-25	-	3-28	2
Totals	6	16	5	27

*Heading numbers under which phases are described.

"midcourse correction" is included in the general sense; that is, no navigation and guidance function is described for the portions of the trajectory when the spacecraft is midway, or approximately midway, between planets. The reasons for omitting these functions are discussed under the following headings.

3-34. Planetary Launch

The basic requirements for the navigation and guidance of a vehicle during launch have been simply stated by Muckler and Obermayer (1964) as, "The problem ... of arriving at a certain altitude, a specific velocity, and a desired geographic coordinate with an intact vehicle." In both the Earth-launch and Mars-launch mission phases, this definition describes the problem: the desired trajectory must be selected from a limited number of possible trajectories which can provide the altitude, velocity, and geographic coordinates required to permit rendezvous without exceeding vehicle or crew limitations. However, other, more stringent, problems overshadow the problems of navigation and guidance. The launch problem from an Earth site, and probably from a Martian site, is primarily a dynamic control problem. Launch studies have been performed in which operators flew against computer simulations of launch situations. Muckler and Obermayer (1964), for example, indicate that their subjects, flying boosters in a computer simulation, could control the trajectory (although not to required terminal constraints) as long as conditions were within the normal limits. However, events that resulted from malfunctions, and many nearly normal conditions that are faced in an ascent, apparently perturbated the vehicle enough to exceed mans' capability to react. Holleman, Armstrong, and Andrews (1960) called attention to a series of factors, such as loss of thrust, windshears, vehicle separation, and burnout, as events that caused loss of control. They also identified vehicle flexibility as a severe constraint on control effectiveness.

The extent to which these parameters exist during Earth and Martian launch differs. For example, because of its soft-landing requirements, a Mars lander must be substantially more rigid than is the typical booster,

and the Mars atmosphere will probably exhibit less of the kinds of turbulence that cause windshear. Environmental and performance factors also differ, indicating that a Mars launch will involve lower g loads, less vibration, and reduced exposure to acoustic noise — all reductions that increase mans' capability to perform. Despite these differences, however, even the Martian launch situation is basically a control problem and, as such, is also beyond the scope of this study.

3-35. Rendezvous

Extensive literature exists in the area of rendezvous and docking. All of it, and flight experience to date, indicate that this mission phase can be accomplished with a minimum of equipment and that, with suitable training, fuel expenditures are not excessive. In general, man appears more capable at close ranges, but he can also perform reasonably well during maneuvers from longer distances.

Levin and Ward (1959) found, for example, that with appropriate displays man performed the docking maneuver with great precision and flexibility, and that with training he could control longer approaches — but with 20 to 30 percent excessive fuel consumption. Farber, *et al.* (1963), Pennington, *et al.* (1965), and Clark (1965) generally agree that this mission phase is clearly within mans' capability, and that only a minimum of information is required for good performance. Further and perhaps more to the point, actual pilot-controlled rondezvous has been successfully accomplished in the Gemini program. Therefore, this function apparently can be safely assigned to an operator, if required, and no great effort need be applied to further analysis of it during this study.

3-36. Landing

The problems of orbital entry and landing partly overlap, and the literature tends to merge terminal adjustments, orbital flight, and landing into a single phase; however, the results can be separated to some extent. Foudriat and Wingrove (1961) concluded that pilots could fly reentry sequences which were of such a nature that they involved skip trajectories, orbital insertions, or direct planetary descents. Wingrove, *et al.* (1964), who studied the Apollo-type vehicle and return trajectory,

also concluded that man could control the nominal entry and could monitor and recover from a skip-out trajectory. Moul and Schy (1965) also reported adequate performance with a blunt-nose type vehicle. Miller (1965) discusses several studies in his review of the available literature, which supports the conclusion that manual control is feasible for low-lift vehicles. It appears, however, that the more highly maneuverable vehicles have dynamic characteristics which make purely manual control undesirable and dictate provision of a relatively complex on-board computational facility and a highly sophisticated automatic system.

The studies noted above, and flight experience, indicate that earth landings with low-lift-ratio vehicles are possible with relatively simple man-operated systems. A Mars landing, or landing with a high-lift vehicle in Earth atmosphere, is more complex, although Apollo studies on LEM, experience in various high-performance aircraft (X-15), and experimental vehicle flights appear to support the conclusion that an essentially manual mode will provide adequate landing control, provided that the proper initial conditions can be established.

Therefore, for this study, it is desirable to exclude the landing phase from consideration because the base mission assumes a ballistic earth entry from orbit with a low-lift vehicle, and the Mars landing involves extensive control-dynamics problems similar to those already noted as implicitly excluded in the launch phase.

3-37. Venus Flyby

The Venus flyby is analyzed only in terms of its phases: a terminal adjustment, a post-planet adjustment, and a flyby adjustment (which is a special case of orbit entry).

3-38. Midcourse Correction

Our study indicates that a midcourse correction would not be desirable with an autonomous vehicle navigation and guidance system because the planet measures used to determine position create a residual error which

becomes more significant as the distance from the planet increases. Ultimately, the planet phonomena measured create an error which becomes larger than any trajectory error that might exist. Thus, it is not feasible to base velocity corrections on sightings taken too far from the planets involved. For Earth, the maximum distance, based on the reference trajectory velocities, is reached in about 20 days; for Venus and Mars, which are smaller, the limit is about 15 days.

Therefore, this study considers only "post-planet" and "terminal" adjustments to the trajectory, and avoids the spindown-spinup sequence that would be required if navigational events occurred at midcourse. This exclusion is not serious, however, because a midcourse correction would use the same equipment and require the same operator activities as the post-planet and terminal adjustments.

SECTION 4

ERROR-SENSITIVITY ANALYSIS

It is vital to the success of any manned interplaneary flight that the spacecraft proceed on the intended trajectory, because uncorrected departure from the design trajectory will cause the spacecraft to miss the intended target. The following analysis was performed in an attempt to determine the sensitivity of the base trajectory to a selected group of possible errors and to determine the velocity impulse that would have to be applied to correct the asymptotic velocity as a function of errors in these variables.

Error-sensitivity analyses were performed on four phases: cis-Martian injection, post and terminal adjustments, Venus flyby and Mars orbit entry. The study was limited to these four specific functions because the analysis results are applicable to the other phases.

The error variables considered in each phase are as follows:

1. Cis-Martian injection -
   Altitude,
   Injection velocity,
   Flight-path angle, and
   Position in earth orbit at time of injection.
2. Post and terminal adjustments -
   Flight-path angle.
3. Venus flyby -
   Magnitude of impact parameter.
4. Mars-orbit entry -
   Mars-orbit entry altitude

In the derivation of all sensitivity coefficients, it was assumed that, the craft is injected at perigee of the departure hyperbola, and that

all thrusting is impulsive. It was also assumed that any departure of the variables from the nominal is small (this allows linearization of any equations involving sines or cosines of angle). N-body effects were not considered nor were errors propagated across the interplanetary phase.

4-1. INJECTION

In leaving earth from a circular parking orbit, the direction and magnitude of the velocity vector at infinity (hyperbolic excess-velocity vector) are a function of the injection velocity, altitude of the orbit, flight-path angle, and location of injection. Any departure in these quantities from the nominal will point the departure hyperbolic asymptote in an undesired direction, and will carve an error in the hyperbolic excess-velocity magnitude. The velocity impulse required to correct the asymptotic velocity can be resolved into two components, δV_T and δV_N. Component δV_T is along the direction of the velocity vector, and δV_N is perpendicular to the velocity vector, but in the plane of the trajectory. (See Figure 4-1).

The δV_N and δV_T components can be expressed as

$$\delta V_T = \left(\frac{dV_T}{dV_i}\right)\delta V_i + \left(\frac{dV_T}{dh}\right)\delta h + \left(\frac{dV_T}{d\Gamma}\right)\delta\Gamma + \left(\frac{dV_T}{dx}\right)\delta x \qquad \text{Eq. 1}$$

$$\delta V_N = \left(\frac{dV_N}{dV_i}\right)\delta V_i + \left(\frac{dV_N}{dh}\right)\delta h + \left(\frac{dV_N}{d\Gamma}\right)\delta\Gamma + \left(\frac{dV_N}{dx}\right)\delta_x \qquad \text{Eq. 2}$$

where

δV_i = error in injection-velocity magnitude,
δh = error in altitude of orbit,
$\delta\Gamma$ = flight-path angle error, and
δ_x = error in location of injection

These relationships are shown pictorially in Figure 4-1.
In deriving these partials, it is assumed that the perigee of the departure hyperbola is the injection point, so that the nominal path angle at injection is zero.

Table 4-1. Injection-Error Partials

Velocity-Impulse Component	Injection-Error Partial*			
	δX	δh	δV_i	$\delta \Gamma$
δV_T	0	$\frac{\mu}{R_i^2 V_\infty}$	$\sqrt{1 + \frac{2\mu}{R_i V_\infty^2}}$	0
δV_N	$\frac{1}{1 + \frac{R_i V_\infty^2}{\mu}} \times \frac{V_\infty}{R_i}$	$\frac{\sqrt{1 + \frac{2\mu}{R_i V_\infty^2}}}{1 + \frac{R_i V_\infty^2}{\mu}} \times \frac{V_\infty}{R_i}$	$\frac{2}{1 + \frac{R_i V_\infty^2}{\mu}}$	$\frac{2 \times \frac{R_i V_\infty^2}{\mu}}{1 + \frac{R_i V_\infty^2}{\mu}} \times V_\infty$

* μ = gravitation constant of planet

R_i = radius of injection

V_∞ = velocity excess at infinity

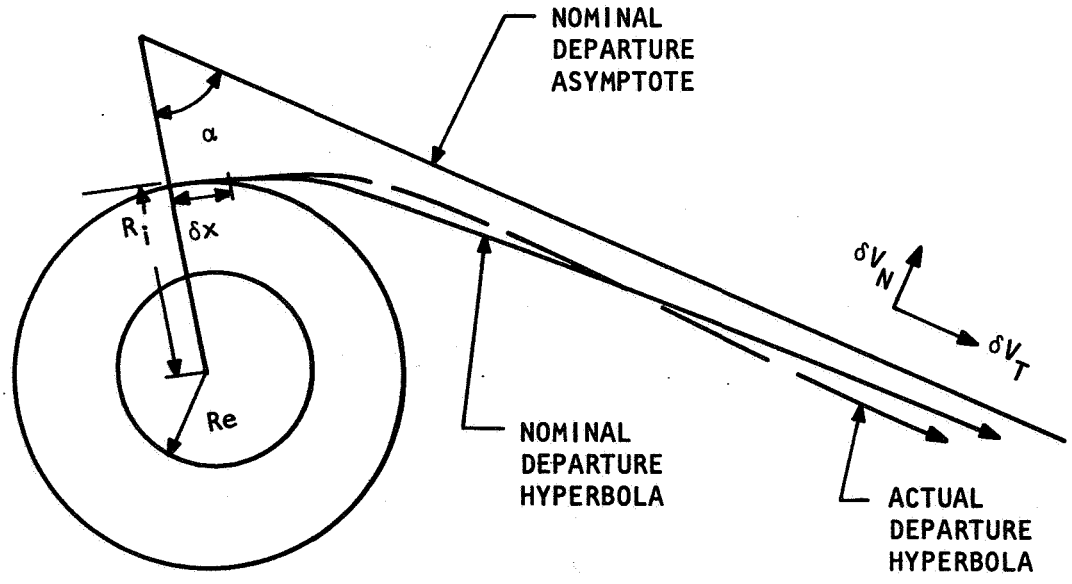

Figure 4-1. Injection Geometry

The partials were derived as follows. The magnitude of δV_N is given by

$$\delta V_N = V_\infty \, \delta\alpha \qquad \text{Eq. 3}$$

but

$$\cos \alpha = -1/e$$

so that equation 3 may be rewritten as

$$\delta V_N = V_\infty \left(\frac{\cot \alpha}{e} \right) de. \qquad \text{Eq. 4}$$

Now δ_e may be expressed as

$$\delta_e = \frac{2R_i V_\infty}{\mu} \, \delta V_\infty \, . \qquad \text{Eq. 5}$$

And since

$$V_i^2 = V_\infty^{\,2} + 2\,\mu/R_i \qquad \text{Eq. 6}$$

and

$$V_i \, \delta V_i = V_\infty \, \delta V_\infty, \qquad \text{Eq. 7}$$

substituting the expression for δ_e in Equation 4,

$$\delta V_N = \frac{2R_i V_\infty \cot\alpha}{e\mu} \, \delta V_i \, . \qquad \text{Eq. 8}$$

In addition,

$$\cot \alpha = \frac{\mu}{V_\infty V_i R_i} \, .$$

Therefore,

$$\delta V_N = \frac{2}{e} \, \delta V_i = \frac{2}{1 + \frac{R_p V_\infty^{\,2}}{\mu}} \, \delta V_i \, . \qquad \text{Eq. 9}$$

The variation of δV_N with δR_i can be similarly found.

$$\delta V_N = V_\infty \frac{\cot\alpha}{e} d_e \qquad \text{Eq. 10}$$

but

$$e = 1 + \frac{R_i V_\infty^2}{\mu} \qquad \text{Eq. 11}$$

so that

$$\delta e = \frac{2R_i V_\infty \delta V_\infty}{\mu} + \frac{V_\infty^2}{\mu} \delta R_i . \qquad \text{Eq. 12}$$

However, from equation 6,

$$\delta V_\infty \quad \frac{\mu}{V_\infty R_i^2} \delta R_i \qquad \text{Eq. 13}$$

Equation 12 then becomes

$$\delta e = \frac{V_\infty^2}{\mu} \left[1 + \frac{2\mu}{V_\infty^2 R_i} \right] \delta R_i . \qquad \text{Eq. 14}$$

Upon substitution, equation 10 becomes

$$\delta V_N = \frac{V_\infty}{\mu e} \frac{V_i^2}{\sqrt{e^2-1}} \delta R_i \qquad \text{Eq. 15}$$

where

$$\cot\alpha = \frac{\mu}{V_\infty V_i R_i} = \frac{1}{\sqrt{e^2-1}} . \qquad \text{Eq. 16}$$

Equation 15 may be rewritten as

$$\delta V_N = \sqrt{\frac{1 + 2\xi}{1 + 1/\xi}} \cdot \frac{V_\infty}{R_i} \delta R_i \qquad \text{Eq. 17}$$

where

$$\xi = \frac{\mu/R_i}{V_\infty^2}$$

4-2. Flight-Path Angle Error

An error in flight-path angle will result in a shift in location of perigee and departure on a trajectory different than the design trajectory. If the path angle at injection is small, the eccentricity of the hyperbola is unchanged; the effect of such an error is to rotate the velocity vector at infinity by an angle equal to that between the nominal and actual perigee as measured from the earth's center.

Then

$$\delta V_N \sim V_\infty \, \delta\nu \qquad \text{Eq. 18}$$

where $\delta\nu$ is the angle (true anomaly) between the actual and nominal perigee of the departure hyperbola.

For small angles, the flight-path angle Γ is approximately related to the true anomaly by

$$\Gamma \simeq \frac{e}{1+e} \, \nu \qquad \text{Eq. 19}$$

then

$$\delta\nu \simeq \frac{1+e}{e} \, \delta\Gamma \qquad \text{Eq. 20}$$

so that

$$\delta V_N \simeq V_\infty \left[\frac{1+e}{e}\right] \delta\Gamma = \left[\frac{2\xi+1}{\xi+1}\right] V_\infty \delta\Gamma \qquad \text{Eq. 21}$$

4-3. Position Error

If injection occurs at the wrong location in the orbit, departure from the planet is not on the nominal trajectory. To correct the resulting error in the direction of the velocity vector, an impulse only in the V_N direction is required. It is assumed that the magnitude and inertial direction of the velocity is unchanged by such an error, the departure geometry is as shown in Figure 4-2.

The angle Θ is given by

$$\Theta = \frac{1+e}{e} \, \Psi \qquad \text{(for } \Psi \text{ small)} \qquad \text{Eq. 22}$$

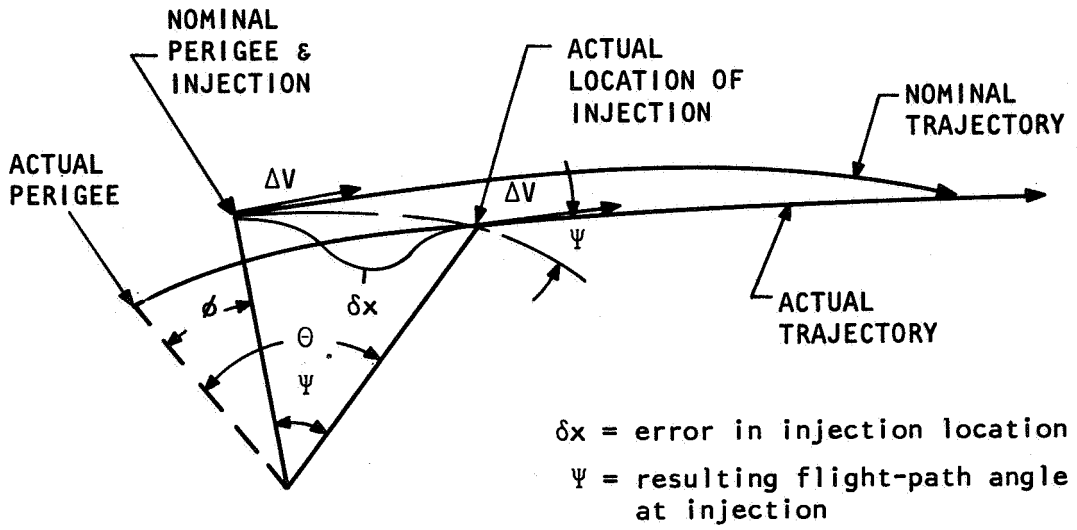

Figure 4-2. Departure Geometry

The actual rotation of perigee is

$$\phi = \Theta - \psi = \left(\frac{1+e}{e}\right)\psi - \psi = \frac{\psi}{e} \qquad \text{Eq. 23}$$

The velocity correction δV_N is just

$$\delta V_N = \frac{\psi}{e} V_\infty = \frac{\delta x}{e} \frac{V_\infty}{R_i} = \frac{1}{1 + 1/\xi} \frac{V_\infty \delta x}{R_i} \qquad \text{Eq. 24}$$

4-4. Axial Errors

Of the error sources being discussed, only errors in altitude and injection velocity also require a δV_T component of velocity to realign the departure velocity vector. Both the errors in the X and M directions require only a δV_N component to correct the trajectory. The desired δV_T partials were found as follows:

$$V_\infty^2 = V_i^2 - 2\mu/R_i \qquad \text{Eq. 25}$$

$$\frac{dV_\infty}{dV_i} = \frac{V_i}{V_\infty} \qquad \text{Eq. 26}$$

$$\delta V_\infty = \frac{V_i}{V_\infty} \delta V_i = \sqrt{1 + 2\xi}\ \delta V_i \qquad \text{Eq. 27}$$

Similarly, differentiating equation 25 with respect to R_i yields

$$\frac{dV_\infty}{dR_i} = \frac{\mu}{V_\infty R_i^2} \qquad \text{Eq. 28}$$

4-5. Sensitivities

A three-dimensional view of the injection normal and axial errors is shown in Figure 4-3. The normal velocity errors caused by path angle (Γ), position (X), injection velocity (V_i), and altitude (h) errors are shown in Figure 4-4.

The parameter values used in the computation of the error sensitivities were

V_∞ = 8 km/sec,

V_i = 13.6 km/sec,

R_i = 3540 n.mi (100-nmi park orbit) or 6550 km, and

μ = 398.6 x 10^3 km^3/sec^2

The axial velocity errors (δV_T) caused by altitude and injection-velocity error are shown in Figure 4-5.

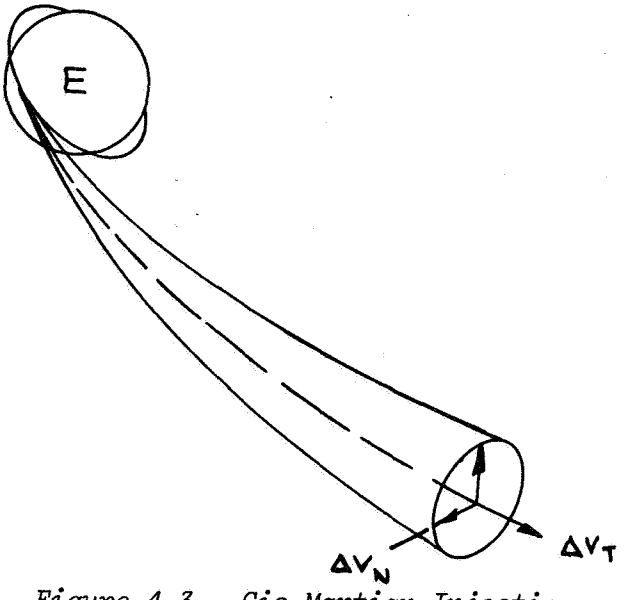

Figure 4-3. Cis-Martian Injection

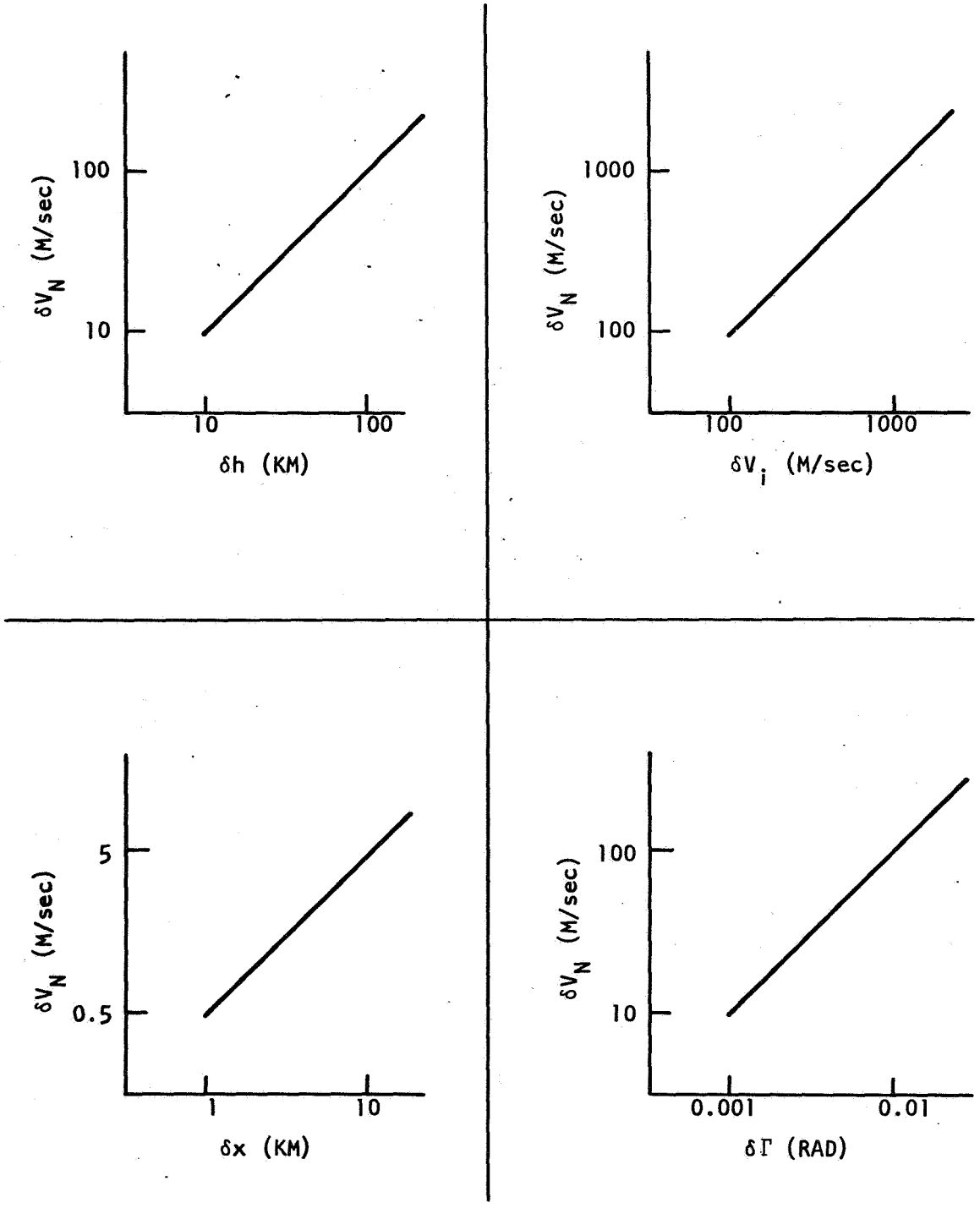

Figure 4-4. Normal Injection Errors (δV_N)

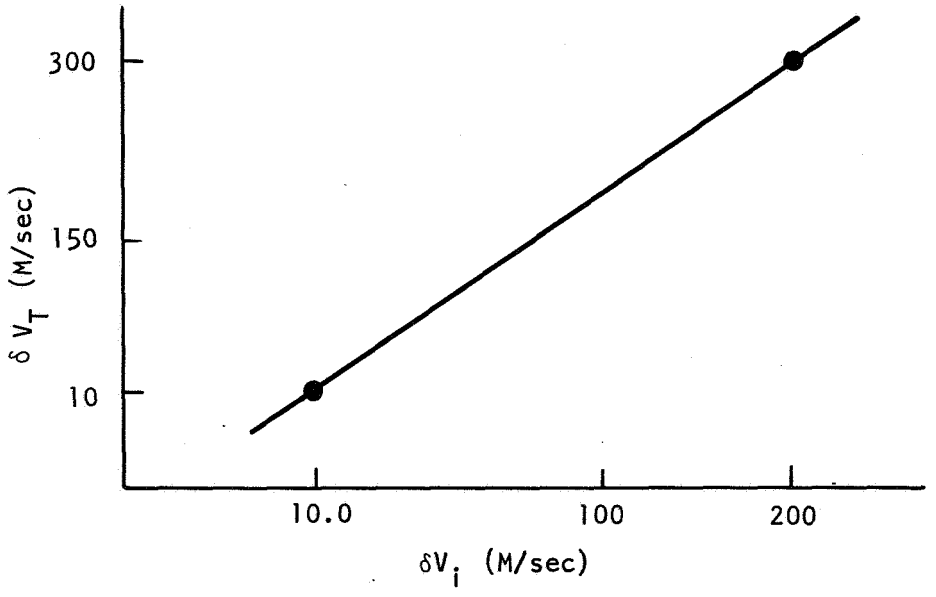

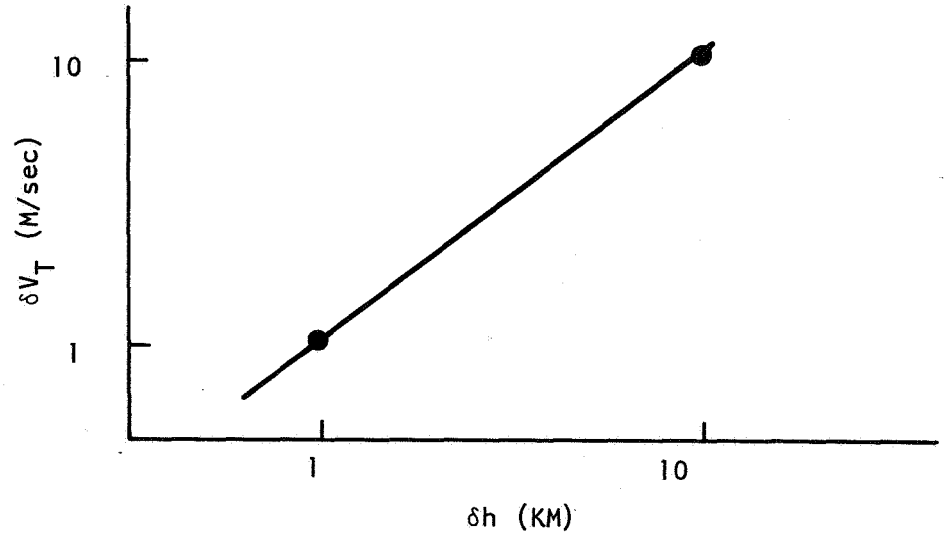

Figure 4-5. Axial Injection Velocity Error (V_T)

4-6. POST AND TERMINAL ADJUSTMENTS

As the spacecraft approaches or leaves a planet, a correction may be desired to place it into a new trajectory. As the craft approaches a planet, the geometry would appear as shown in Figure 4-6.

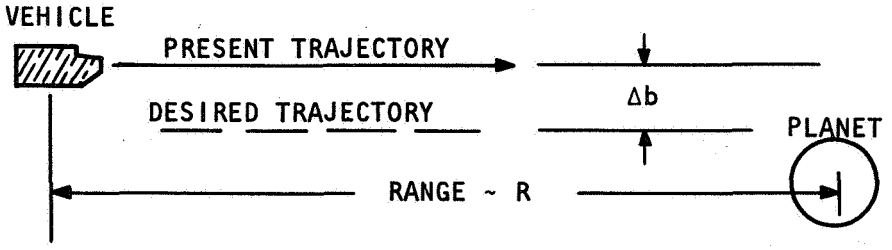

Figure 4-6. Terminal Adjustment Geometry

The minimum velocity impulse needed to deflect the spacecraft to the desired trajectory is in a direction perpendicular to the trajectory and of magnitude $\frac{\Delta b}{R} V_\infty$; the departure and arrival geometry and error sensitivities are shown in Figures 4-7 and 4-8. For a planet flyby, the planetocentric trajectory (Figure 4-9a) is hyperbolic. The direction of the departure asymptote is a function of the impact parameter, b.

A deviation in b from the nominal causes a change in Θ. The velocity impulse required to realign the velocity vector at infinity after the encounter normal to the trajectory and is given by

$$\delta\Delta V \simeq V_\infty \delta\Theta \qquad \text{Eq. 29}$$

From Figure 4-9a, it can be seen that

$$\sin\alpha = \frac{b}{\Gamma p + a} = \frac{V_\infty^2 b}{\mu}\cos\alpha \qquad \text{Eq. 30}$$

Differentiating with respect to b yields

$$\delta\alpha = \cos^2\alpha \frac{V_\infty^2}{\mu}\delta b \qquad \text{Eq. 30}$$

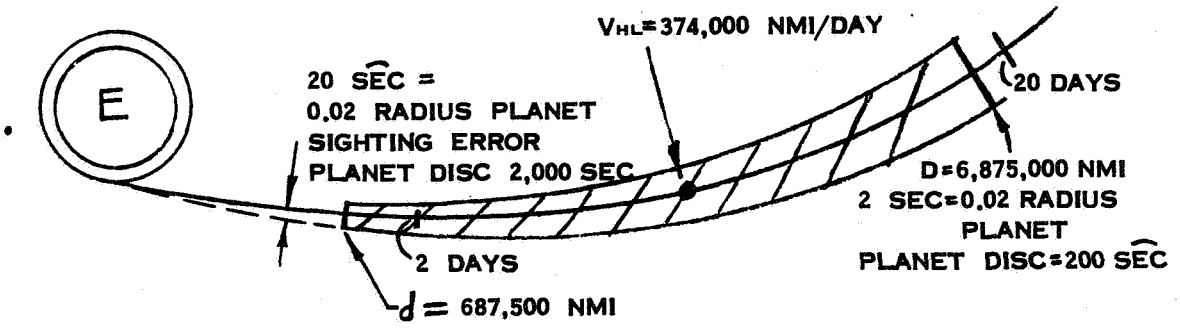

a. Geometry

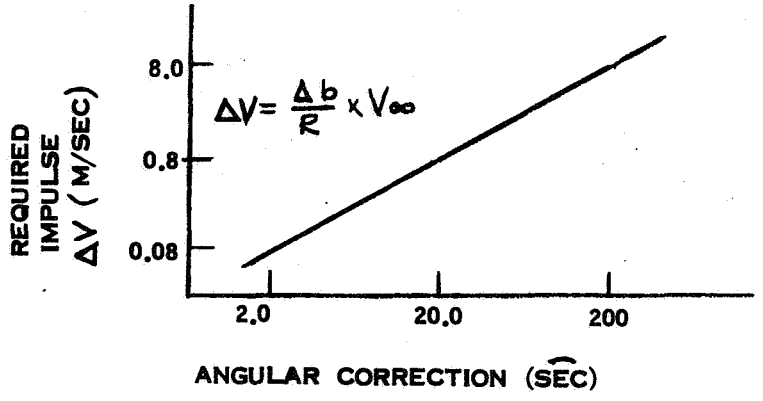

b. Error Sensitivity

Figure 4-7. Post-Earth-Correction Geometry and Error Sensitivity

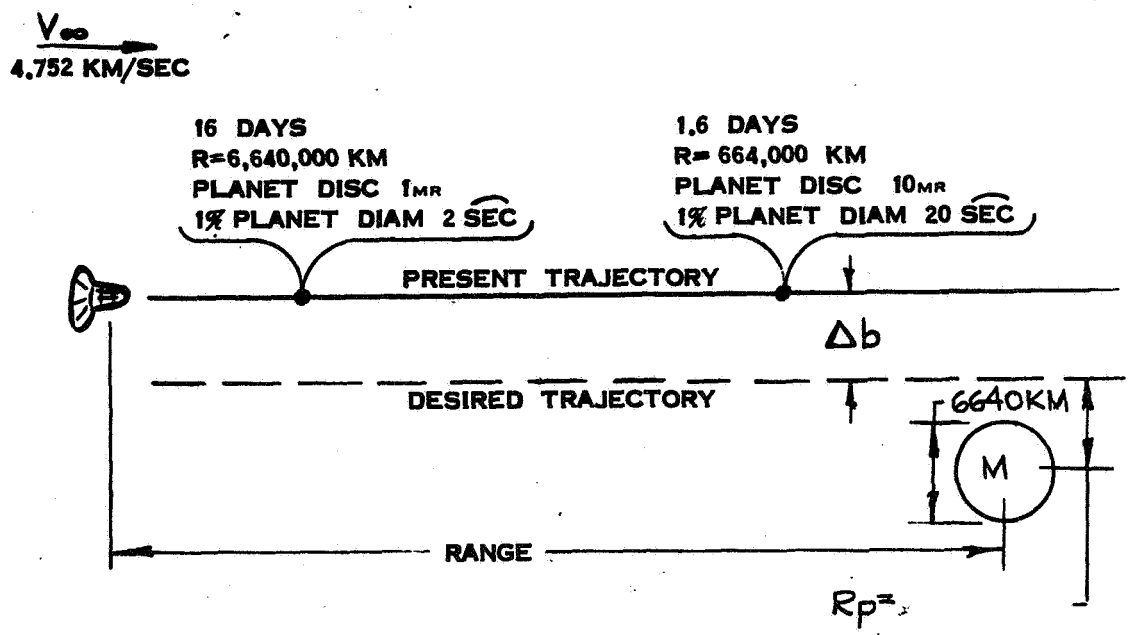

a. Geometry

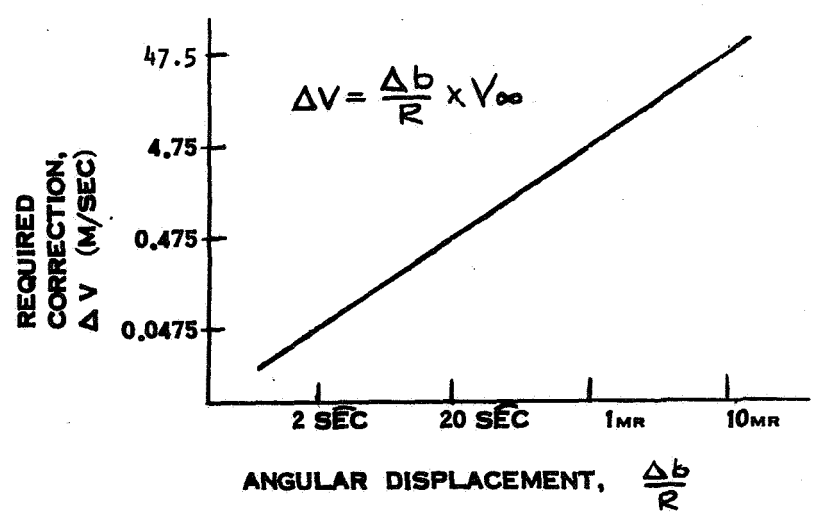

b. Error Sensitivity

Figure 4-8. Mars-Terminal-Adjustment Geometry and Error Sensitivity

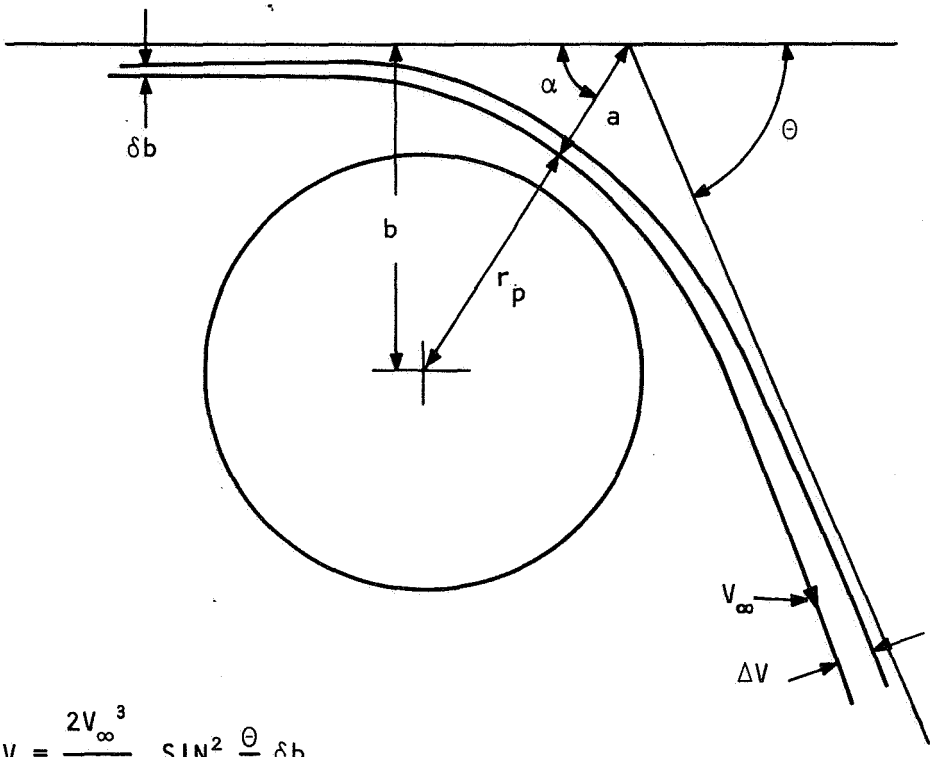

$$\Delta V = \frac{2V_\infty^3}{M} \text{ SIN}^2 \frac{\Theta}{2} \delta b$$

a. Geometry

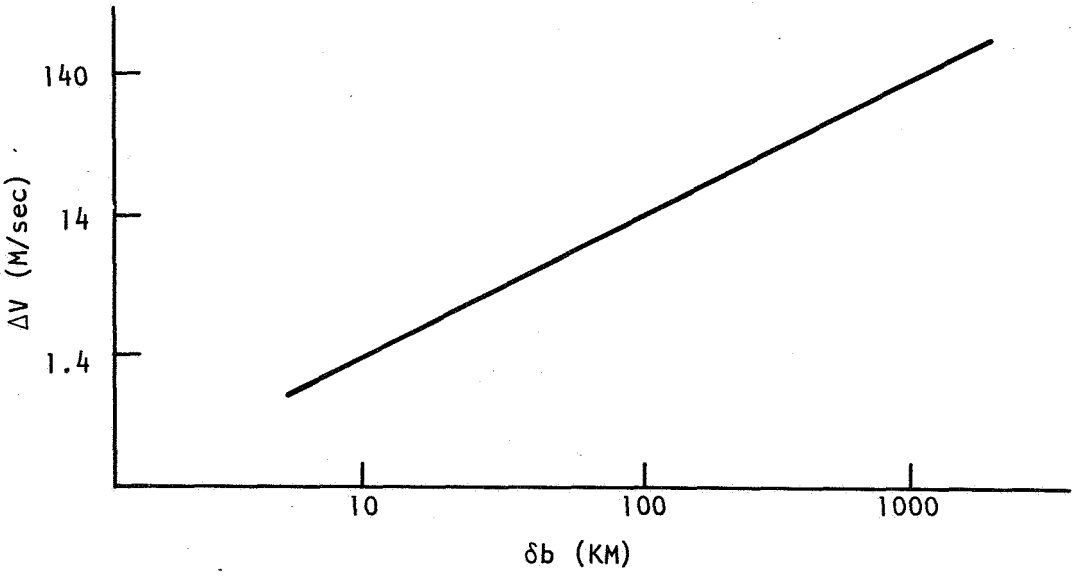

b. Error Sensitivity

Figure 4-9. Venus Flyby Geometry and Error Sensitivity

Since $\Theta = 180 - 2\alpha$, equation 29 reduces to

$$\delta\Delta V = \frac{2V_\infty^3}{\mu} \sin^2 \frac{\Theta}{2} \delta b \qquad \left\{ \begin{array}{l} \delta_{\Delta V} = \frac{2\ (167)}{325 \times 10^3} \times 0.14 \times \delta b \\ \delta_{\Delta V} \simeq 0.14 \times 10^{-3}\ \delta b \end{array} \right\} \qquad \text{Eq. 32}$$

For a Venus flyby, typical values for the various parameters in equation 31 are

$$\mu\text{Venus} = 325 \times 10^3\ \text{km}^3/\text{sec}^2$$
$$V_\infty \sim 5.5\ \text{km/sec}$$
$$\Theta \simeq 45°$$

When these typical values are used, the variation of $\delta_{\Delta V}$ with δb for Θ Venus flyby is as shown in Figure 4-9b.

4-7. ORBIT ENTRY

If, as the spacecraft approaches a planet, it is desired to transfer from a hyperbolic to circular orbit, a velocity impulse of magnitude ΔV is needed to decelerate the spacecraft to circular velocity. If the altitude at which this impulse is applied is correct but an error in the magnitude of the impulse occurs, the vehicle will enter an elliptical orbit which has a perigee radius equal to that of the nominal circular orbit. An example of such an orbit for Mars is shown in Figure 4-10a.

The increase in apogee altitude over the nominal circular altitude is

$$\delta h = \frac{4R_p}{V_c} \delta\Delta V_i \qquad \text{Eq. 33}$$

The increase in apogee altitude is found from the expression

$$Ra = (1 + e)a \qquad \text{Eq. 34}$$

where Ra = radius at apogee, and
a = semimajor axis

or

$$\delta Ra = (1 + e)\delta a + a\delta e \qquad \text{Eq. 35}$$

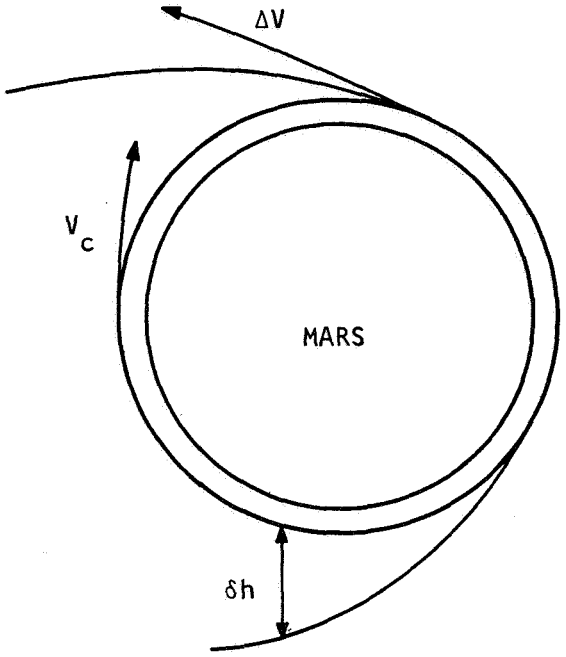

a. Geometry

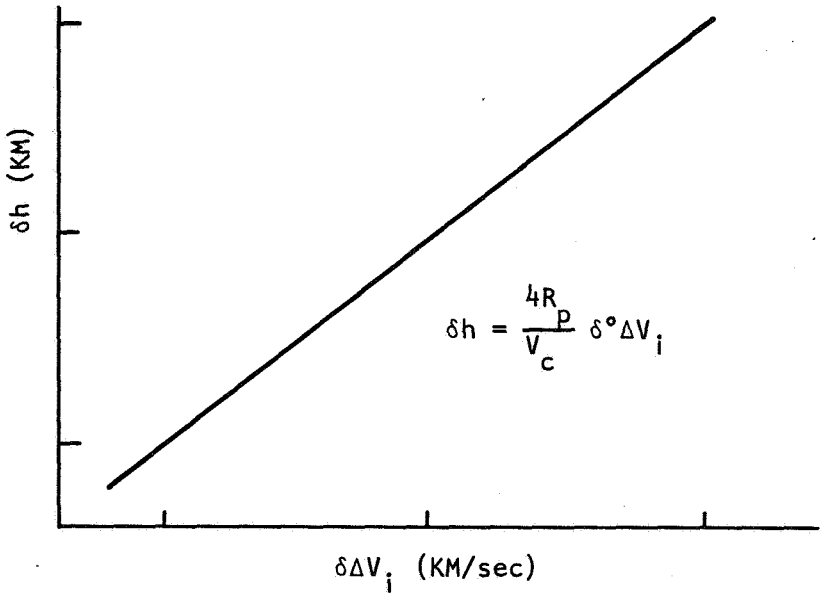

b. Error Sensitivity

4-10. Mars Entry Geometry and Error Sensitivity

Because the perigee radius does not increase, an expression for a can be found:

$$R_p = a(1 - e) \qquad \text{Eq. 36}$$

$$\delta R_p = 0 = \delta a(1 - e) - a\delta e \qquad \text{Eq. 37}$$

or

$$\delta Ra = 2\delta a \qquad \text{Eq. 38}$$

The semimajor axis is given by

$$\frac{1}{a} = \frac{2}{R} - \frac{V^2}{\mu} \qquad \text{Eq. 39}$$

Differentiating with respect to V yields

$$\frac{da}{a} = \frac{2\ aV^2}{\mu}\ \frac{dV}{V} \qquad \text{Eq. 40}$$

or

$$\delta Ra = 4a \left(\frac{aV^2}{\mu}\right) \frac{dV}{V} \qquad \text{Eq. 41}$$

If the nominal orbit is curcular, the following relations obtain:

$$\frac{aV^2}{\mu} = 1, \qquad \text{Eq. 42}$$

$$a = R_p, \qquad \text{Eq. 43}$$

and

$$V = V_c \qquad \text{Eq. 44}$$

Thus,

$$\delta h = 4R_p \frac{dV_i}{V_c} \qquad \text{Eq. 45}$$

For a "typical" Mars flight,

$$R_p = 4300 \text{ km}$$

$$V_c = \sqrt{\frac{\mu}{R_p}} = 3.0 \text{ km/sec for h } \sim 1000 \text{ km}$$

Using these values, the relation of δRa with δV_i is as shown in Figure 4-10b.

4-8. SUMMARY

The derived error-sensitivity curves for cis-Martian injection show that for moderate altitude (10-km), position (10-km), path-angles (1-mΓ), and injection-velocity (10-m/sec) errors, the resulting normal velocity (δV_N) errors will be approximately 12 m/sec or less. The axial-velocity errors, δV_T, are 17 m/sec or less for altitude and injection-velocity errors of 10 km and 10 m/sec, respectively.

Post- and terminal-adjustment errors are directly related to the post- and terminal-trajectory angle errors. Therefore, for a hyperbolic excess velocity of 8 km/sec, the required trajectory velocity correction will be less than 10 m/sec for a milliradian error. Measurement accuracies of 20 arc-seconds will hold the correction error to less than 1 m/sec.

The accuracy of the Venus flyby angle is a function of the trajectory displacement error. A trajectory displacement error of 100 km in Venus flyby will require a velocity impulse of less than 15 m/sec δV.

Orbital-entry injection-velocity errors are extremely serious. For example, a 10-m/sec, δV, error will result in approximately an 80-km δh error at the 180-degree orbit phase point.

SECTION 5
NAVIGATION AND GUIDANCE

The navigation and guidance functions of a manned mission to Mars, and return by way of Venus, can be accomplished using a wide variety of techniques. This section discusses the navigation and guidance information requirements and general methods that will satisfy the navigation and guidance requirements of the manned Mars mission.

Two basic approaches will be considered: the "semiautomatic" approach requires only a moderate amount of manual operation; the "aided-manual" approach is more manual in concept. The consideration of two basic approaches does not mean that one or the other would be selected; elements of both approaches probably would be incorporated into the equipments selected for a Mars mission.

Semiautomatic and Aided-manual approaches will be discussed for orbit determination, injection, post and terminal adjustment, orbit entry, and station-keeping mission phases.

In general, the crew can participate in all navigation and guidance activities, including obtaining basic data, processing data, and guiding the vehicle. The *extent* of man's contribution, however, varies in the two approaches.

5-1. ORBIT DETERMINATION

The parameters that must be obtained to identify and adjust planetocentric orbit are orbit size and shape, orbit orientation in the celestial sphere, and the position of the vehicle in the orbit as a function of time. The size and shape of the orbit may be expressed in terms of eccentricity and the major or minor axis. The orientation of the orbit may be expressed by a set of direction cosines or Euler angles defining a line normal to the orbital plane. The orientation of the

orbital elipse in the orbital plane can be stated as an angle measured from the ascending node. Orbital vehicle position at any time can be expressed as an angle from some fixed point on the orbit, such as the ascending node, or periapsis.

5-2. *Orbit Geometry*

Figure 5-1 illustrates the geometry of an earth-centered coordinate system and the optical observations required to determine the orientation of the orbital plane. The observations consist of measuring a latitude star-horizon angle (L_a), and a longitude star-horizon angle (L_N) (Figure 5-2). The orbital shape and major axis orientation within the orbital plane is determined by vehicle altitude measurements.

5-3. *Semiautomatic Orbit Determination*

Figure 5-3 shows the data-acquisition information flow for a semiautomatic orbit-determination approach. The optical instrumentation could consist of a horizon scanner and a star tracker; these instruments would provide data from which the latitude and longitude star-horizon angles could be obtained. An instrument is also required to provide ranging or altitude information.

The sequence of principal operations for a semiautomatic approach to orbit determination is as follows:

1. The IMU is operated in the gimbaled stabilization mode with stellar drift correction from the star trackers to provide a stabilized plane nominally parallel to the orbital plane.
2. The vehicle is rotated about an axis normal to the nominal inertial orbital plane by use of the horizon-scanner local vertical data.
3. Gyrocompassing is used to determine the normal to the orbital plane.
4. Inertially derived orbital-plane calculations are verified and corrected by stellar gyrocompassing. The star-orbit plane angle will cone unless the star offset line of sight is normal to the orbital plane.

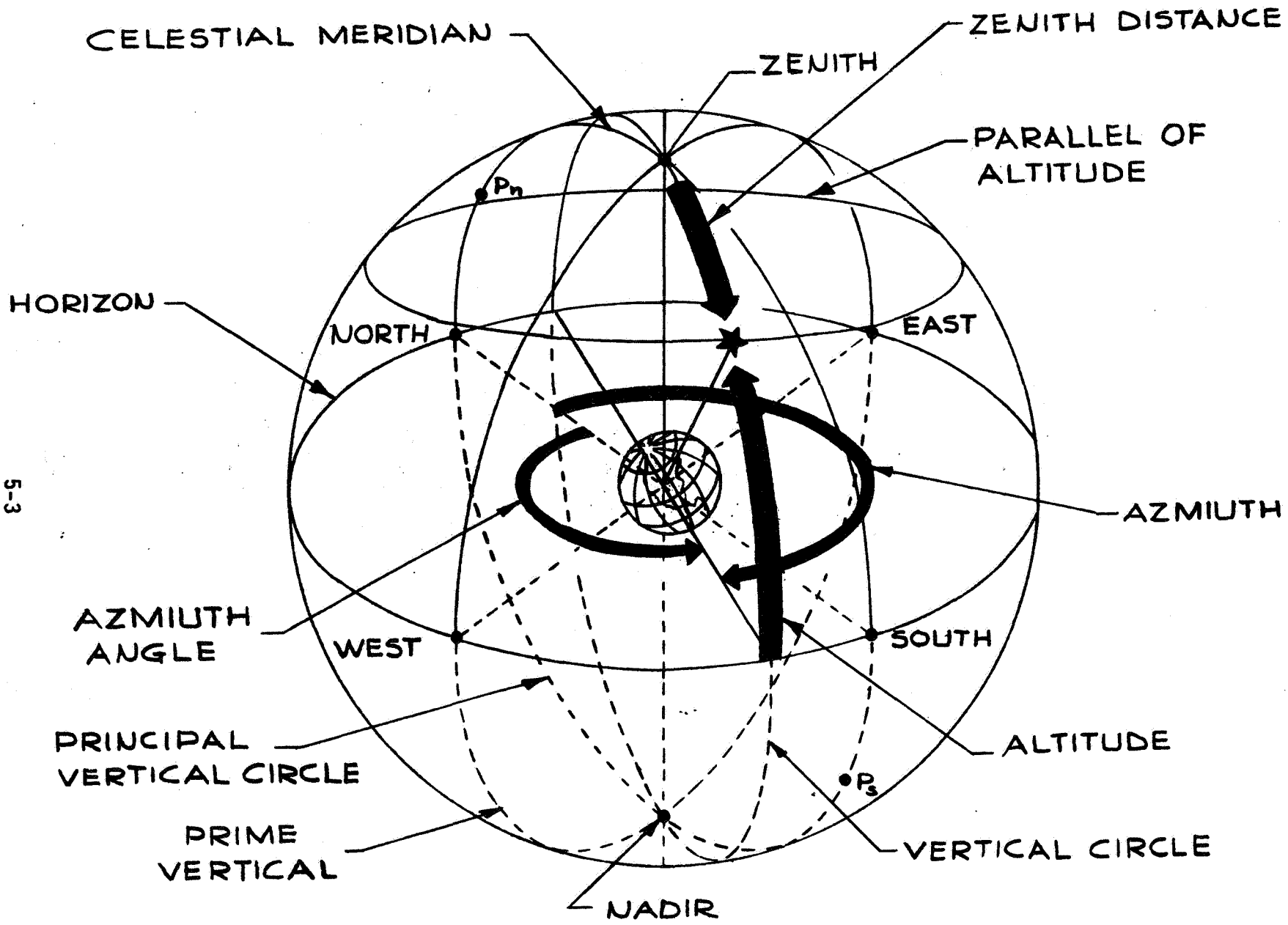

Figure 5-1. Horizon System of Coordinates

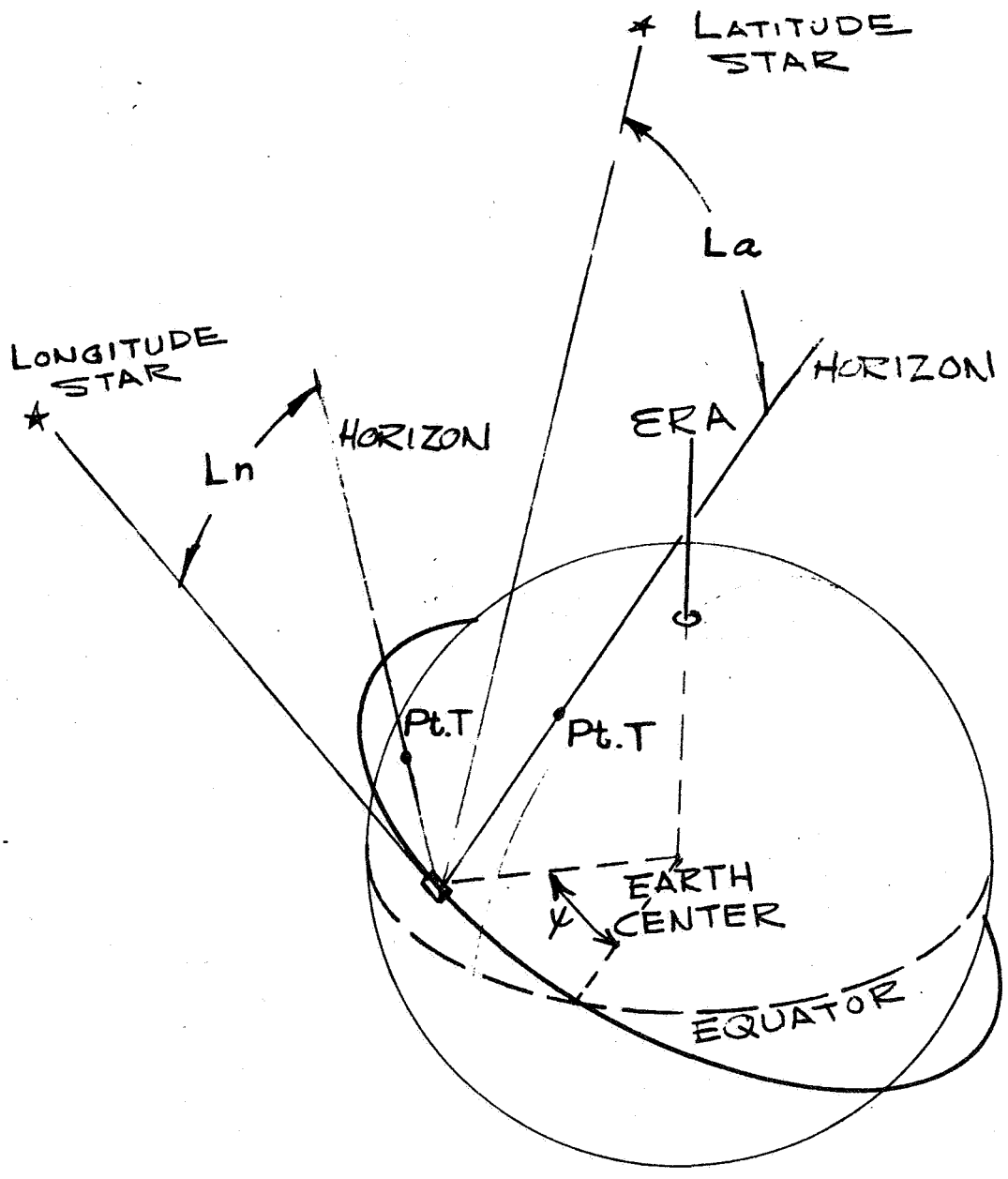

Figure 5-2. Space-Sextant Measurement Geometry

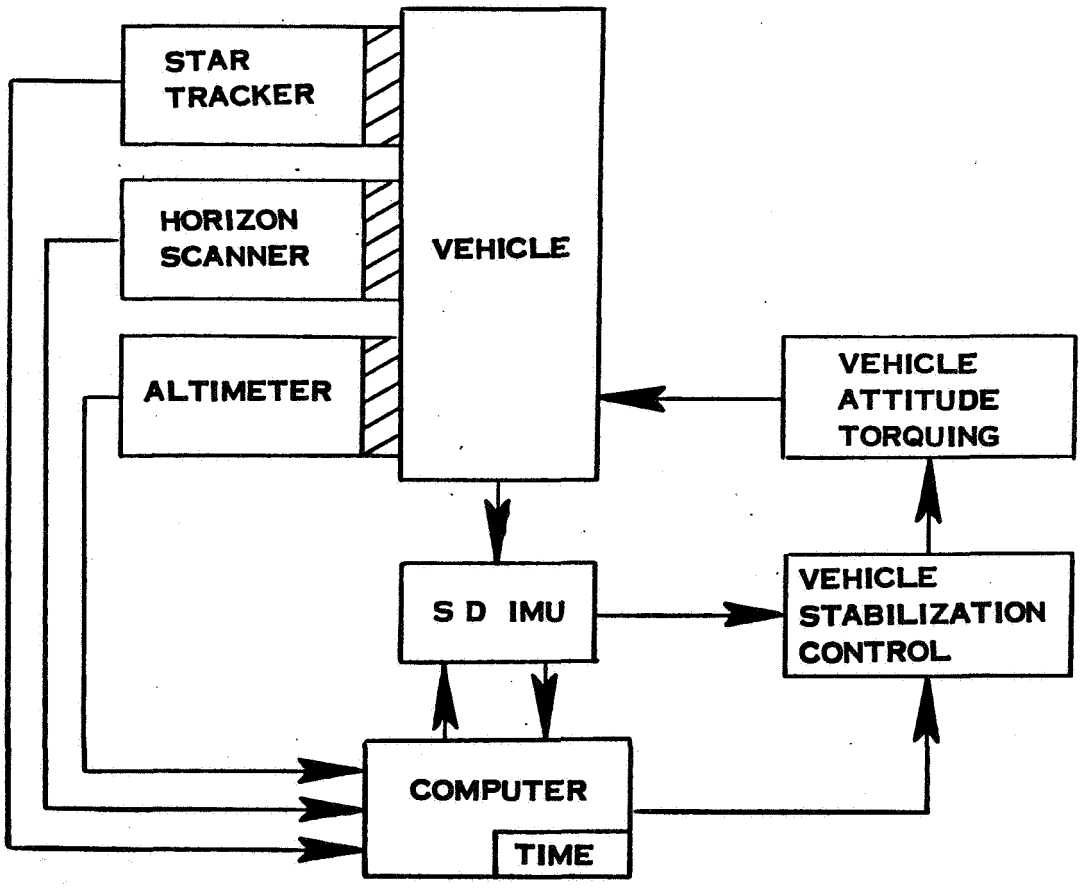

Figure 5-3. A Method of Semiautomatic Orbit Determination

5. Planetocentric position measurements are now obtained by the automatic equivalent of conventional celestial marine navigation through use of the horizon scanner and star trackers, and computer-supplied time.

6. Orbital height is obtained from the automatic altimeter data.

7. Final orbit calculations are made by the computer, which weighs the various inertial planet and stellar data to provide the best estimate of the planetocentric orbit.

5-4. *Aided-Manual Orbit Determination*

Figure 5-4 is a data-acquisition and information-flow diagram for an aided-manual orbit determination. Optical data are supplied by a sextant and a stadimeter. The sextant provides direct measurements of the latitude and longitude stars (Figure 5-2), and the stadimeter is used to provide altitude data. These instruments are described in Section 6.

The sequence of principal operations for aided-manual orbit determination is as follows:

1. The vehicle is brought to the proper attitude for navigational observations.

2. The vehicle is maintained at this attitude to keep the optical targets within the sensor field in view. Methods of accomplishing manual attitude control required for navigational observations are discussed in Section 6.

3. A series of stadimeter sightings are taken to obtain altitude data.

4. Smoothed stadimeter data is used to compute the orbital elements which determine orbit size and shape.

5. A series of sextant sightings are taken to obtain a number of star-horizon angle pairs at various points in the orbit.

6. The sextant dataare used to determine the orbital elements which fix the plane of the orbit and the position of the vehicle in the orbit as a function of time.

5-5. *Orbit Correction*

Having determined the orbit, the next step is to correct the orbit so that it lies in the plane of the preselected cis-Martian

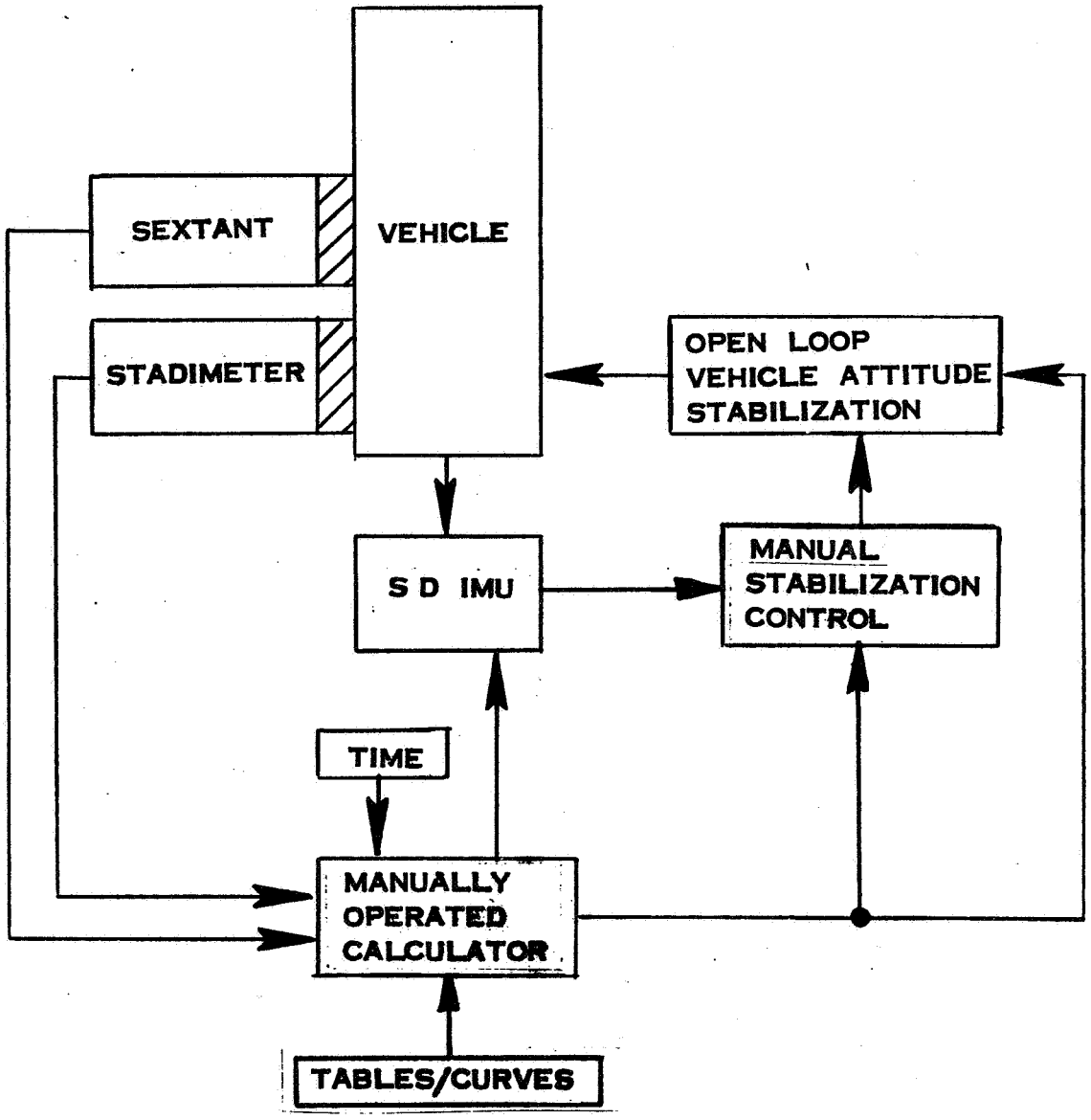

Figure 5-4. A Method of Aided-Manual Orbit Determination

trajectory. Since the techniques and procedures for correcting the orbit are essentially the same as those for other guidance events, this function will not be discussed here. For the purposes of this study the major difference between orbit correction and other guidance events is the computation requirements. These will be discussed in detail in the Phase II report.

5-6. INJECTION

The injection of a space vehicle orbiting a planet into a heliocentric transfer to another planet requires the application of an impulse of velocity to the spacecraft at the proper point in its planetocentric orbit. A heliocentric cis-Martial orbital geometry is shown in Figures 5-5 and 5-6. The orbit passes through a plane determined by three points: the Earth's position at launch, the Sun, and the position of Mars at arrival. This plane may be defined by a set of direction cosines which analytically fix the normal to the orbital plane, the inclination angle of the orbit plane to the ecliptic plane, and the angular location of the intersection of the orbital plane with the ecliptic plane.

The cis-Martian injection velocity for the base-line trajectory is 13.62 km/sec and the excess hyberbolic velocity reaches a value of 8.02 km/sec as the vehicle departs from the earth.

The navigational and guidance requirements of injection can be divided into two steps. The first step consists of determining the correct planetocentric position and proper heliocentric orientation, and determining the required ΔV. The second step consists of achieving and maintaining the correct attitude during the injection-impulse engine burn. A mission timing is assumed which places the vehicle in the correct heliocentric position.

Planetocentric position as a function of time is obtained from the previous orbit determination phase. From this data, and on the basis of a precomputed cis-Martian trajectory, the time of impulse and

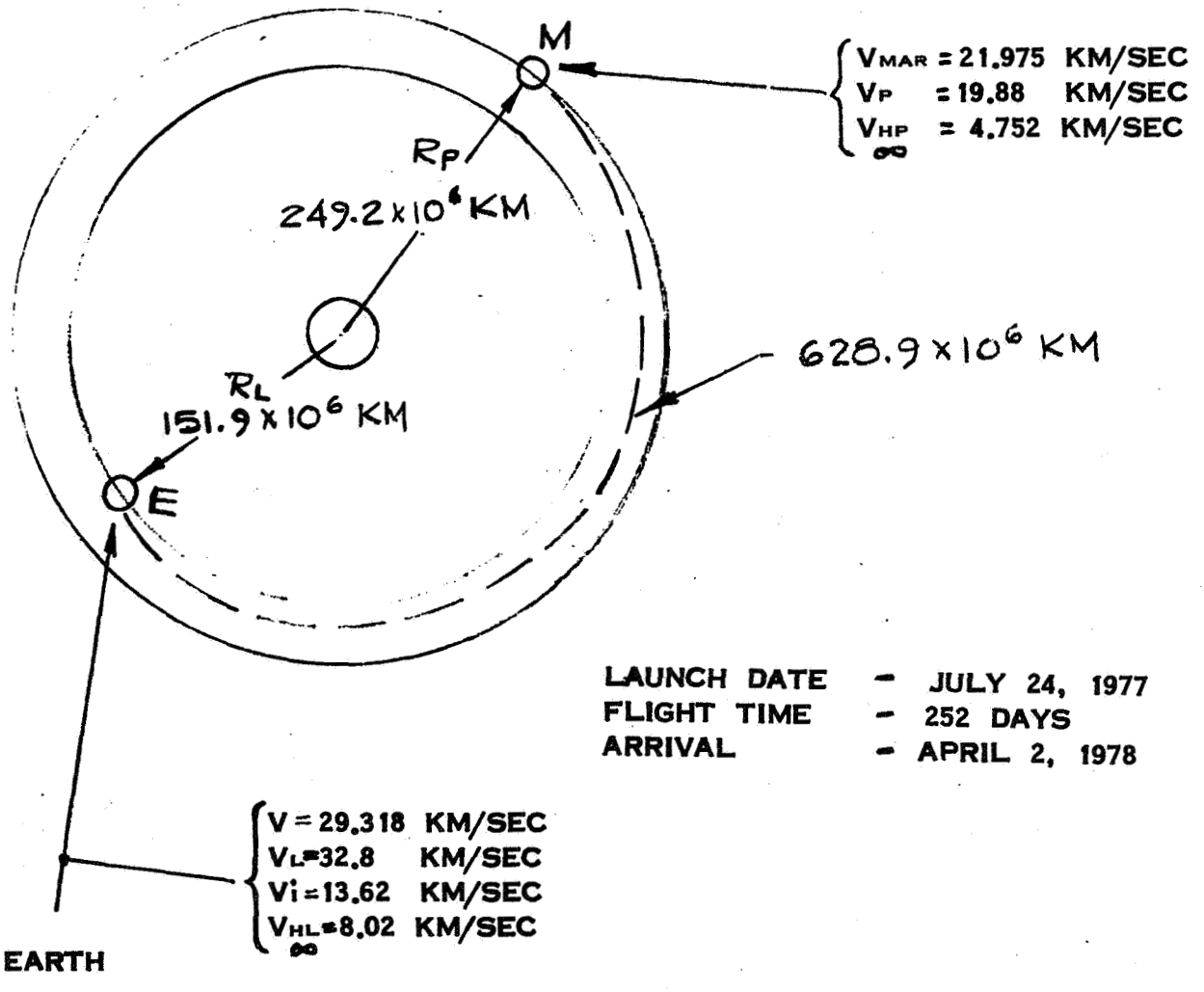

Figure 5-5. Geometry of a Cis-Martian Orbit

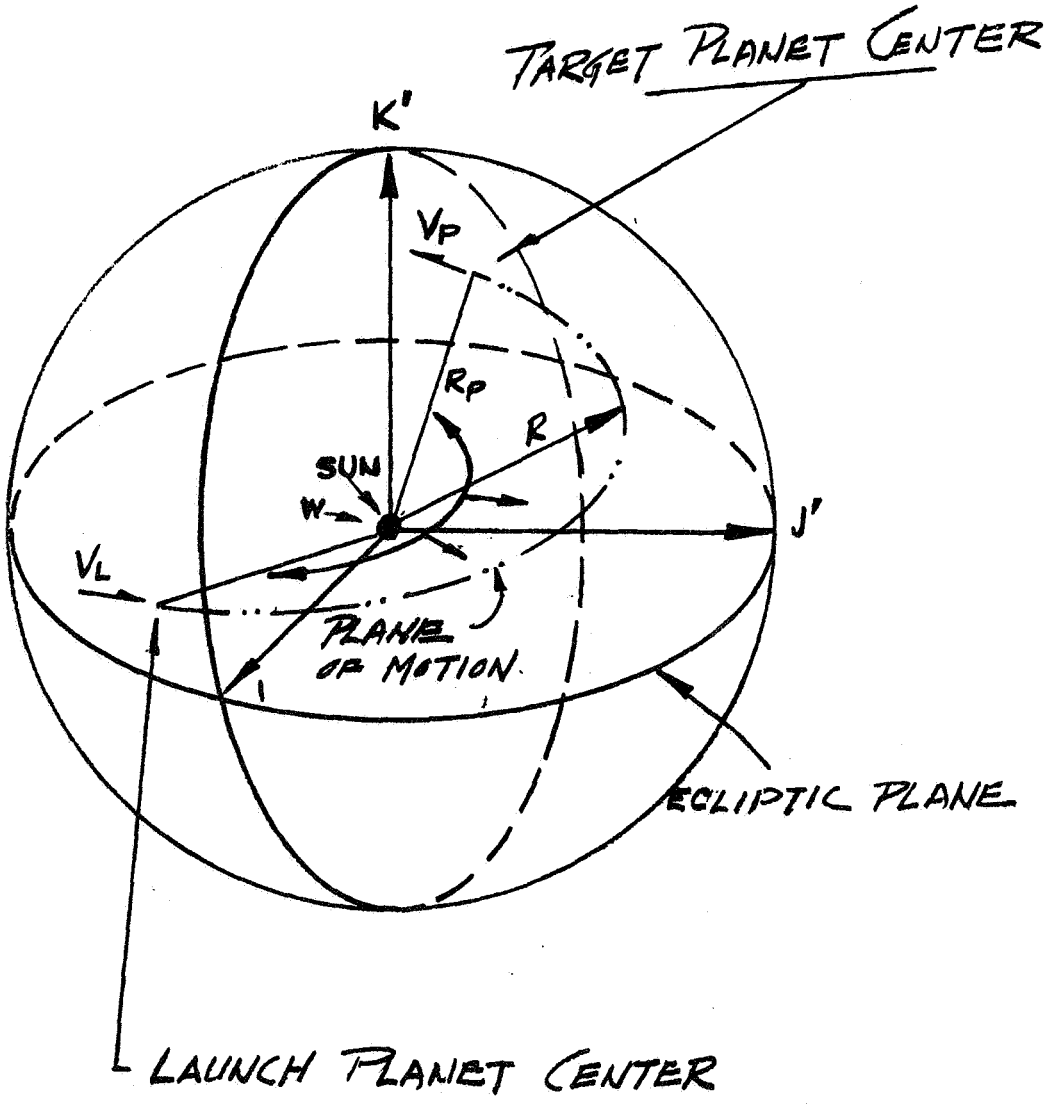

Figure 5-6. Heliocentric Transfer Geometry

the ΔV may be computed. The vehicle orientation or attitude within the celestial sphere for thrusting may be expressed in terms of two stars measured relative to a stable reference frame. This is a precomputed direction based on the nominal earth orbit. If the stars selected are within several degrees of the desired vehicle-injection attitude, the geometry is simplified as shown in Figure 5-7. This figure shows orientation of the injection-velocity impulse (nominal star track reference) and two stellar attitude references. The injection alignment error is shown as the difference between the injection target attitude and the vehicle star tracker reference. Proper mechanization of the injection phase requires a guidance which utilizes this difference to minimize the error between the velocity impulse attitude and the injection target attitude.

5-7. Semiautomatic Injection

Figure 5-8 illustrates the data acquisition and information flow for a generic semiautomatic cis-Martian injection approach.

The first step of the injection phase,determining the proper time, attitude and impulse, is accomplished by the on-board computer.

The second step of the injection phase,applying the required thrust, is accomplished by the following equipment:

2-2 axis star tracker (attitude),
Horizon scanner (local vertical),
Altimeter (altitude),
Time reference,
Computer,
Vehicle stabilization subsystem, and
Inertial navigation and guidance system.

The inertial navigation and guidance system could consist of a strapdown inertial measuring unit (SD IMU) a computer, vehicle-stabilization control, vehicle attitude torquing, and an engine with associated ignition, cutoff, and gimbaling.

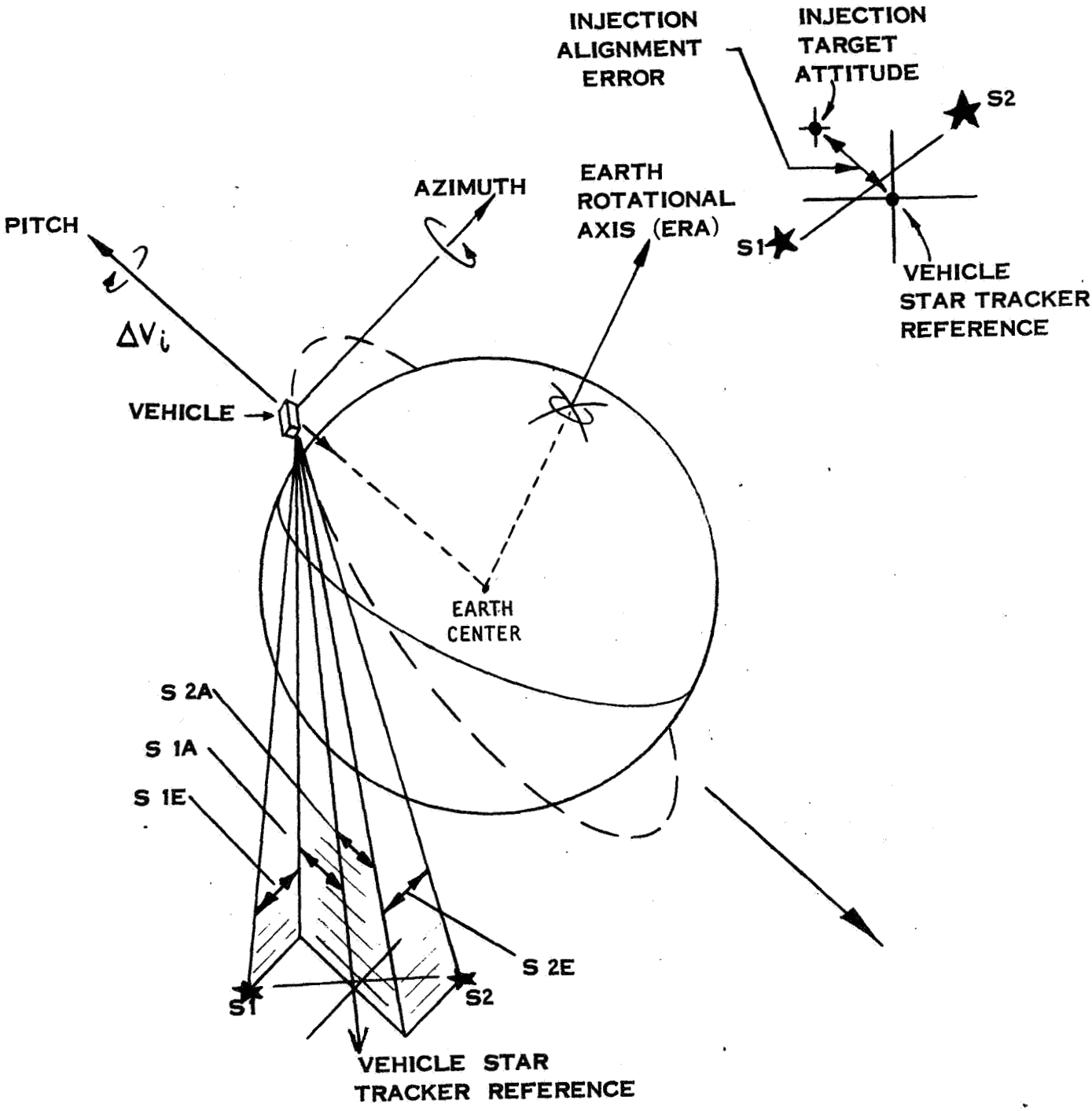

Figure 5-7. Cis-Martian Injection Star Tracker Alignment

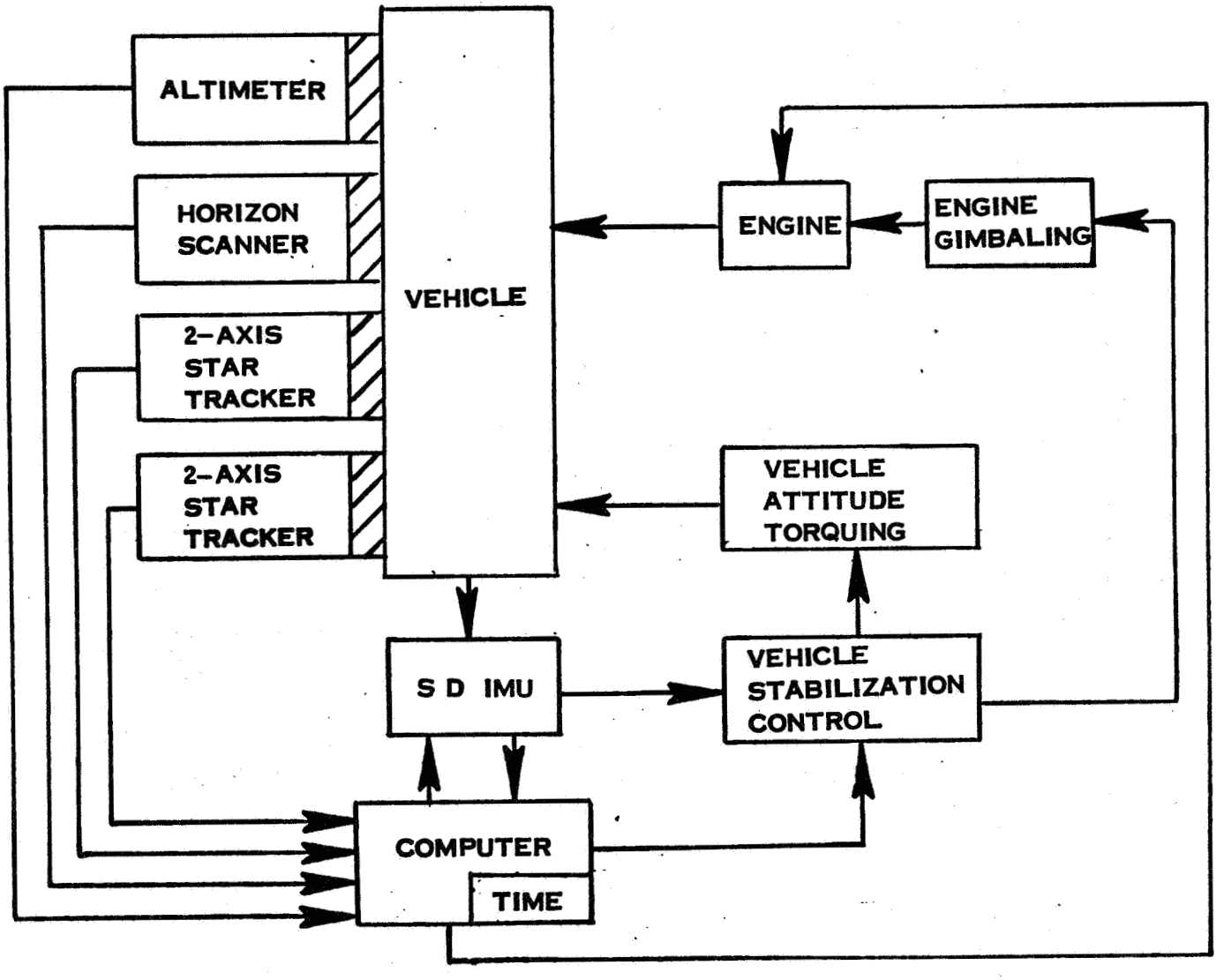

Figure 5-8. Semiautomatic Cis-Martian Injection

Navigation and guidance requirements for this phase are a two-step process. To initiate and terminate the burn at the proper time, the crew will use information brought from earth and previously calculated during the planet orbit phases.

The nominal trajectory on which the mission is based will define the orbit from which the vehicle should inject, the time of injection, the burn time, and the celestial attitude which should be held during the injection process.

Orbit-determination processes already completed will enable the crew to determine any changes which are required; however, once the earth-orbit plane is corrected, only two adjustments need be made—turn-on time or burn time. The former is most likely and would be used to compensate for the effect of improper orbital altitude which, if it were other than nominal, would change the time when the vehicle arrived over the ground track point which represented the proper on-time.

Since the vehicle would not pass over this point if the angle of inclination of the orbit were other than nominal, this condition would be compensated for by a slight variation in celestial attitude and an increased burn time.

The injection would then involve the following operations:

1. The vehicle attitude stabilization system is set to proper injection attitude.
2. Star trackers are aligned with selected stars (1 and 2 in Figure 5-7).
3. The vehicle is oriented to minimize the injection alignment error.
4. The vehicle is placed in the gimbaled inertial stabilization mode with stellar updating providing inertial drift correction.
5. Engine ignition is commanded when the vehicle reaches the correct planetocentric position.
6. The vehicle is then placed in a navigation-and-guidance mode to measure and control the applied injection-velocity vector (ΔVi); during engine burn, the navigation-and-guidance system controls engine gimbaling, vehicle attitude, and engine cutoff.

The operational complexity of the instrumentation is considerably reduced by the introduction of man into the system. Man is available to provide control for operation sequencing, to make decisions when there is ambiguity in discrimination, to replace pattern-recognition devices, and for memory functions.

5-8. *Aided-Manual Injection*

Figure 5-9 illustrates the data acquisition and information flow for a generic aided-manual cis-Martian injection. As previously noted, the first step of the aided-manual injection, determining engine turn-on time and ΔV, is directly derived from the orbital phases and can be accomplished manually with the aid of tables and a simple arithmetic calculator.

The proper vehicle attitude for injection may be attained and maintained by use of a wide-angle (5 degrees) manually pointed star tracker which provides a view of several injection-alignment stars, the injection direction, and the injection-alignment error. With the use of the alignment-error presentation (described in Section 6), a crew member can manually adjust the vehicle attitude torquing to minimize alignment error.

The cis-Martian injection will utilize a comparatively high thrusting level and, consequently, require a high activation response and correct error interpretation for the proper guidance of the spacecraft. The practicality of manual control would be improved if the injection-impulse duration were increased, and thus the total change in velocity were made over a longer time, so that the effect of misalignments were less critical.

The manually controlled injection could consist of the following grouping of equipment:

Wide-angle star tracker,
Integrating accelerometer (part of SD IMU),
Manual engine igintion-and-cutoff subsystem,

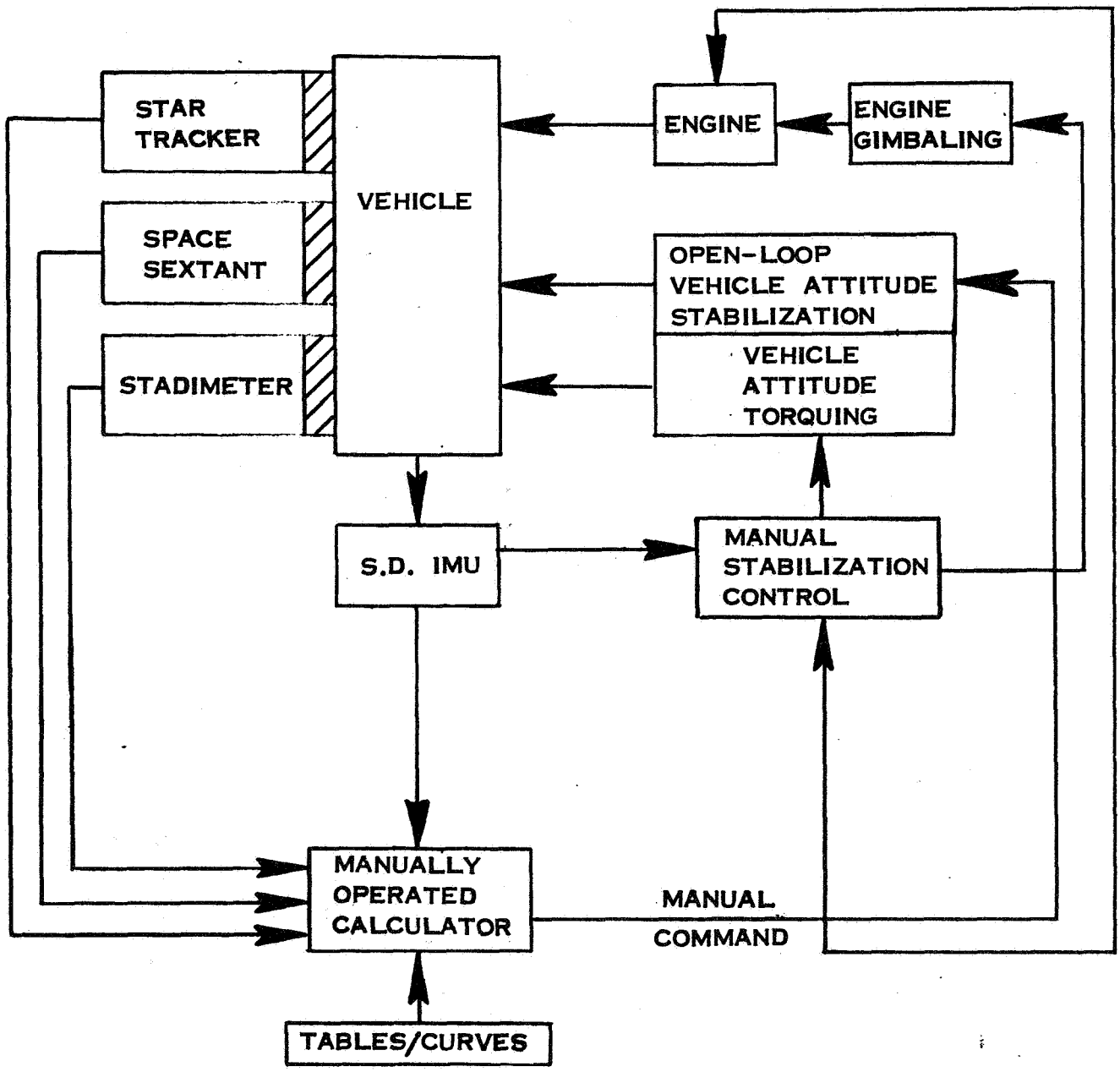

Figure 5-9. Aided-Manual Cis-Martian Injection and Orbit Entry

Open-loop vehicle-attitude-stabilization subsystem,

Vehicle-attitude torquing, and

Moderate-thrust injection engine.

In this navigation-and-guidance configuration, the wide-angle star tracker provides pointing-error information, which is used to determine the manual vehicle attitude torquing required to maintain proper vehicle orientation.

Components normal to the desired line of thrust or velocity impulse may be corrected by observing a display of the normal output of the IMU and manually nulling the normal integrated impulse by gimbaling the thrust engines, or by adding normal thruster impulses.

Engine cutoff will be executed when the in-line integrated acceleration measured by the IMU's accelerometer reaches the desired injection ΔV.

The sequence of principal operations for the aided-manual injection is as follows:

1. The crew member manually controls the vehicle-attitude stabilization subsystem to the proper injection orientation relative to the celestial sphere.

2. Manual servocontrol of the vehicle-attitude stabilization subsystem is maintained by monitoring injection-alignment error on the wide-angle star tracker.

3. Engine ignition is manually commanded at the time precalculated for the correct planetocentric position.

4. Manual guidance may be performed by "flying" the space vehicle along the predetermined injection-star alignment path. Flying the spacecraft consists of manually controlling the vehicle attitude for proper orientation. The engine may be manually gimbaled or normal thrusters activated to minimize any accrued velocity normal to the preselected injection attitude.

5. Engine cutoff is manually executed when the in-line integrated acceleration reaches the requisite injection velocity.

5-9. POST AND TERMINAL ADJUSTMENT

Post and terminal adjustment of interplanetary trajectories will be required at many points in the mission. These adjustments will be

performed 1 to 20 days after leaving or before arrival, at the gravitation influence of a planet. The purpose of these adjustments is to ensure a correction of the injection errors before the error buildup becomes excessive. Post-Earth correction geometry and Mars terminal-adjustment geometry were presented in Figures 4-7a and 4-8a, respectively; the line-of-position geometry for Earth-departure trajectory, and solar-position-fix geometry are shown in Figures 5-10 and 5-11, respectively.

Post and terminal adjustments may be effected by the near-planet line-of-position approach or the solar-position-fix approach. The data required for a solar-position fix is two sun-star measurements and one planet-sun measurement. The geometry of the solar-position fix is shown in Figure 5-10. Geometrically, the two sun-star measurements form two conics with their conic axis along the sun-star line and conic intersection along the sun-space vehicle line of sight. Measurement of the sun-planet angle provides sufficient data to solve the sun-planet-vehicle triangle and obtain the vehicle's solar position. The above method is described in detail in Battin (1964).

The near-planet approach described below has the advantages of providing comparatively high accuracy coupled with simplicity, while the solar-position-fix approach provides data from which absolute solar position may be calculated. The error in the solar-position calculation is not particularly sensitive to the midcourse region in which the measurements are made; however, it apparently is not as accurate as the near-body approach, even though the near-body measurements are limited to a period of 1 to 20 days distance from a planet. The solar-fix approach could be used to check navigation during the midcourse trajectory.

5-10. Near-Planet Line-of-Position Approach

The near-planet line-of-position approach consists of determining the attitude of the vehicle-planet line of sight by comparing it with known attitudes of adjacent stars. Figure 5-10 shows an observer taking a near-planet/star view, and visually measuring an elevation and azimuth angle.

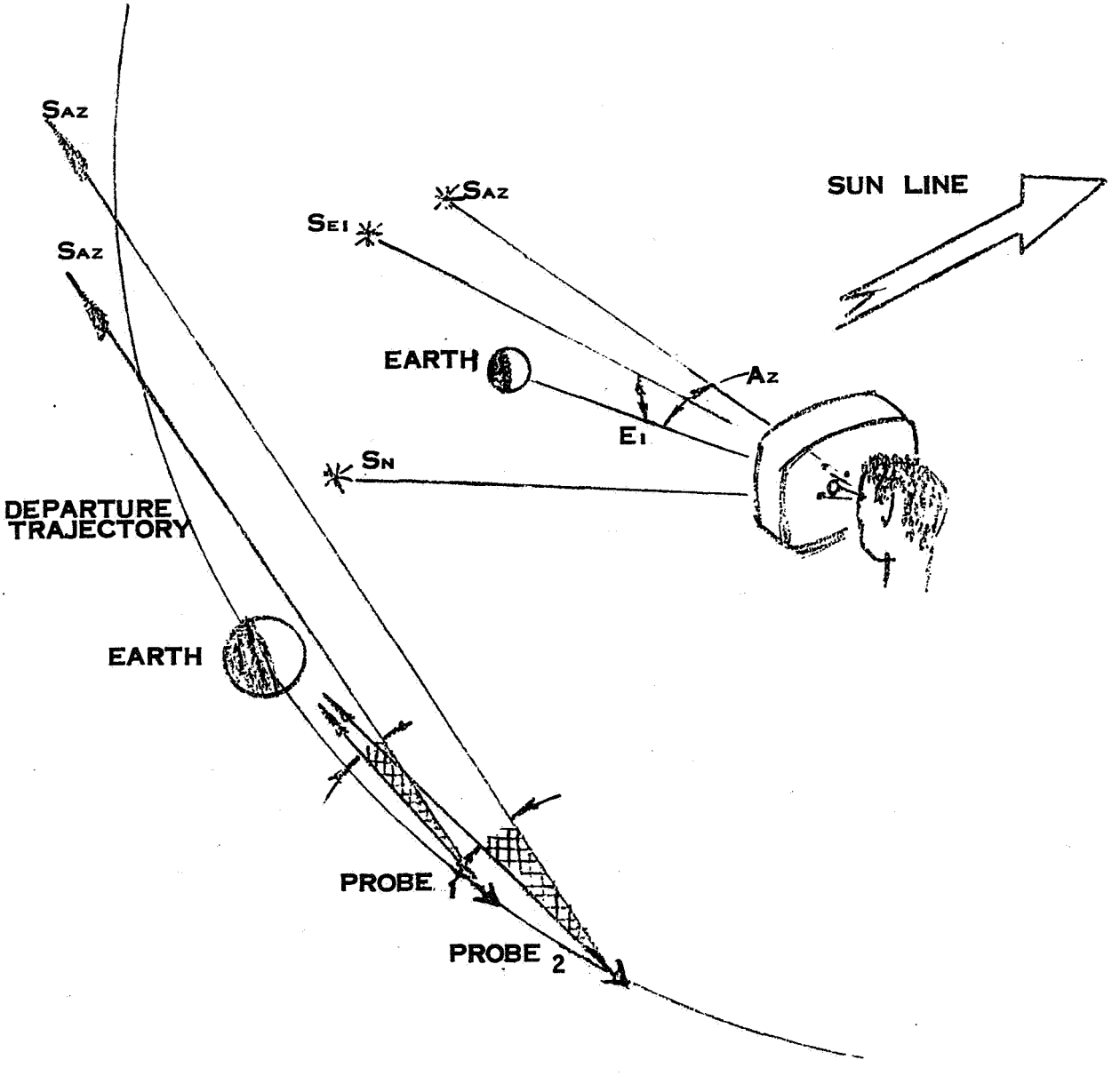

Figure 5-10. Earth-Departure Trajectory Line-of-Position Geometry

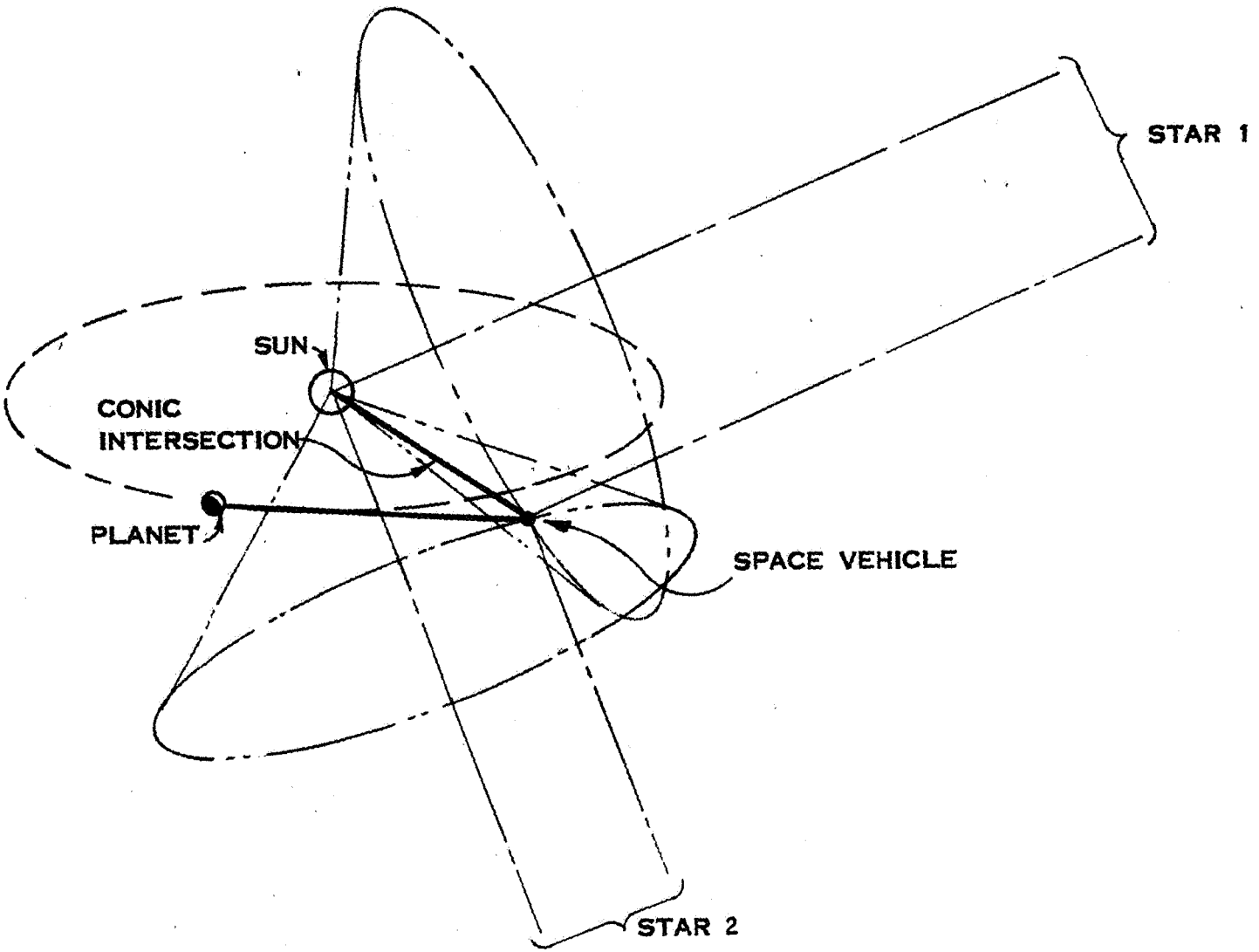

Figure 5-11. Solar-Position-Fix Geometry

The near-planet sightings probably will be performed in a region of approximately 1/2 to 10 million miles from the departure or arrival planet, as was shown in Figures 4-7a and 4-8a. This distance corresponds to a time period of approximately 1.5 to 20 days after departure or before arrival.

The zone in which the line-of-position measurements are performed is determined by the accuracy of the planet tracking. Figure 4-7a shows that, for the post-earth correction phase, there is no value in taking a planet sighting at too close a range; that is, at a departure time of 1.6 days from the earth and at a distance of 687,000 nm, the pheonomena-limited planet tracking accuracy is 20 arc seconds. As the distance from earth increases, the planet tracking error improves. At a departure distance of approximately 7,000,000 nm, the phenomena-limited planet tracking accuracy is at best, 2 arc seconds. Considering the limitations of associated planet tracking instrumentation of roughly 2 arc seconds, there is no value in taking planet-star measurements past a range of 7 million miles.

When a sufficient set of planet-vehicles line-of-sight data has been obtained, this information, together with range data, may be used to determine the trajectory error relative to the nominal trajectory. This method assumes a variational guidance analysis technique.

5-11. Semiautomatic Post and Terminal Adjustment

Figure 5-12 shows the data acquisition and information flow for a generic semiautomatic post and terminal adjustment system. Data are acquired by use of a star tracker, a planet tracker, and a ranging stadimeter.

The star-tracker and planet-tracker measurements of the planet and nearby star provide two sets of two-axis gimbal angle data. These data are related to a common reference frame and therefore can be used to compute the planet-star angles. This comparison will permit a simple calculation of the attitude of the vehicle-planet line of sight.

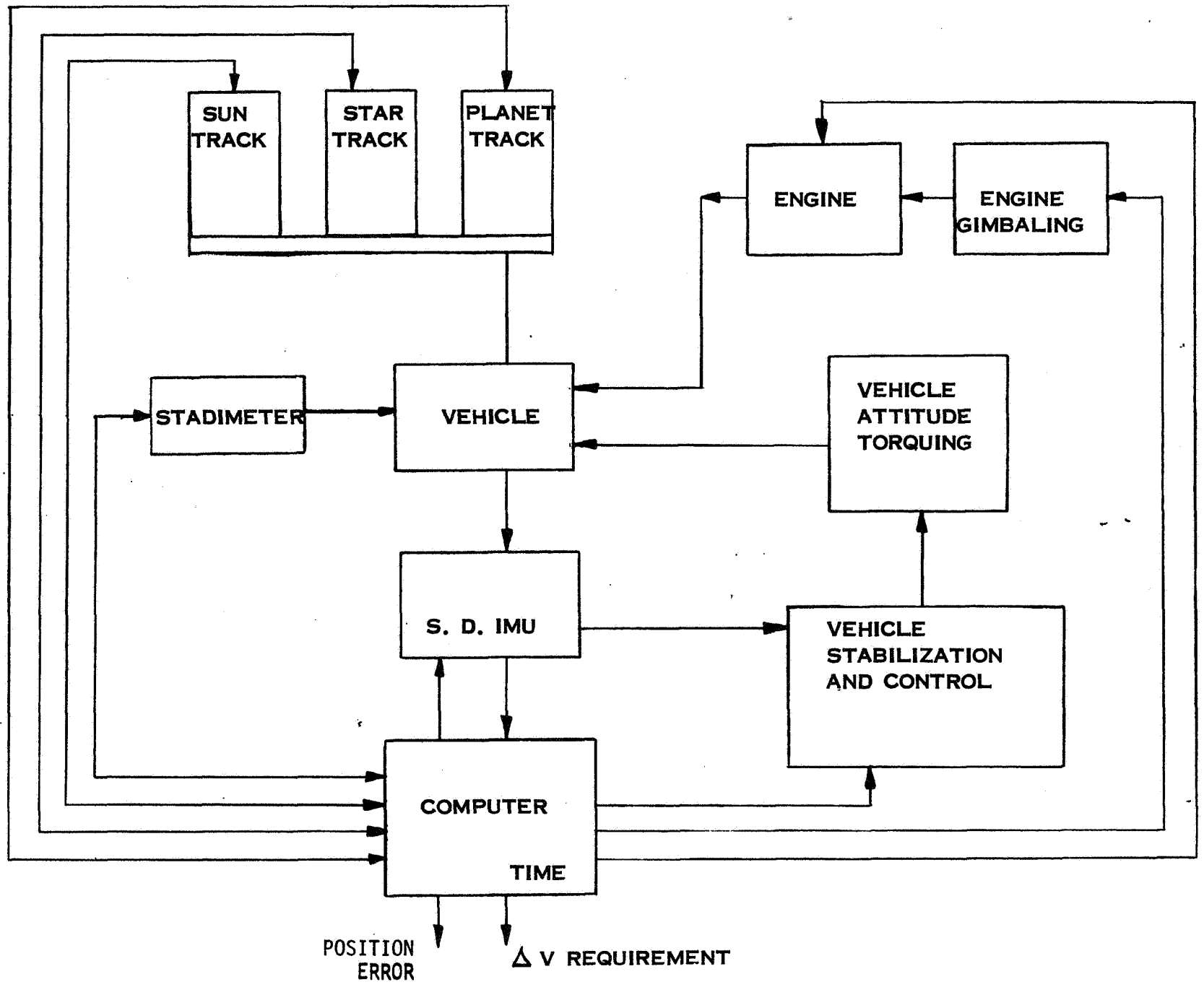

Figure 5-12. Semiautomatic Post and Terminal Adjustment

Vehicle-to-planet range information can be most accurately obtained from the injection trajectory computations. The stadimenter, however, can also be used to obtain range data. At departure and terminal adjustment ranges, the stadimeter is primarily making a planet-disc diameter measurement. Although a disc can be measured with extreme accuracy, the phenomenal limitations of measuring the angle subtended by the planet will result in large range errors. The addition of a sun tracker can supply sufficient data-acquisition capability to the star and planet trackers to allow for a solar-fix computation.

The sequence of principal operations for semiautomatic post and terminal adjustments is as follows:

1. Orient vehicle attitude to permit optical sensors to take position fix measurements.

2. Hold vehicle attitude stabilized by use of the SD IMU's gyros as part of a gimbaled servo loop. The loop consists of the SD IMU gyros, vehicle stabilization and control circuitry, and the vehicle attitude torquing hardware. Star-tracker data provide the inertial stabilization drift correction.

3. The computer commands optical track operations consisting of the sun track, two selected star tracks, and a planet and/or stadimeter track.

4. The computer computes vehicle position, vehicle-position error, and the requisite velocity increment for proper post or terminal course adjustment.

5. The computer commands the vehicle-attitude stabilization loop to the computed attitude for the course-correction engine firing.

6. The computer controls the engine firing time while the SD guidance and navigation system measures and controls the course-correction velocity impulse.

7. The navigation system commands engine cutoff when the desired course-correction velocity impulse has been achieved.

8. Repeat steps 1 through 4 at appropriate time intervals to check effect of course correction.

9. Compute impulse required for secondary course correction and compute desirability of initiating secondary course-correction impulse.

10. The semiautomatic instrumentation may also compute a trajectory correction by use of the planet-star comparison technique. For use of this technique, replace step 3 and 4 with step 3A and 4A.

3A. The computer commands optical track operations, consisting of a planet track, and track of adjacent elevation and azimuth stars.

4A. The computer computes the attitude of the planet-vehicle line, and the requisite velocity increment for proper post or terminal course adjustment.

5-12. Aided-Manual Post and Terminal Adjustment

Figure 5-13shows the data acquisition and information flow for a generic aided-manual post and terminal adjustment system. The data acquisition may totally consist of planet-star comprisons if range data are obtained by dead reckoning; the planet-star comparator is an instrument which permits the direct measurement of the angle between a planet and an adjacent star or stars. Selection of the comparison stars in, and normal to, the orbit plane will simplify the calculation of departure or arrival trajectory line-of-position errors (Figure 5-10).

The planet-star comparison may be made by a number of different techniques, including a vidicon, space sextant, "optical-wedge" comparator, photographic techniques, and a simple optical-screen presentation with a grid background. Several illustrative techniques are described in Section 6.

The inherent capability of obtaining high precision in a small-angle measurement makes the planet-star comparison technique attractive. Small-angle techniques for measuring mechanical rotations have been implemented to precisions in excess of 0.1 arc second (Razdow Midarm); this capability is based on the ability to divide accurately a given angle by a factor. Due to the smaller division factor required for small-angle measurements, these measurements have generally been simpler and more precise.

The sequence of principal operations for aided-manual post and terminal adjustment is as follows:

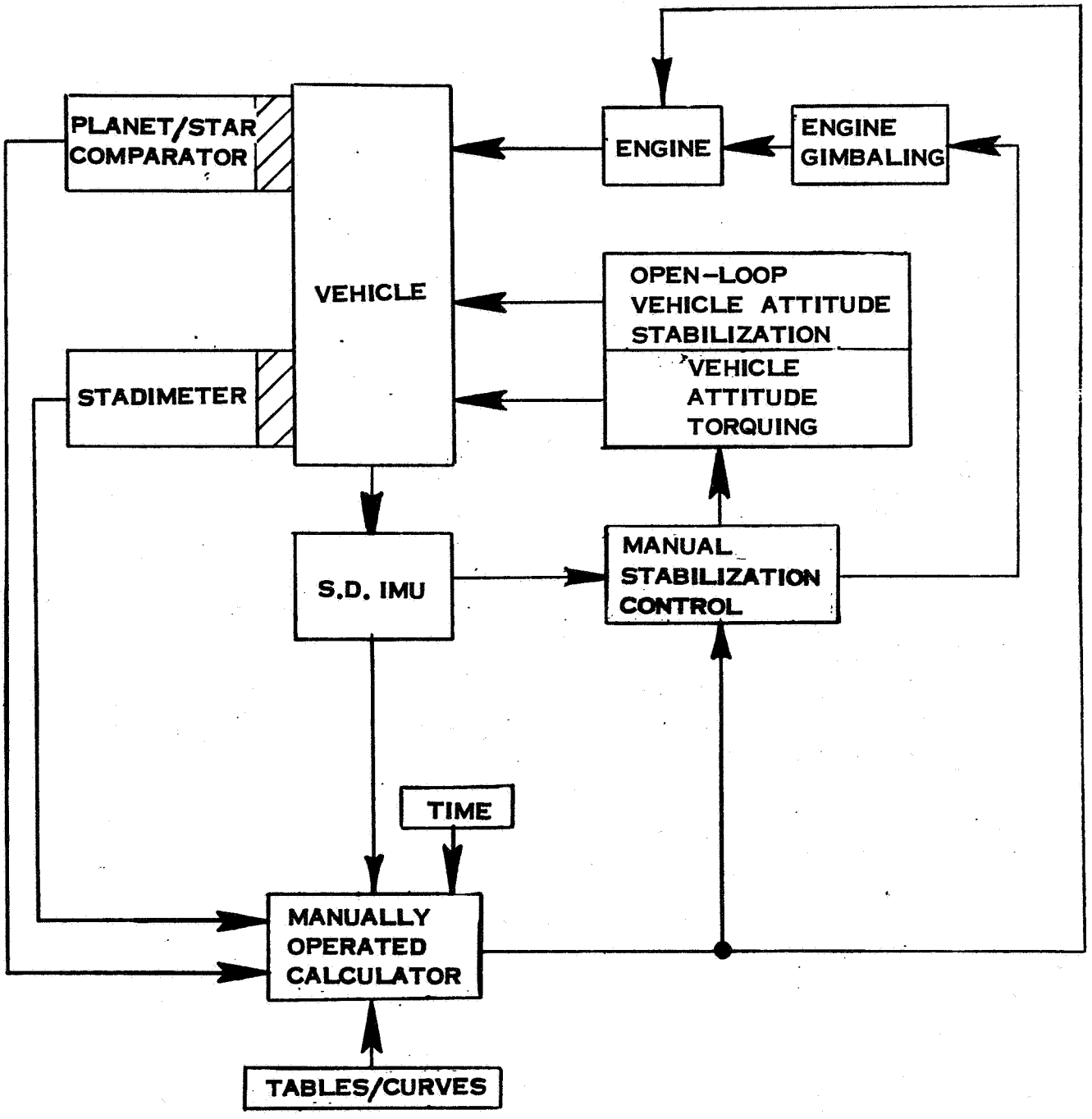

Figure 5-13. Aided-Manual Post and Terminal Adjustment

1. Manually control vehicle attitude torquing to place planet-star comparator in viewing position of the planet.

2. Maintain vehicle attitude by open-loop vehicle-attitude stabilization subsystem, and by intermittent manual vehicle attitude torque bias adjustments.

3. Crew members take a set of planet-star comparator measurements.

4. Calculate line-of-position and trajectory errors.

5. Compute post or terminal course adjustment ΔV.

6. Manually control vehicle attitude torquing to computed vehicle orientation for course correction engine firing.

7. Execute manual engine-ignition command executed.

8. Open-loop vehicle attitude stabilization coupled with manual control of vehicle attitude is utilized to maintain course-correction impulse attitude. The error signal for the manual attitude-control loop may be derived in a manner similar to that employed in the aided-manual injection stellar alignment.

9. Monitor in-line and normal velocity increments to minimize the normal component and to command engine cutoff when the computed course-correction ΔV has been attained. Manually controlled engine gimbaling and/or use of manually controlled multiple thrusters may be utilized in effecting the desired vehicle guidance.

10. Repeat steps 1 through 5 to determine whether or not any secondary course correction is required.

5-13. ORBIT ENTRY

Orbit entry may be attempted only after the terminal adjustments have accurately oriented the vehicle trajectory. With the predicted terminal trajectory established from the terminal-adjustment phase, orbit entry is essentially the reverse of the injection process described under heading 5-6.

Figures 5-7 and 4-10a are a three-dimensional and a plane view of the orbit-entry geometry, respectively. Orbit entry requires that the vehicle engine attitude be aligned with the computed ΔV attitude, and that the entry velocity impulse be applied at the proper range and/or range rate. Planetocentric position data may also be used to initiate the orbit-entry velocity impulse.

The vehicle engine attitude may be aligned to the proper orbit-entry attitude by use of a two-star reference. This reference can be used to generate an entry alignment error in a manner similar to the technique used to generate the injection alignment error (heading 5-6).

Range data may be readily supplied by an altimeter and/or a stadimeter.

Planetocentric position or latitude and longitude may be computed star-horizon measurements, as described under heading 5-1.

5-14. Semiautomatic Orbit Entry

Figure 5-14 shows the data acquisition and information flow for a semiautomatic orbit entry. The equipment utilized is the same as that required for a heliocentric injection.

The automatic horizon scanner and star tracker can provide sufficient data for a planetocentric position fix. This data, coupled with the altimeter for ranging and the set of star trackers for celestial attitude, provides complete sensory information for the initiation-orbit-entry guidance.

With the vehicle at the proper position and attitude, reverse thrust may be applied and the vehicle's automatic navigation-and-guidance system utilized to measure and control the precomputed orbit entry ΔV.

The two-axis star trackers track the celestial orbit entry attitude alignment stars to provide alignment-error data for the stabilization of the vehicle. The SD-IMU provides memory for the star-tracker alignment data.

The star trackers are also utilized with the horizon scanner to determine planetocentric position data. The utilization of the star trackers and horizon scanner is similar to that described under heading 5-1. The combination of planet range and range-rate data from the

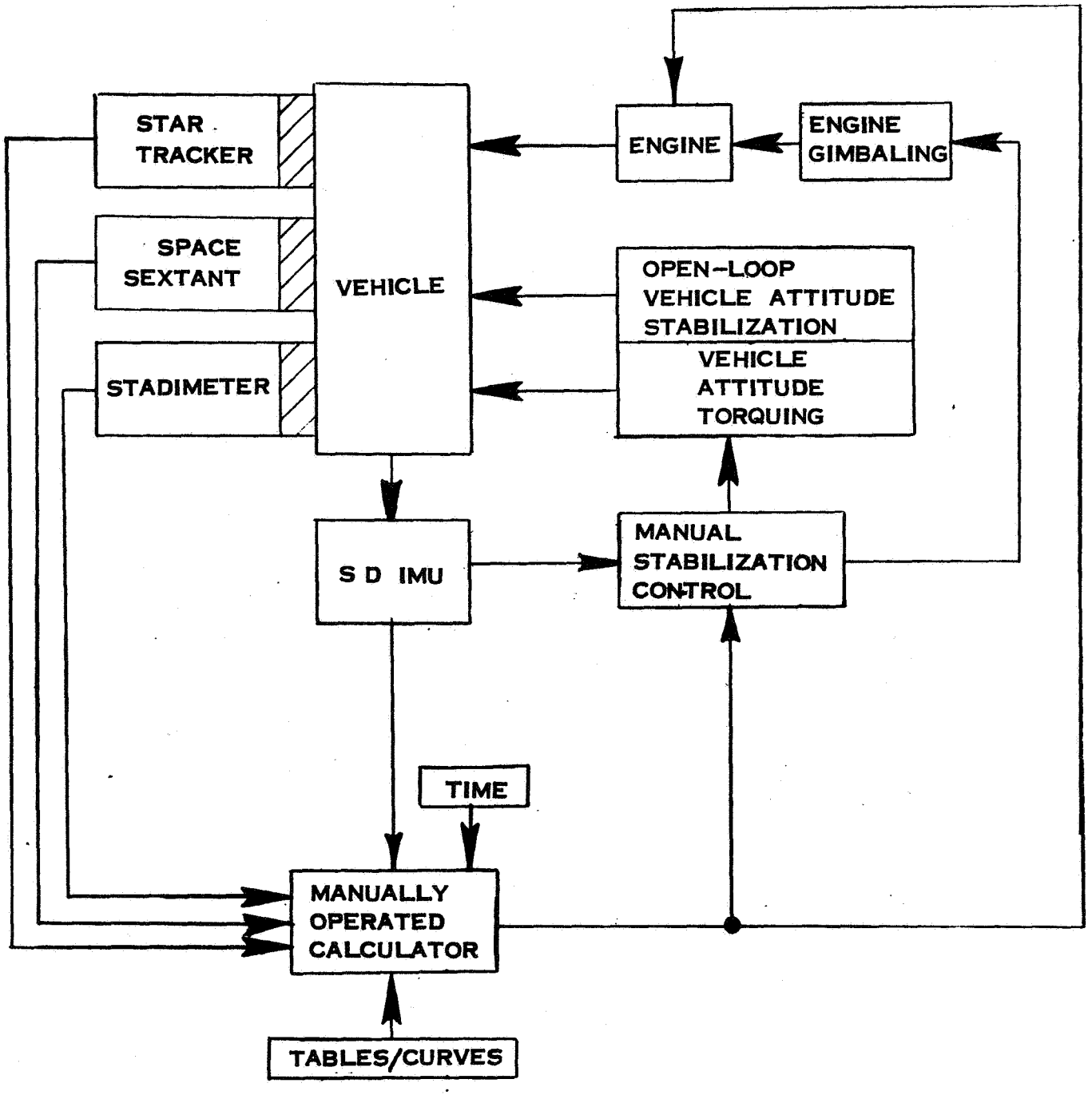

Figure 5-14. Aided-Manual Approach for Cis-Martian Injection

stadimeter provides an additional parameter of planetocentric information for the precise determination of engine ignition.

The sequence of principal operations for semiautomatic orbit entry is as follows:

1. The vehicle is stabilized in the precomputed attitude for proper orbit entry based on the terminal trajectory attitude calculations performed in the previous phase.

2. Vehicle attitude is held in stabilized mode by use of the SD IUM's attitude or rate reference, updated by the stellar alignment error display.

3. The computer commands operation of optical tracking, and navigation subsystems.

4. The optical-tracking operation consists of tracking the planet and an azimuth elevation star (equivalent to marine sextant measurement).

5. Altimeter subsystem activated to provide planet range and range-rate data.

6. The computer commands the automatic stabilization system to control the vehicle to the precomputed orbit-entry attitude.

7. Engine ignition is commanded when the measured range, range-rate and/or planetocentric position information are in agreement with the precomputed values for entry.

8. The vehicle's inertial guidance and navigation system is utilized to measure and control the orbit-entry impulse.

9. Engine cutoff is commanded when the strap-down navigation system has measured the requiste orbit-entry velocity impulse.

5-15. Aided-Manual Orbit Entry

Equipment for data acquisition and information flow for an aided-manual orbit-entry system are the same as those used for a heliocentric injection (Figure 5-4).

The space sextant and stadimeter supply the sensory data necessary for fixing planetocentric position. Vehicle attitude may be determined by taking a set of star sightings with the vehicle's inertial attitude-stabilization subysystem providing a short-term attitude memory.

The engine-burn portion of the orbit entry may utilize either an automatic or aided-manual mode of operation. As previously discussed in the section on injection, automatic operation is desired when high thrust levels are involved. This desirability, however, does not necessarily preclude the use of aided-manual guidance during the engine-burn portion of orbit entry.

The sequence of principal operations for aided-manual orbit entry is as follows:

1. The attitude of the vehicle is manually stabilized in the precomputed attitude for orbit entry.
2. Vehicle attitude held in desired preceding orientation (step 1) by star-sighting updating.
3. Crew members take sextant and stadimeter sightings.
4. Strapdown - IMU energized.
5. Engine ignition initiated at point where estimated planeto-centric position and range match precomputed entry corridor.
6. Automatic inertial navigation-and-guidance system controls vehicle during engine burn.
7. Engine cutoff executed when the strap-down navigation system measures the requisite orbit-entry velocity impulse.

5-16. STATION KEEPING

The station-keeping phase contains the following navigation and guidance operations:

Orbit determination, correction, and maintenance;

Mapping;

Excursion-vehicle calculations for descent or landing and launch;

Rendezvous; and

Injection calculations for return trip.

The orbit determination is similar to the orbit-determination phase of Section 5-1, except for the time involved and number of orbit-determination iterations. The time period covered in the Earth-orbit determination should be less than 1 day, while the Martian-orbit determination phase will last approximately 50 days.

The mapping function covers a detailed mapping of the planet's surface to evaluate further preliminary site selections for the excursion vehicle and whatever mapping may be required for scientific information. To ensure a high-quality mapping of the planet's surface, a precision pointing subsystem may be required for the camera; this problem was investigated by Lozins (1964). The report indicated that camera pointing could be achieved to a high degree of precision (2 to 10 arc seconds).

One configuration that may be considered in the planet-mapping operation is to use a body-mounted camera instead of a gimbaled mounted camera. The high inertia provided by the body-coupled camera will provide superior pointing performance for a given pointing bandwidth and disturbance torque level.

Determining the excursion-vehicle landing and launch trajectories is primarily an energy management problem. Navigation and guidance of a vehicle from one point to another can be optimally defined by advanced control theory energy management techniques. For the case under study, the points are a function of time with a common planetocentric reference frame.

The energy management technique will define specific optimized point-to-point trajectories for descent and launch, depending on the criteria to be satisfied. For example, it will be necessary to consider such variables as vehicle stress, vehicle acceleration limits, skin temperature, and fuel consumption in selecting a descent trajectory. These computations are complex and may require an on-board computer if the entire process is performed in orbit. It is quite likely, however, that, given a preselected landing point and a nominal Mars orbit, much of the computation can be performed on the Earth prior to the mission. The on-board process would then be reduced to a much simplified variational technique based on tables, charts, nomographs, and the like to account for deviations from the nominal orbit. Control of the actual descent and launch operations involves the excursion vehilce with its specialized systems and will not be treated in this study.

Rendezvous after station keeping is similar to the Earth rendezvous problem and will not be discussed here. Rendezvous should not impose any special problems for the Mars orbital phase that are significantly different from the Earth-orbit rendezvous.

The navigation and guidance for injection into the Venus-Earth return trajectory is similar to the cis-Martian injection calculation. The Venus-Earth injection calculations will be performed and updated to provide detailed injection navigation and guidance requirements throughout the station-keeping period.

SECTION 6
INSTRUMENTATION

In this section, the characteristics of sensors required to produce navigation data are discussed in detail. This discussion provides basic information on sensors required for the consideration and study of alternative navigation-system configurations.

The state of the art in navigation sensors is based largely on automatic approaches; this is reflected in the heavy emphasis on automation in the sensor systems described below. The mission under consideration, however, is manned, and the presence of a human crew provides an opportunity to use human skills and capabilities to reduce the complexity and enhance the reliability of essentially automatic sensor systems. In any of these activities, the crew can simplify equipment requirements by performing mode selection and sequencing, monitoring and acting as a link between systems.

It is meaningful to discuss these general crew functions in more detail only in the context of a specific configuration and this will be done during Phase II of the study. However, man can perform several functions with respect to specific sensor systems.

With respect to planet and sun trackers and horizon scanners, the crew can perform three functions which simplify navigation considerably: the crew can "fly" the vehicle to the correct attitude and then provide the necessary stabilization to keep the target bodies within the sensor field of view; the instrument operator can resolve the true null position, where there are secondary gradient null indications; and the operator can ensure that the instrument is operating and tracking properly.

With respect to star trackers, in addition to the functions described above, the operator can recognize patterns and identify stars; and, having brought the sensor to the correct orientation, he can ensure that the correct star is being tracked.

6-1. PLANET TRACKERS

The planet, or disk, tracker is related in function and mode of operation to the horizon scanner. The main difference is a somewhat artificial division based on the angular subtense of the planetary body. Horizon scanners may be thought of as those devices that work in the 20-to-180-degree angular subtend region, while planet trackers work at angles less than 20 degrees. The goal of either device is to find the direction to the geometric center of the planet.

Planet trackers can be separated into two general types. The first type depends on the planetary body radiating sufficient energy in the infrared region to make use of the total planet circumference, whether or not it is illuminated by sunlight. The second type depends on the sunlit crescent or gibbous phase. In either case, much of the recent work depends on the use of electronic image tubes. Using either the infrared image (full circumference) or visible-light image (crescent or gibbous phase), the positions of three points spaced along the outer circumference are sufficient to determine the center.

One lunar tracker, which uses visible light and mechanical edge scanning rather than complete imaging, is stated to have an accuracy of 20 seconds of arc. The instrument performs with a subtended lunar angle of between 0.5 and 9 degrees.

Another study on the use of electronic image tubes for planet tracking concluded that, with a 1000-line scan (regardless of tube type) and terrestial template matching on a monitor display, the center of Mars can be found within 8 arc seconds with Mars 2,000,000 miles distant. The angular subtense of the planet at this distance is 420 arc seconds. Similarly, it was concluded that the angular separation of the planet center and a nearby star could be determined to ± 0.029 degrees or $\pm$ 100 arc seconds.

Another method advocates a vehicle spinning with a known rotational velocity about an axis normal to the ecliptic plane with a rigidly mounted electro-optical telescope aboard. The telescope is made up of a lens, a focal plane containing slits parallel to the axis of rotation, and a photomultiplier that responds to the visible light signals passing through the slits. As the vehicle rotates, a time sequence of varying length pulses is obtained. The pulse is defined by the location of the celestial body along the azimuth and elevation directions, the angular subtense of the body, its state of terminator or edge definition, and the bias and spectral cutoff level of the photomultiplier. In a cislunar mission, the accuracy of finding a star position or the lunar center is quoted to be slightly greater than 5 seconds of arc, the larger part of the error being instrumental.

In a June 1966 study report on the Voyager mission, General Electric proposed the use of a single image tube, possibly the ABC image orthicon developed by General Electric. The television system will continually transmit a mosaic containing images of Canopus, the Sun, and Mars. Accuracy of navigational measurement is based on the least television line readout position on the tube. The error is expected to be in the region of 0.1 milliradian (20 arc seconds).

All planet trackers that employ television or related pickup tubes are limited by the least-resolution interval, usually one or several television lines, and the dynamic range limitation. Nevertheless, television image methods have many advantages. These are the possibilities for earth-bound readout, wide-field recording which might include the planet and several surrounding stars, and high sensitivity in any one of several spectral regions.

6-2. HORIZON SCANNERS

Horizon scanners are automatic tracking devices which operate as multiple elements of a larger system to provide data for the system that is used to obtain the direction to the center of a planetary body.

As an instrument class, horizon scanners usually include only those infrared devices used for maintaining the local vertical direction for orbiting satellites. The orbital mission precludes the use of any optical device which operates only in the visible region, because the vehicle passes periodically over completely dark regions. By necessity, the celestial body for which local vertical is being determined must have certain characteristics to ensure success: it must be warm enough that a detectable thermal discontinuity exists at the horizon; the discontinuity or gradient should be sharp; and the radiance should be reasonably uniform over the planet surface.

The accuracy with which the horizon can be determined depends on the steepness of the horizon gradient, which, in turn, is dependent on the atmospheric characteristics. The moon exhibits a near infinite gradient, although extreme terrain discontinuities near the horizon detract from the otherwise ideal horizon signal. The earth has its well-known atmospheric windows, but the signal also suffers degradations because of low energy or a very gradual gradient in the window regions. Less information is available on the horizon gradients of Mars and Venus. There are indications that the atmosphere of Mars is very tenuous and will therefore not diffuse the horizon significantly. Venus has a very dense atmosphere of unknown depth, but exhibits a well-defined top of the cloud deck. Consequently, fewer difficulties are to be expected in the horizon sensing for Mars and Venus than for the Earth or Moon.

Because planetary temperatures vary from 120 to 380^{o} K, the thermal detectors used must respond in the region of 8 to 40 microns. The use of the more sensitive photoconductors, such as zinc or copper-doped germanium, are not feasible for long space missions because of the requirement for maintaining the detectors at liquid-helium temperatures. Only thermal detectors, such as thermistor and metal bolometers and thermocouples, are suitable.

Horizon scanners can be grouped into three general categories:

1. Conical scan,
2. Edge tracking, and

3. Radiometric balance.

In the conical scan, a relatively small detector field is made to scan along the periphery of a large hollow cone; the mechanism of the scan is supplied by mechanically rotating optical prisms or mirrors. The cone may have an apex angle as large as 180 degrees, although 30 to 120 degrees is more common. Two such scanners with orthogonal or parallel scan axes provide two sets of pulses which are related to the dwell time of the detector field within the planet envelope. An analysis of the relative lengths of the two pulses, and the positions of the pulse leading and tracking edges within the scan cycle, provide for measurement of the pitch and roll attitude angles of the vehicle. The The mean length of the pulses can also be used to measure range or altitude.

Edge tracking provides more accuracy than the conical scan. An array of detectors, each with an optical dithering means, is pointed (with the aid of an auxiliary coarse pointing device) such that the direction of each member of the array can be oscillated locally across the edge of the planet. The arrayed elements are spaced evenly about the circumference of the body. Fine pointing involves the adjustment of the entire detector group direction such that the output signals from all detectors are the same.

The radiometric balance technique, which does not involve any scanning or moving parts, is the simplest of the three methods. In effect, the planet disk is imaged onto four detectors in quadrature. Comparison of the four signal levels indicates the direction of imbalance. Proper pointing of the detector with reference to the basic coordinate system provides the directional angles to the planet center.

The major limitations on the three methods are related to the chief data for the respective modes of operation. In the conical horizon scanner, it is the time definition of the planet pulse edges; in the edge tracker, it is also the definition of the pulse edges, but in addition there is a limitation due to the resolver readout accuracy; the limitations on the radiometric balance sensor are due to false

additive signals in each quadrant, such as unequal planetary temperatures, drift in the thermopile combination, or the sun in a portion of one quadrant. Table 6-1 defines accuracies of several horizon-scanner types for different planetary bodies.

6-3. SUN TRACKERS

Sun trackers, as self-contained, automatic devices for obtaining the line of sight to the sun, usually differ in their mode of operation from other trackers because of the vast difference in the target object itself. Because of the high solar irradiance supplied at the sensor, the solar disk need not be imaged in the usual sense. The simplest sun tracker, for instance, is a photocell whose output is proportional to the cosine of the angle of incidence of the sun's rays; these devices, manufactured by Ball Brothers Co., Inc., have demonstrated accuracies of 2 to 3 degrees. Limitation on the accuracy is that due to slowly varying cosine curve in the null region.

Other gated sensors indicate when the solar line of sight is in a selected direction. This is done, in effect, by allowing the sunlight to pass through a slit to a masked detector, where the masking configuration is related to the desired line of sight. Accuracy is stated by Adcole Corporation to vary from 0.25 to 5 degrees, depending on the total acquisition field of view.

Further refinements in the above Adcole Corporation approach have led to solar trackers with a digital readout of the solar angle. This is done by using digitally coded masking at the "focal plane" of this slit. The output is an absolute readout of the solar angle which is limited by the least significant bit in the encoded mask. Models are available which read to 1 and 0.5 degrees. One such device is capable of single-axis readout only. Because of its simplicity, complete two-axis readout is obtained by using two similar elements with orthogonal slits. Readout again is absolute, the least reading for each axis being 1 or 0.5 degrees.

Table 6-1. Summary of Horizon Sensor Accuracies

Horizon Sensor Type	Range of Accuracies Against Venus (degrees)	Range of Accuracies Against Earth (degrees)	Range of Accuracies Against Mars in First or Last Quarter Phase (degrees)	Range of Accuracies Against Moon in First or Last Quarter Phase (degrees)
Conical scan sensors				
a. Simple conical scanner	±0.1 to ±0.3	±0.2 to ±0.3	±0.3 to ±1	Requires elimination of trailing-edge error.
b. "Space-scan" conical scanner	±0.05 to ±0.1	< ±0.1	±0.1 to ±0.3	<±0.3
Edge tracker	±0.05 to ±0.1	±0.1 to ±0.3 (Atmospheric CO_2 band used)	Requires means for discrimination of true horizon edge from cloud edges.	Requires means for discrimination of true horizon edge from crator edge.
Radiometric balance sensor	±0.5 to +2	±0.5 to ±2	±3 to ±10	Not applicable except for very coarse pointing.

Although the least significant bit of the encoded mask defines the resolution of the output, resolution is also limited by the subtense of the solar disk at the point of measurement. If the solar direction is to be measured in the vicinity of the earth with one of these slit trackers, the slit must pass a 0.5 degree unfocused beam, which results in a resolution of about that magnitude in the readout.

The accuracy of the basic Adcole digital-slit and encoded-mask approach can be enhanced by using phase information in the output signal. The position of half the encoded mask of a typical one-axis tracker is changed such that the output signals from each half are in quadrature. The resultant phase of the signal can then be determined and an order of magnitude gained in accuracy. Solar angles have been measured to $\pm$ 0.06 degree.

Ball Brothers have also accomplished accuracies of $\pm$ 0.1 degree by using shaded mosaic arrays of solar "eyes".

Solar tracking capability at this time is of the 0.05 - to 0.1-degree order of accuracy, which is similar to that of other disk-tracker types. It is expected that at least an order of magnitude gain can be made by improving the electronic circuitry and by using imagining techniques and manual aid.

6-4. STAR TRACKERS

Star trackers are electro-optical instruments used in spacecraft to provide navigational and stabilization information. In current state-of-the-art devices, the information provided is the deviation between a predetermined line of sight and the actual line of sight formed by the spacecraft, the tracking star, and other reference targets. This information is in the form of an electrical signal which, upon exceeding a selected deviation, pulses small, cold-gas nozzles.

Star trackers utilize an objective mirror which collects and images to a point the impinging star irradiance. A modulator scans the image and encodes it into a usable form from which angular deviation

can be reduced. A radiation-sensitive detector then accepts the encoded information and transduces it into a usable electrical signal.

Photomultiplier tubes and image-dissector tubes are commonly used as the photodetector. If a photomultiplier tube is used, a mechanical modulator must be utilized. This is a scanning device usually utilizing either a spinning reticle or a vibrating slit with an assemblage of gears, cams, and other moving parts. When an image-dissector tube is used, modulation is accomplished using the small, electrostatically focused beam which, as part of the image dissector tube, electronically scans the photo-surface.

System characteristics for star trackers are usually described in terms of initial acquisition capability, detectable star magnitude, and output accuracies. Other important characteristics are size, weight, life, power consumption, and ruggedness.

The characteristics for several typical star trackers are listed in Table 6-2. The status of these trackers is either "flown" or "flight prototype". In general, the accuracies of the flown trackers are more realistic than the prototypes. The accuracies are mostly limited by the inherent noise of the photodetector and the limitations of the tracker field of view.

For a representative tracker, in which the photodetector is a photomultiplier tube, dark-current noise is 3.08608×10^{-9} amps. When a star is tracked, a change in signal current is produced as the star image is linearly displaced along an axis defined on the photocathode. When the ratio of signal current to dark current is one, the star image is displaced 0.0001288 inch, which is then the displacement error caused by noise. The angular error, which is the output error, is arrived at by dividing the displacement by the focal length of the collecting optics. For this example, the output error is 3.8 arc seconds.

The output error can be decreased by increasing the focal length. This change, however, is limited by the field-of-view requirements, since the field of view decreases as the focal length is increased. An

Table 6-2. Summary of Star-Tracker Characteristics

Identity	Manufacturer*	Scanned Field of View	Accuracy	Axes	Sensitivity (Star Magnitude)	Detector†	Size (inches)	Weight (lbs)	Power (watts)	Life	Status (12/31/65
OAO Startracker	Kollsman	1° x 1°	30"	2	+2	PM	11 x 17 x 16 + 11 x 16 x 4	23.6 + 18.5	17.5 + 10.0	1-yr mission	Flown
Canopus Tracker	Barnes Eng. Co. / JPL	5° x 11°	0.1° null	1	+2.3	ID	4 x 5 x 11	5	1.5	2.0 x 10^5 hr	Flown
Dual Mode Startracker	ITT	8° x 8° or 32'x32'	5" rms	2	+3	ID	5 x 10-1/2 x 5	9.5	8.0	-	Prototype
Sun/Star Sensor	Nortronics	30'	10"	2	+3	PM	105 cu in.	9	8.0	-	Prototype
Canopus Tracker	Santa Barbara Research Ctr.	±2° x 5°	0.1°	1	can. ±0.5	PM	-	4.9	-	2-week mission	Flown
NCN 121 Startracker	Nortronics	10 min.x 10 min.	2.8" x 1.0"	2	+3.5	VID	265 cu in.	9.5	12	1.8 x 10^3 hr	Prototype
OAO Back-up Startracker	Bendix Corp. / ITT	1° x 1°	9"	2	+2.5	ID	5-5/8 x 5-1/4 x 5-1/4	6	4.5	1-yr mission	Prototype

*JPL = Jet Propulsion Laboratories
ITT = International Telephone and Telegraph Corporation - Federal Laboratories

† PM = Photomultiplier tube
ID = Image dissector tube
VID = Vidicon tube

increased focal length will also result in a larger package. For example, a tracker with an accuracy of 10 seconds and field of view of 30 minutes can be housed in a 105-cubic-inch package, whereas a tracker with accuracy of 2.8 seconds and field of view of 10 minutes require a package of 265 cubic inches.

Field of view also is important in the initial-acquisition capability and the tracking-star selection. The initial acquisition is complicated when stars of similar magnitude are in the field of view. A tracking star with magnitude bright enough to be distinct in a limited field of view is desired. In a 1-degree field of view, one star is brighter in the field when a +8-magnitude star is chosen; this is large when compared to the 0.013 stars in the 1-degree field when a +4-magnitude star is chosen, or the 0.0014 stars in the field when a +3-magnitude star is chosen.

The tracking star, however, can be disqualified on the basis of signal level. The just-detectable star magnitude is a function of the sky background, the photodetector noise, and the aperture size of the collecting objective. If the sky background and photodetector noise are fixed, then for a particular star magnitude there is a unique aperture size which yields a photodetection signal-to-noise ratio of one. Taking sky background to be 1.2×10^{-15} watts/cm^{2}degree^2 (background outside the atmosphere), and considering the noise of the 1P21 photomultiplier tube, the aperture required to just detect a +2.5-magnitude star is 0.45 cm^2. When tracking a +5.0-magnitude star, the aperture required is 4.5 cm^2.

Increasing the aperture area to 78 cm^2 (10 cm diameter), the signal-to-noise ratio for a +2.5-magnitude star is approximately 150. As shown in Table 6-2, sensitivities (in star-magnitude units) range between +2.0 and +3.5. This is indicative of the good acquisition capability and the workable signal-to-noise ratios afforded by this magnitude range.

6-5. RADAR ALTIMETERS

An accurate measurement of altitude is required for controlling the parking orbit. Parking orbits are needed leaving the earth and also before landing on Mars. A nominal parking orbit may be considered to be at 500 nautical miles (approximately 1000 km) above the surface of either planet. To adjust the flight velocities effectively, it is desirable to measure the orbital altitude to a 1-percent accuracy.

Present-day radar altimeters have been designed to operate from aircraft altitude ranges to ground level with the extreme accuracy desired near ground level. However, it may be feasible by state-of-the-art techniques to design a satellite radar altimeter of the desired accuracy and range.

Radar altimeters are designed on the basis of measurement of the pulse echo delay in a pulsed-radar system, or measurement of frequency shift in a frequency-modulated, continuous-wave (FM-CW) radar system. The choice of system depends on the size and weight *versus* complexity tradeoff. Pulsed radars may be larger and heavier due to the peak powers required, but they are less complex; FM-CW radars are smaller and lighter, but more complex. The complexity factor affects reliability, so that consideration is usually given to both designs when design tradeoffs are made.

To obtain some insight into the complexity factor and size and weight factors, it is instructive to evaluate typical designs. For a bandwidth-limited, pulsed radar, the 3σ accuracy can be determined from the following relation:

$$\text{Range accuracy } (3\sigma) = \frac{c}{4BR\sqrt{S/N}}$$

where c is the speed of light, B is the power bandwidth, R is the range, and S/N is the signal power to noise power ratio. At a 1000-km range, a 20-db signal-to-noise ratio and an accuracy of 1 percent, the 3-db bandwidth is 1200 cycles per second.

The equivalent equation for the FM-CW radar is

$$\text{Range accuracy } (3\sigma) = \frac{c}{4R\Delta f}$$

where Δf is the frequency shift. For the same conditions, the frequency shift is 7500 cycles per second; thus, the FM-CW radar requires a much wider band system. HOwever, the average transmitter power required can be approximately the same for either system with the pulsed radar peak power being may times higher. It is estimated that approximately 10 watts average power would be required, provided that a low-noise-figure, high-sensitivity superheterodyne receiver is considered. Present FM-CW crystal-video radar altimeters operate at C-band with an average power of 1.5 watts at an altitude of 20,000 feet, with an antenna beamwidth of 60 degrees. Thus, with a superheterodyne and an antenna beamwidth of 2 degrees, the power required is only an order of magnitude higher, even though the range is between two and three orders of magnitude greater, and power increases as the fourth power of range.

If radar altimetry is employed beyond the 500-nm orbital range, its utility is limited by rapidly increasing required power, and by antenna-pointing accuracy. Therefore, at large range values, it is undesirable to depend on radar altimeters, since at these distances planet subtending systems are more effective.

6-6. MANUALLY OPERATED SENSORS

A series of navigation experiments carried out on the Gemini 4 and 7 flights (Jorris and Silva, 1966) have demonstrated man's ability to obtain accurate navigation data in space by means of a manually operated space sextant. The sextant is used for the same type of angular measurement provided by the automatic trackers described above. A second manual instrument, the stadimeter, can be used to obtain range information. Such instruments take maximum advantage of man's ability to recognize star patterns, and to identify individual stars. Perhaps the most important human skill which makes a manually operated sextant attractive when compared with an automatic system is the ability of a man, given

the proper visual information, to locate the center or edge of a planet disk. Man is capable of compensating for gibbous effects, ellipticity, and terrain irregularities, which are the limiting phenomenal factors in automatic planet trackers.

6-7. *Sextants*

All sextants operate on the principle illustrated in Figure 6-1. An undeviated line of sight to a reference feature, such as a planet marking, planet limb, or a star, is maintained by manual, gimbaled, or vehicle thrust correction. A second line of sight to another object, usually a star, is made through an adjustable mirror which is used to superimpose the second object image on the first. The amount of adjustment that is applied to the rotating mirror is a measure of the angular subtense between the two objects.

The ability to measure the angle between the two objects depends on several effects which have been evaluated on space simulators and the actual manned Gemini flights GT-4 and GT-7*.

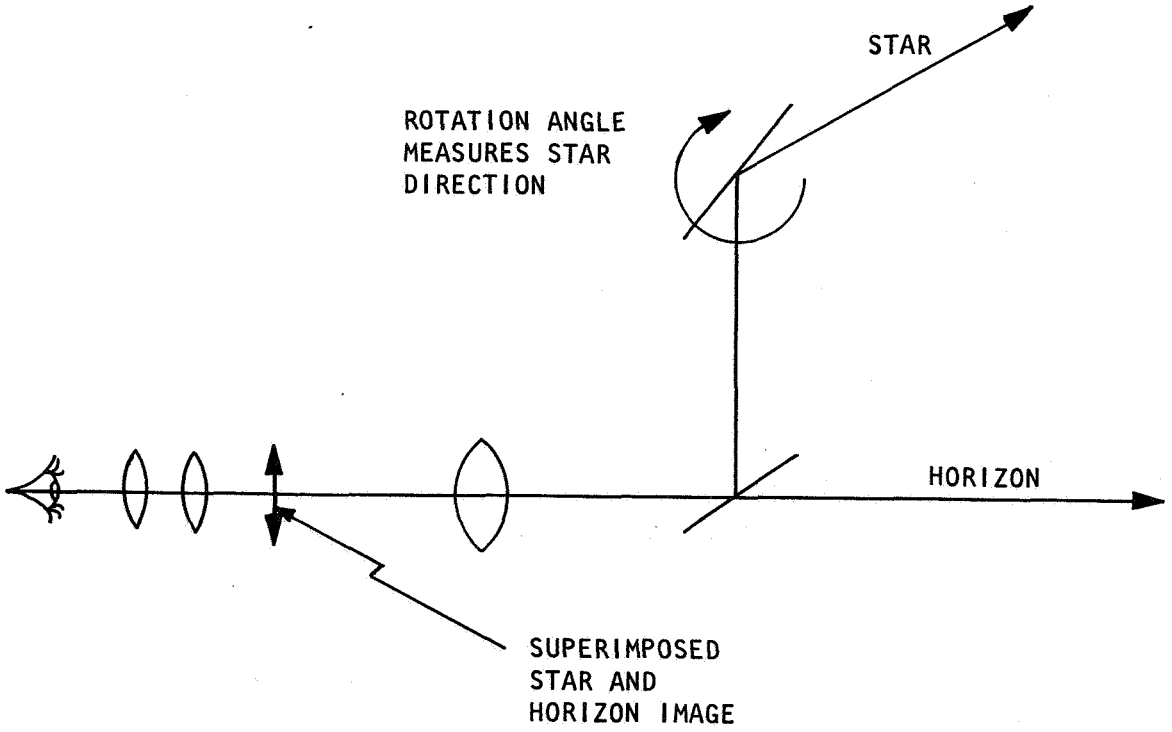

Figure 6-1. Celestial Sextant

Lampkin and Randle (1965) used the Ames Mid-course simulator to determine the accuracy with which observers can make star to star angle measurements using hand held and gimbaled sextants. After two weeks of training, observers were able to make star to star readings with standard deviations ranging from 15 to 30 are seconds depending on conditions. Increasing the yaw rate of the sighting station had no effect on sightings taken with a hand held sextant; but the repeatability of gimbaled sextant sightings decreased as yaw rate increased. However this apparent sensitivity of the gimbaled sextant to yaw rate was largely an artifact of the sextant mounting since at the extremes of the sighting station oscillation, the gimbaled sextant was out of the range of the columated beam eminating from the simulated stars. Although subjects indicated a slight preferrance for the gimbaled sextant it provided no consistant performance advantage. Both the hand-held and gimbaled sextant used in this part of the study had three power telescopes. It is possible that with higher levels of magnification the greater image stability provided by a gimbal mounting would have proved beneficial.

A second part of the study was devoted to sextant observation of real stars. The device used was the Plath Micrometer Sextant with three interchangeable telescopes providing magnification of 2.5, 4.0 and 6.0.X. The observers took with the three different telescopes and with and without a space helmet face shield. Performance was consistently worse and the shield in place. When the shield was not used the repeatability of the observation as measured by the standard deviation improved with increased telescope magnification.

Studies were also performed by Lampkin (1966) on the Ames Mid-course simulator to determine the ability of human subjects to measure the angle between a simulated star and a moving blinking light source. While this simulation was developed to represent a rendezvous sighting problem, aspects of it are relevant to the star to star sextant sighting task.

The sextant used was a modified Plath Marine Sextant with a six power telescope. The minimum vernier readout was six arc seconds. Three independent variables were studied: the flash rate of the signal light, the motion of the sighting station and the apparent angular rate of the target light. Since this review is concerned with star to star observations, the data summarized below is limited to that obtained under those conditions in which the target light was on steadily.

Under these conditions the standard deviations of sextant sightings ranged from about 18 to 25 arc seconds. The variable errors increased slightly as apparent target motion increased from 25 to 100 arc-seconds per second. Performance was also slightly better when the sighting station cab was stable than when it was oscillating at plus a minus 1° about the three rotational degrees of freedom. No hypothesis testing statistics were reported, however, it is likely that the effects of cabin and target motion were too small for statistical significance.

Constant errors of measurement were more strongly affected by the motion variables. Bias errors were larger by several arc-seconds when the cab was in motion than when it was static.

It was found that a navigator training technique which included immediate error feedback information significantly reduced the bias errors. In a second phase of the study subjects rated each of their individual measurements as good, bad, and undecided. When all bad and undecided rated measurements were eliminated, average bias error was reduced by approximately five seconds of arc.

Arken (1966) performed a study in which star to star and star to lunar limb sextant measurements were made from a CB-990 aircraft flying between 35,000 and 47,000 feet at night. Two sighting stations were installed in the aircraft. One station, incorporated a gimbal-mounted sextant, adjustable in roll, pitch and yaw. The second sighting station was designed to be used with hand held modified, space

rated D9 Air Force sextant. The gimbaled sextant had a ten power telescope and a 5° field of view permitting a readout to one arc second. The handheld D-9 sextant had a 4.5 power telescope and a 15 field of view. This sextant could be read to 3.6 seconds of arc. The sighting station windows were of optical quality glass. Observed angles were corrected for various sources of refraction error and distortion. The observation flights took place over the NASA high range and the true angles between the observation targets was based on radar obtained air craft position data and was accurate to within one second of arc.

With the handheld sextant, the average standard deviation of star to star observations was around 15 arc seconds and the average bias error between 0 and 15 arc seconds. With the gimbaled sextant the standard deviation of star to star measurements was considerable lower; the average standard deviation with the gimbled sextant was about 7½ arc seconds with bias errors close to 0. Star to near lunar limb standard deviations with the handheld sextant ranged between 15 and 20 arc seconds; with the gimbaled sextant the standard deviations were about 5 arc seconds less. Average bias areas ranged from 10 to 30 seconds with the handheld sextant and from 0 to 20 seconds with the gimbaled sextant.

There were considerable differences between subjects; however with the gimbaled sextant, the best subject was able to make star to star and star-lunar limb measurements with a standard deviation of well under 10 seconds. The results suggest that with a properly designed gimbaled sextant with high magnification, a trained observer can make both star to star and star planet sightings with bias errors and standard deviations of less than 10 arc seconds.

Duke and Jones (1964) performed a study of navigation sighting accuracy in a simulation of the Apollo mid-course navigation task. The sighting task required that the observers superimpose a simulated star and a simulated landmark by manipulating two hand controls. One

hand control moved only the star and thus simulated the sextant split image control; the other control simulated an attitude controller and was used to keep both the simulated star and the landmark in the sextant field of view. To determine the effect of spacecraft motion on sighting accuracy, several different rates of target motion ranging from 170 to 440 arc seconds per second were simulated. Two different levels of sextant magnification were used: 26-power and 40-power.

By an criterion, performance with either telescope was very good. Average bias errors and standard deviations were, for the most part, below 5 arc seconds. Performance deteriorated very slightly, perhaps by one or two arc seconds, at the higher spacecraft motion rate. Performance with the 40-power telescope was consistently better by one to two arc seconds than the 28-power telescope.

Observers were able to identify bad readings with better than chance accuracy and the authors suggest that some form of reject control is desirable in spacecraft apllications to allow the navigator to discard any questionable sightings. As in other studies in this field, it was found that observer performance increased with practice.

Jorris and Silva (1967) report the results of the sextant experiments conducted on the Gemini 4 and 7 flights. The purpose of the experiment was to determine the ability of astronauts to make the sextant sightings required for on-board orbital navigation. The authors concluded that, in general, the astronauts' performance indicated that it is feasible for man to make celestial sightings from a spacecraft. Astronauts were able to identify and use stars down to the 7th magnitude on the night side of the orbit. Light scatter on the observation window made it impossible for astronauts to observe stars on the day side of the earth. At night the green glow 5577-angstrom horizon and the natural earth horizon are available for measurements. However, the natural earth horizon is generally less well defined under the night lighting conditions. The star-to-star and star-to-horizon sextant angle measurements made by the astronauts were of sufficient accuracy to permit subsequent ground track computations which coincided very closely with tracking network

radar derived ground track data. It was concluded that astronauts are capable of consistent and accurate performance with a space sextant in an actual space environment.

It is clear from these findings that the accuracy of sextant readings is strongly dependent on the power of the sextant's telescope. In the absence of spacecraft vibration, or line of sight motion due to space-craft rotation, sextant readings to a fraction of an arc second would be possible. However, it can be anticipated that residual attitude rates will exist and that on-board machinery will produce some vibration. These factors limit the maximum feasible sextant magnification. Research is required to establish the motion and vibration environment of a spacecraft in freefall and to determine the effects of these disturbances on the ability of the astronauts to use sextants of various levels of magnification.

A second problem associated with very high power sextants is that the resulting field of view will be too small to accommodate many potential target pairs. One solution to this problem is to develop a sextant with two levels of magnification. An initial superimposition would be made with a low magnification lens with a large field of view. The observer would then select the higher magnification and complete the superimposition of the targets. To minimize image disturbances, induced by the unsteadiness of the observer, highpowered sextants should be gimble mounted.

Another important limiting factor in sextant reading accuracy is the optical distortion of the space-craft window. White (1967) performed a study to determine the line of sight deviations associated with various characteristics of space craft windows such as the angle of incidence between the viewer and the window, pressure loading, flatness and refraction effects. Irregularities in Gemini type space craft windows induced line of sight distortions as high as 180 seconds of arc. It was concluded that with

analytical and experimental means presently available an accurate map of the window induced line of sight deviations can be provided. Thus, it is entirely feasible to develop a system of window calibration for correcting optical measurements taken to a space craft window.

A second problem associated with space craft windows is the effect of light scatter in the windows on the visibility of stars. Gemini 4 and 7 astronauts observed that when the spacecraft was on the day side of the earth and sunlight fell on the observation window, the resulting light scatter in the window was such that the stars were not visible. One solution would be to limit the sextant observations to targets whose orientation with respect to the sun and the spacecraft windows as observation ports and to mount the sextant directly through the hull of the space craft.

In summary, the major findings of these studies were as followed:

1. *Star-star measurements give the greatest accuracy.* 20-arc-second accuracy was obtained using a hand-held sextant having a 4.5 power telescope, a 15-degree field of view, and a resolution of 3.6 arc seconds. Another experiment with the same type of sextant showed standard deviations of 10.5 arc seconds around a mean error of 7.5 seconds for the star-star, and 16.5 arc seconds about a mean of 20.5 seconds for a star-near planet limb measurement.

2. *Increasing the magnifying power of the telescope improves the accuracy.* The results of a simulated Apollo midcourse navigation problem has demonstrated errors having standard deviations of 1.5 to 3.0 arc seconds with mean errors of 3.0 and 6.0 seconds. The telescope powers were 28x and 40x as compared with 4.5x for the Gemini mission described above. The errors were also consistently smaller by 1 or 2 arc seconds with the 40x setting.

3. *Measurement between two objects of more nearly equally brightness improved accuracy.*

4. *Gimbaled sextant readings invariably show better results than hand-held readings.* However, the difference is not as great as one would suspect. For instance, with star-star readings, the hand-held sextant had a standard deviation of 10.5 seconds about a mean of 7.5 seconds, while the gimbaled sextant gave a standard deviation of 6.0 seconds about a mean of 5.0 seconds.

5. *Measurements made with simulated constant or sinusoidal vehicle angular rates showed higher repeatability than that for the random vehicle motions.*

6. *Performance varies greatly with operators.* In one experiment, the individual standard deviations varied from 10 to 100 arc seconds.

The results of these experiments indicate that man can use a space sextant to good advantage in an interplanetary mission. The sextant chosen for the job should have reasonably high magnifying power, possibly in the 6x to 50x range. It is desirable to mount the sextant in gimbals and possibly use remote control; however, satisfactory accuracy levels may be achieved with a properly designed hand-held instrument.

6-8. *Planet-Star Comparator*

The use of man as a functioning element in the navigation system permits consideration of a great variety of nonconventional instruments. Man has the ability, for instance, to recognize a particular star pattern at a glance. He can determine with some precision the position of the geometrical center of a planet in its crescent or gibbous phase. The same ability is evident in bringing a star image to the planet horizon, much as in terrestrial sextant fixes. He can detect quite accurately the very slight wobble of minutely decentered objects in a rotating field of view. All of these capabilities would require unusual complexity in instrumentation designed for the same task.

An example of the type of manual device that could be used for measuring the angle between a star and a planet center or edge is illustrated in Figure 6-2. This device, which may be regarded as an ultrasophisticated sextant, utilizes the convenience of a narrow field of view both for improved accuracy and practicality for observation through a narrow spacecraft window. Figure 6-2 shows an imaging objective lens in front of which a beamsplitter superposes two lines of sight. One line of sight passes straight through the beamsplitter toward the planet. The upper line of sight is directed by a Risley prism. By proper adjustment of the optical wedges about the optical axis, the star image can be made to appear at the center or edge of the planet image as shown. A readout of the two wedge angles will then furnish both the azimuth angle of the star relative to any assigned direction on the face of the planet image, and the total angle between the star and planet center or edge. The duplication of the star line-of-sight deviator indicates that two or more stars can be included simultaneously in the celestial fix.

It has been mentioned that the human operator is very sensitive to the wobbling motion associated with a slightly decentered rotating object. The effect has been used, for instance, in truing up work in a lathe or in centering and edging optical elements. Provision can also be made in this device for such capability. A Dove prism is shown immediately in front of the objective lens. It is intended that the man rotate the prism manually or with a variable-speed motor, as needed, to rotate the field of view. With the Dove prism at the position shown, all objects in the field of view will rotate together. If either the stars or planet are slightly off-center, the wobble will be quite noticeable and corrective measures can be taken.

The planet image in its gibbous or crescent phase will exhibit wobble or flickering under all conditions. Rather than eliminate wobble, the object of the rotation is to adjust the telescope line of sight to the planet such that the *smallest diameter* blurred disk is seen. The planet is then rotating about its geometric center and its circumference will exhibit a very sharp unwavering outline against black space.

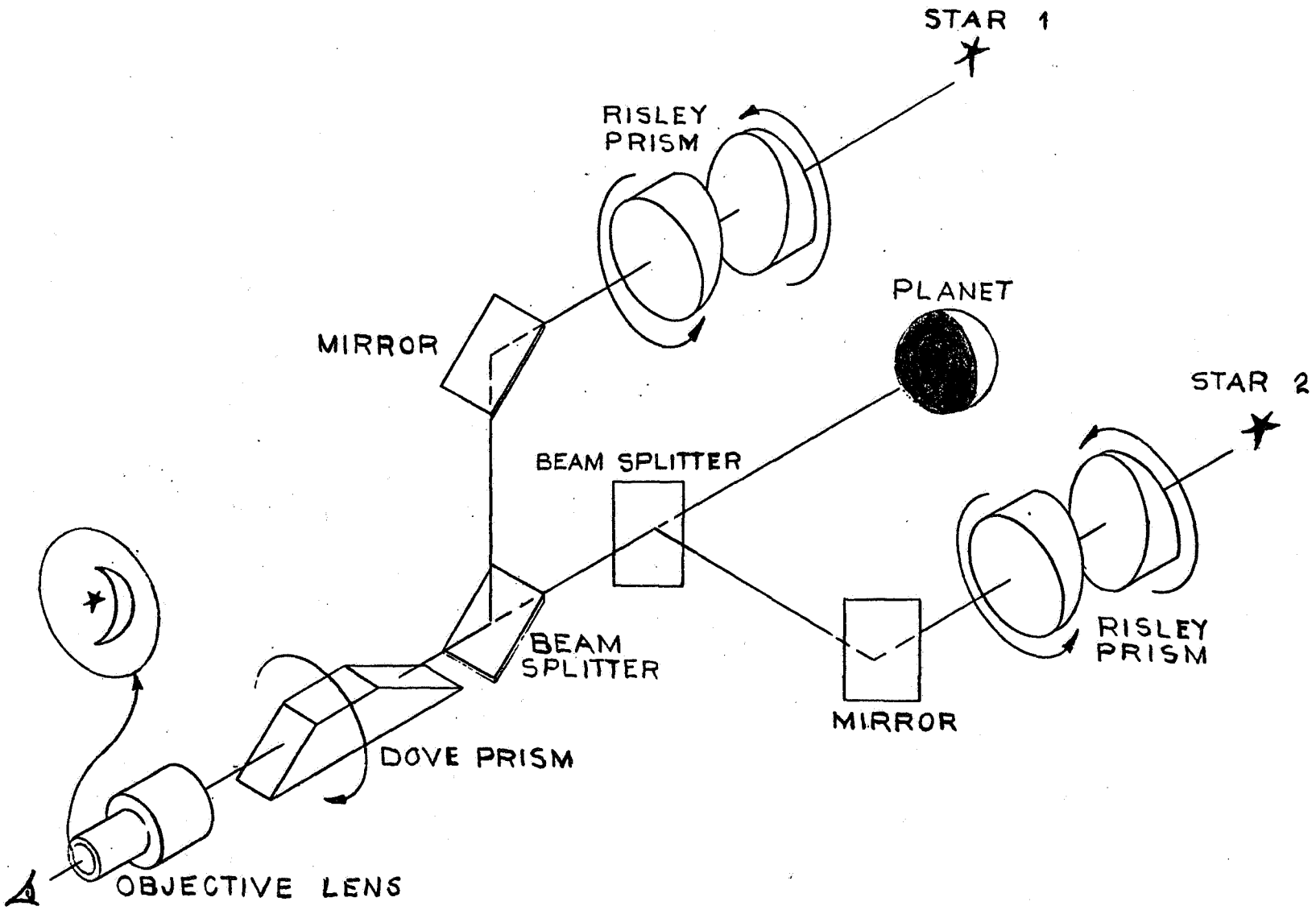

Figure 6-2. Planet-Star Comparator

Although man's capabilities for such activities as locating the center of a circle, wobble detection, constructing right angles unassisted, and so forth, have not been studied extensively, estimates can be made of his accuracy. An experiment with a hand-held space sextant has demonstrated an accuracy of 18 arc seconds. The truing up of a lens element in a centering and edging machine by unassisted observation of the wobbling of a reflected light image at the lens surface can be shown to be accurate to several seconds. A very sensitive test for the accuracy of the 90-degree roof angle on Amici prisms is to study the reflected image of the observer's own pupil, where a very few arc seconds of error results in a cat's eye or a doubled pupil appearance, depending on the direction of the error.

6-9. *Stadimeter*

The hand-held stadimeter optically determines range from a spacecraft to Earth, Moon, or other neighboring planetary bodies. The instrument determines range as a function of the measured curvature of the portion of horizon viewed through a sight-angle-limited flat viewing window of the spacecraft. By optically measuring the angle between two chords through three equidistantly spaced points on the horizon, the stadimeter determines the curvature of a limited region of the viewed horizon.

Three 14-degree portions of the horizon are viewed. These portions, separated by 45 degrees, and centered around the intersection of the chords with the horizon, are superimposed utilizing a pair of special deviation prisms. Rotation of one prism relative to the other results in the intersection of the three horizon sections. The rotational angle is related to the orbital altitude through a mathematical relationship or auxillary graphs. The general characteristics of a stadimeter manufactured by Kollsman Instrument Co. for the Air Force are listed in Table 6-3.

Table 6-3. General Characteristics of a Stadimeter

Characteristics	1-Inch Focal-Length Eyepiece	2-Inch Focal-Length Eyepiece
Size (L x W x H) in inches	$6\frac{57}{54} \times 6\frac{7}{32} \times 5\frac{17}{32}$	$7\frac{17}{64} \times 6\frac{7}{32} \times 5\frac{17}{32}$
Weight	8 lb, 3 oz	8 lb, 8 oz
Magnification	4.5X	2.25X
Field of view (degrees)	14	14
Exit pupil (mm)	7	14
Eye relief (mm)	19	74
Diopter adjustment	-3 to +4	-2 to +2
Resolution (seconds)	10	10
Image	Erect	Erect
Range (degrees)	-1 to 21	-1 to 21

6-10. *Photographic Approaches*

An alternative to real-time optical measurements can be provided by a photographic system. The advantages of such a system are that stabilization requirements are far less stringent; measurements are made more carefully; background stars provide for self-calibration of each photograph; and, given batch-processing of photographs, a series of navigational sightings can be made in less time than would be required for an equal number of direct sightings.

Havill (1963) describes a photographic technique to provide navigation data for midcourse corrections. While Havill's technique is designed to obtain distances and line-of-sight angles to the Earth from a Moon-Earth trajectory, the measurement techniques are generally applicable to near-body navigation procedures.

Havill's technique involves taking a series of photographs of a near celestial body with two stars of known angular separation in the background. Using the stars for calibrations, the distance to the body is obtained by measuring the diameter of the image. The line-of-sight angle traversed in successive images is obtained by superimposing the background stars and measuring the center-to-center distance between two successive images. In Havill's study, the near body was the Earth; given the time between successive images, the angular separation of the background stars on the celestial sphere, and the diameter of the Earth, the trajectory parameters can be computed.

To evaluate the accuracy limitations of this procedure, a series of tests was conducted in which subjects performed the measurements on photographic images of disks tilted so as to correspond to the Earth's ellipticity as seen from various points in space.

Two devices provided accurate measurement of the photographic images: a transparent overlay with accurately inscribed circles, and a small 30-power shop microscope. The inscribed circles on the transparent overlay were drawn with a radial separation of 0.1 inch and a line weight of about 0.002 inch. The smallest division of the shop microscope was 0.001 inch, and it could be read to about half this distance. A 1/32-inch hole was drilled at the common center of the circles inscribed on the overlay and a sharp tool which fit tightly into this hole marked the photographic image at its center.

The maximum error in measurement of disk diameter was 0.0029 inch or 0.035 percent of the disk's diameter. Maximum center-to-center error was 0.25 percent of the diameter; at the ranges simulated in the study, these figures correspond to angular errors of about 2 and 7 arc seconds, respectively. The time required to perform each measurement was about 10 minutes, and the time to perform the required calculations to obtain orbital elements was about 15 minutes.

Havill concludes that the technique studied could provide a basis for an adequate navigation system. He points out that a system of tables and nomographs could be employed to reduce the number of calculations required.

6-11. ATTITUDE CONTROL

Attitude control must be exercised at two points in a navigation-and-guidance sequence: (1) to permit navigational observations to be made, the vehicle must be brought to and stabilized at an attitude which maintains the target objects within the sensor field of view; and (2) for thrusting, the vehicle must be brought to and stabilized at some precomputed attitude to ensure the correct thrust angle throughout the thrust period. The required attitude control may be accomplished by the crew in several ways.

If an IMU is available, the pilot can simply "dial" the desired attitudes into the IMU in terms of the inertial coordinates. The IMU would then simply slew the vehicle to that attitude and provide the necessary stabilization.

However, given the presence of a human pilot, the attitude-control system can be simplified by having the pilot fly the craft to the appropriate attitude. This can be accomplished by providing the pilot with an optical display of the necessary visual information. Pointing data for thrusting or observation would be given in the form of two angles along and normal to the line between two reference stars. An example of how such an instrument might work is as follows.

The geometrical information required to fix the point could be fed into the display by having the pilot maneuver the spacecraft so as to place both reference stars on a horizonal crosshair, with one star at the center of the reticule. Dialing in the two angles, horizontal with respect of the star in the center, and normal to the horizonal line would geometrically fix the thrust orientation point on the display, and would optically drive one of the two reference stars to that point. The pilot's task would then be to maneuver and maintain the reference star in the center of the display by means of a crosshair sight. Given a very low gain mode in the manual attitude control system, a human pilot could provide the alignment with a very high degree of accuracy, eliminating the need for a star tracker. At this point, having accurately

aligned the vehicle, the pilot could select an automatic stabilization mode to maintain the correct attitude during the thrust period.

Alternatively, stabilization during thrust could be provided by the pilot by controlling attitude directly with reference to the display described above. For small, low-thrust corrections, this seems feasible. However, large thrust corrections are likely to produce attitude rates and noise of a magnitude and frequency beyond the ability of a human operator to control.

6-12. VELOCITY-INCREMENT MEASUREMENT

In the execution of necessary enroute trajectory corrections, some incremental velocity is generally applied to spacecraft. The measurement philosophy associated with this correction can be of the open-loop tracking type, or, in various degrees of complexity, a true on-board measuring system. If the thrust source is of a very low value, the trend would be toward an open-loop system, in which the correction is made by controlling the engine on time; the effect is then determined by using the basic navigation system to redetermine the new trajectory. With higher thrust levels, however, a direct velocity-increment measurement would be required.

An inertial measurement unit capable of providing the needed instrumentation could be employed in either a gimbaled or strap-down configuration. If a strap-down angular measurement system were used for attitude stabilization, the same gyros could be used as a measurement system with the addition of an accelerometer triad. Three accelerometers mounted to the same substructure as the gyros with parallel aligned input axes result in a simple configuration. When this approach is used, the ΔV thrust is converted into a stabilized computational reference frame. The reference frame is computed from the base rotation data as measured by the gyros. The accelerometer data are then rotated into the stabilized computation frame, so that velocity increments can be computed in a fixed inertial reference frame.

Because strap-down inertial navigation techniques are mechanically simple, good reliability may be expected over the comparatively long Mars mission time. To improve reliability, a grouping of six SD IMUs, together with appropriate spares, could be considered.

A gimbaled IMU might be considered as a means of supplying vehicle-attitude data and velocity-increment measurements. The gimbaled IMU differs primarily from the strap-down unit in that the accelerometers are maintained in a physical inertial-measurement frame by a set of three or four gimbals and associated torquers. Although this configuration provides better inertial reference drift performance, because the gyros operate at a null, the gimbaling mechanization and readout equipment are mechanically complex. Reliability estimates indicate strap-down performance may be thousands of hours, while gimbaled performance is limited to hundreds of hours.

SECTION 7
MANUAL NAVIGATION

7-1. CREW SIZE AND WORKLOAD CONSIDERATIONS

Before assigning specific navigation roles to crew members, it is first necessary to determine how much crew time will be available for navigation and guidance functions in each phase of the mission. It should be noted, however, than an exhaustive phase-by-phase task analysis is not required as it is beyond the scope of this paper to develop a completely integrated and optimized crew subsystem. For the purposes of the present study, the work load analysis need only go far enough in each phase to indicate whether or not there is crew time available for the performance of navigation and guidance functions. The first step in the analysis is to specify the total pool of available man-hours, that is, the crew size.

In ground based man-machine systems, where there are no significant restrictions on crew size, the number of operators employed is determined by the requirements of the system. In manned space vehicles, however, to a large extent it is crew size that determines the nature of man-machine subsystems. The system costs associated with an increase in crew size are so large that in most cases it is highly unlikely that anything is to be gained by replacing hardware with an additional crew member. Crew size is thus determined by the nature and purpose of the mission, mission duration, reliability considerations, and other considerations of larger scope than those used in the optimization of individual subsystems. In the Apollo mission, for example, the requirement for a three man crew stems largely from the need to split the crew during the lunar excursion phase: one man must remain in orbit to monitor and provide a backup function in the orbiting vehicle while prudence dictates a minimum of two men for the surface excursion. Thus, the operational requirements of a single phase dictate the crew size for the entire Apollo mission.

Similar considerations provide a preliminary basis for determining crew size in the present Mars mission. It appears almost certain that

the Mars excursion will impose a greater operational load on the crew than any other phase in the mission; thus, the manning requirements of the Mars excursion phase will dictate the crew size for the entire Mission. At the time of the Mars surface excursion, part of the crew stays on board the orbiting Command Model (COM) while the excursion team descends to the surface of the planet. The Ares study specifies a six-man crew; three for the surface excursion and three to reamin behind on the orbiting vehicle. Considering the relatively long stay on the surface (30 to 40 days) a three-man COM team is a reasonable minimum size assuming the following conditions.

(1). The COM crew is on 24-hour communications/alert throughout the excursion phase with the excursion team, i.e. the COM crew must be ready to execute abort procedures at all times.

(2). The condition of the COM is actively monitored on a 24-hour basis. This includes station keeping functions as well as subsystem monitoring.

(3). Updated abort navigation data must be continuously available.

(4). A certain amount of crew time must be set aside for scheduled preventative maintenance and unscheduled emergency maintenance.

(5). The nominal length of stay on the surface can be up to 40 days.

Over a 40-day period a work/rest ratio of 1.0 is the maximum consistent with the maintenance of alertness, accuracy and reliability. On this basis a two man crew is capable of supplying 24 man-hours per day of duty time. This does provide continuous coverage but any time spent in non-monitoring tasks such as maintenance or scientific observation is at the expense of monitoring and hence detrimental to reliability and responsiveness of the vehicle. Further, and perhaps most important, in view of the length of the mission, a two-man crew provides very little mutual backup capability. For example, in two of the Gemini missions the result of relatively minor "emergencies" was an overloaded crew and the abandonment of several important experiments.

A three-man crew, on the other hand, can supply 1.5 men on a continuous basis, (i.e. 36 duty man-hours per 24-hour period). This is

sufficient to provide continuous monitoring coverage plus 12 man-hours per day of non-monitoring tasks. Further, three men can provide considerably more mutual support and backup than two. Hence, on the basis of the above assumptions, it is felt that a minimum of three men is required to man the COM during the excursion phase.

The size of the excursion team follows directly from two assumptions:

1. A team member never goes out alone in any surface exploration.
2. The surface vehicle is always manned to provide a continuous communication link with the orbiting vehicle and to insure continuous readiness.

These requirements yield a minimum Mars excursion team size of three men. Admittedly, the team's size arrived at above follow from a set of relatively hard assumptions about Mars excursion-phase operations. However, even if these assumptions were relaxed somewhat, the need for a strong backup capability remains. For example, suppose it were decided that five men represented a sufficient but minimum crew. The probability that one of these men would suffer a significant physical disability in the 280 to 290 days prior to Earth return can be considered dangerously high. Thus, in view of the length of the mission the redundancy afforded by at least one additional crew member would be highly desirable. The criticality of the Mars excursion phase with respect to crew size argues against a Venus flyby on the outbound leg since this can lengthen the outbound trip considerably, depending on the launch date.

On the basis of the above analysis, it appears that the operational requirements of the Mars excursion phase, plus the need for some redundancy in the crew, dictate a crew of six men. As it is highly unlikely that the manpower requirements of any other mission phase will exceed this figure, a six man crew will be assumed for the mission. However, it will be assumed that the sixth man is redundant, i.e., that all non-navigation tasks critical to mission success must be performed by five men with the sixth man acting as backup.

On the assumption of a six-man crew, each mission phase was evaluated to determine the manpower available for navigation and guidance functions. On the basis of in house studies at General Electric, it

was determined that for the major portion of the mission, the inbound and outbound legs, critical activities, including subsystem and vehicle status monitoring, scheduled maintenance, physical subsystem checkout and regular extravehicular inspection would require 36 man-hours per day as an upper limit. It was assumed that each man will be scheduled for duty for 10 hours per day. This means, of course, that during steady state flight the crew is, if anything, underloaded, and that over 12 man-hours per day is available for navigation and guidance functions. In fact, the analysis identified only four periods during the mission when critical task peak loading becomes severe. These are

1. Checkout and activation of the Mars vehicle after Earth orbit rendezvous at the beginning of the mission;
2. Checkout of and activation of the MEM prior to the Mars surface excursion;
3. The excursion phase; and
4. Checkout of the Earth landing module prior to re-entry.

The three phases involving checkout and activation of a major vehicle system are somewhat critical as regards task loading. This is especially true of the Main Vehicle checkout as prudence dictates that each subsystem be checked out very thoroughly before leaving Earth orbit. However, during such peak activity phases, five men are capable of supplying as much as 80 man-hours per day for several days, i.e., 6 to 12 man-hours per day could be made available for navigation and guidance functions. Further, unless the navigation and guidance tasks are of such a nature that they impose a continuous load, there is no reason why they cannot be scheduled for before and after periods of peak checkout activity. The problem becomes severe only when continuous crititical task high-activity periods coincide with continuous navigation periods.

The problem is more severe during the Mars excursion phase precisely because of a need for more or less continuous navigation functioning, dictated by abort readiness requirements, while at the same time a high degree of systems alertness and reliability must be maintained. Orbital parameters and MEM launch data must be updated frequently to maintain the capability for rapid reaction to emergencies. Just how critical the

situation is will depend on the amount of time required to generate this information. If it turns out that a significant amount of time is required for navigation, then it will be necessary to perform a detailed task analysis of the crew activities in the COM during the Excursion phase to determine with some degree of precision the time available for navigation.

On the basis of the foregoing, it is concluded that the task load imposed by non-navigation and guidance functions are problematical only during the Mars excursion phase. At all other times a five-man duty schedule is capable of supplying as much as 12 man-hours per day for navigation and guidance functions; thus, ample time is available for navigational observations. Jorris and Silva (1966) and Weber (1966) reported that experience both in the Gemini 6,7, and 10 missions and in simulator studies indicates that complete and accurate orbital parameters could be determined by a single crew member in less than 30 minutes. The procedure was entirely manual, employing hand-held sextant and stadiometer, and using tables in conjunction with minimal calculations performed on a slide rule. An acceptably accurate "quick look" estimate of apogee, perigee, and period could be made in less than 2 minutes. Clearly, the time required to make a single set of observations and to perform the necessary calculations to determine trajectory is well within the time available. The problem arises, however, from the necessity of making repeated observations. The accuracy of the observations made by the Gemini pilots was sufficient for orbital parameter determination. However, the accuracies required for ejection into the midcourse trajectory, midcourse correction, and injection into planetary orbit are greater than for orbital parameter determination. Thus, it is likely that a manual system will require repeated observations with averaging to obtain sufficient accuracy. Depending on the required frequency of the observations, the time required to perform the observations and to implement an optimal averaging scheme may become prohibitive if a purely manual system is employed. This problem will be considered in detail as part of the evaluation of alternate manual concepts.

7-2. OPERATIONAL DESCRIPTION

This section contains a detailed narrative description of the crew functions in navigation and guidance. The purpose of this narrative is to set forth in an organized, coherent way, a detailed operational account of a minimum manual navigation-and-guidance system. The narrative will serve as the basis for developing a detailed time line task analysis. Four mission phases are considered: earth-orbit determination and correction; injection into Mars orbit; post and terminal Mars trajectory adjustments; and Mars orbit entry. In each phase, the narrative will describe the crew roles in navigational observation, data processing, and the control of guidance maneuvers.

7-3. Phase 1. Earth-Orbit Determination and Correction

7-4. Navigational Observations

Summary. Two sets of observations are required for orbit determination. Orbit size and shape are determined by altitude measurements, while star-horizon angle measurements are required to fix the plane of the orbit and to determine the position of the vehicle in the orbit as a function of time.

Equipment Requirements. A gimbal mounted stadimeter and two gimbal-mounted sextants are used respectively to obtain altitude and star-horizon angle measurements. The sextant permits selection between at least two levels of magnification. Both the sextant and the stadimeter have a "mark" feature. When the astronaut is certain of his reading he depresses the "mark" button, which locks the last reading in place and also displays the time of the last reading. Both instruments incorporate a clock which can be synchronized with the vehicle master clock. The stadimeter and one sextant are mounted on gimbled brackets at an observation port. When not in use the instruments are stowed. The other sextant is mounted in front of a second observation port so situated with respect to the first port that simultaneous observation of stars 90 degrees apart is possible.

Given the duration of the mission, some form of automatic attitude stabilization is assumed to relieve the astronauts of the burden of maintaining attitude control throughout the mission. This feature provides vehicle line-of-sight stabilization during navigation observations. A strap-down IMU provides the attitude sensing and a torque wheel system provides the torque required to maintain the vehicle at the attitude established manually by the pilot. To hold the vehicle in a specific alignment, the pilot first establishes the desired alignment manually using a two-axis hand controller (pitch and yaw) and rudder pedals (roll). When the vehicle has been manually stabilized at the desired attitude, the pilot selects the hold mode of the attitude-control system.

A microfilm table is used to determine which star pairs will be in position for viewing at various times in the orbit so that sextant observation periods can be scheduled. Microfilmed star charts are used as an aid in located and identifying specific stars.

Procedure. The sextants and stadimeters are unstowed and set up on their gimbled mounts at the observation ports. The stadimeter and sextant clocks are manually synchronized with the vehicle clock as follows. The navigator sets the instrument clock to an even time increment some tens of seconds ahead of the master clock whose output is displayed at the navigators station. When the master clock reaches the time set into the instrument the instrument clock start button is depressed, and the two clocks are synchronized.

When the navigator indicates to the pilot that he is ready to begin taking stadimeter observations the pilot maneuvers the vehicle to bring the earth horizon into the stadimeter field of view. The pilot then places the attitude-control system on attitude hold. The navigator turns the stadimeter on, unlocks the gimbal, and manipulates the stadimeter until the earth horizon is in the stadimeter field of view. The stadimeter is manually traversed along the horizon until the vertical hairline intersects a known star. This is done to provide an earth-vehicle

orientation reference so that subsequently corrections can be made for the oblateness of that portion of the earth's horizon in computing altitude. The prism control knob is rotated until the three separated sections of horizon are superimposed. When the navigator is satisfied with his adjustments, he presses the mark button which locks in the last reading and time. A second reading of a different portion of the earth's horizon is performed immediately after the first. This procedure is repeated three times at 20-minute intervals.

Between stadimeter observations, sextant sightings are taken of known pairs of stars. The times at which the earth, the vehicle, and the observation stars will be in a relationship appropriate for making observations are determined by the navigator, by reference to a microfilm table based on the precalculated nominal orbit. In the table, under each of the selected observation stars, is a list of the times that each star pair may be observed. When the viewing in time for an observation star pair approaches, the navigator alerts the pilot. The pilot manually rolls the vehicle to bring the earth's disk and the two navigation stars into the sectants' field of view and then places the vehicle attitude system on automatic hold. To avoid the additional computational complexities associated with nonsimultaneous observation of two star-horizon angles, the two star-horizon measurements are made at the same time. Separate sextants are used since the only reference found describing tri-sextant measurements suggested severe accuracy limitations. Thus, the follwing procedure is performed simultaneously by the navigator and a second crew member stationed at the second observation port. While the pilot is maneuvering the vehicle, the navigator(s) turns the sextant on, selects the appropriate filter, and unlocks the gimbals. With the aid of a star chart, the navigator visually locates on navigation star and then locates it in the sextant wide angle field of view. When the pointing of the sextant has been adjusted to bring both the star and the horizon into the field of view the sextant gimbals are locked. The prism control is then rotated until the star and the horizon are superimposed. The navigator then selects the higher-magnification, narrow-field-of-view lens, again superimposes the star

and the horizon, and maintains the superimposition. When both observers are simultaneously satisfied with their settings, the "mark" buttons are simultaneously depressed, and the time and angle readings logged.

Immediately following each star-horizon angle measurement, the angle between two known stars is measured. This data is used to provide sextant calibration error corrections.

A second pair of simultaneous observations is made immediately after the first. Two pairs of sextant observations are made after each pair of stadimeter observations. A total of six independent stadimeter readings and six pairs of sextant readings are performed per orbit. Subsequently, a number of different estimates of the orbital parameters are made based on independent sets of observations. If the variability between the resulting sets of parameters is low, no further observations are required.

7-5. Data Processing

Summary. The stadimeter sextant measurements at the times of the observations are processed to yield orbital elements. The orbital data is then used to determine the guidance corrections necessary to obtain the nominal orbit.

Equipment and Procedures. Since data-processing algorithms have not yet been developed for this study, it is not possible to give explicit description of the data processing and procedures. However, it appears entirely feasible to assume that all of the data processing required in this phase can be performed, with the aid of microfilmed tables, on a simple mechanical or electrical calculator. Computation tables can be stored on microfilm. While the amount of film that can be stored depends on the amount of reduction, extremely small microfilm chips require relatively sophisticated viewing devices. Standard microfiche chips are approximately 1 x 1.5 centimeters. Using microfiche, 15,000 page-size tables can be stored on a *single 10-inch* reel of 35mm 5-mil film.

Since two altitude observations and the time between the observations are sufficient to determine the eccentricity and major axis of the orbit, an estimate of these parameters can be obtained directly from the tables for any time separated pair of altitude observations. Several pairs of altitude observations will be used and the resulting set of size and shape parameters subjected to a smoothing and combining process.

The orientation of the orbit in the celestial sphere is determined from the star-horizon angle measurements. Most of the computations can be tabled; however, it is anticipated that some intermediate hand calculation will be necessary. Since the computation tables will be based on the nominal orbit precalculated before launch, the tables for orbital calculations can be restricted to the computation of orbits which deviate only slightly from the nominal. As with the stadimeter data, several sets of sextant data will be used to obtain independent estimates of the orbit orientation and these subjected to an averaging process.

Once the true orbit has been determined the next data processing step is to determine the guidance corrections that must be made to alter the plane of the orbit so that it is coincident with the plane of the nominal earth-Mars trajectory. The size and shape of the orbit are not altered since deviations in these parameters affect only the total ΔV required to achieve a Mars trajectory.

The guidance information required for orbit correction is determined by entering microfilmed tables with the parameters of the true orbit. The guidance information is given in the tables in the form of two celestial attitudes which define the attitude of the thrust vector, a thrust onset time, and a total ΔV. The thrust attitude is given as an angle along the line between two known stars and an angle normal to this line. Thrust onset time is given relative to apogee. As was the case with the orbital calculations, it is feasible to table the guidance calculations since the tables can be restricted to cover a limited set of orbits.

7-6. Guidance

Summary. At the proper time, the vehicle is maneuvered to align its thrust axis in accordance with the tabled values. Thrust is manually initiated and is terminated automatically when the correct ΔV has been achieved.

Equipment. A stellar reference viewer is required to permit the pilot to bring the vehicle into a specific alignment with respect to two navigation stars. The line of sight of the viewer is parallel to the vehicle's nominal thrust axis and its field of view is imaged on a large lens on the pilot's instrument panel. A prism system is used to provide an adjustable split image. The adjustable image is controlled by the pilot by means of knobs, and can be blanked out as desired. The IMU, incorporating three orthogonal linear accelerometers and provision for integrating and displaying its output, is required for the control of thrust. This sytem includes a provision for pre-setting the correct ΔV and will terminate thrust automatically when the correct ΔV has been achieved. Nonaxial velocity errors caused by misalignment of the vehicle during thrusting are displayed as orthogonal components. The pilot nulls orthogonal components by controlling the position of the gimbaled thruster by means of a two-axis hand controller.

Procedure. When the time for the guidance correction approaches, the pilot maneuvers the vehicle to correctly align its thrust axis.

To do this, the pilot first slues the vehicle to bring the reference stars into view through the spacecraft windows. The pilot then locates the reference stars in the field of view of the stellar reference viewer, and maneuvers the vehicle so that two stars lie on the horizontal reticle of the instrument with the left-most star aligned with an indicator mark on the extreme left-hand side of the reticle. The line between the two stars now defines the vehicle yaw plane.

Using the knobs that control the adjustable split image, the pilot dials the two guidance attitudes into the attitude display. The guidance attitudes are given in the form of an angle α along the line between the

two stars, at an angle β to the line between the two stars. When these values have been set in, the adjustable image of the left-most star will now occupy that point on the image which defines the correct line of sight for thrusting. The pilot then pitches and yaws the vehicle to place the adjusted image to the intersection of the reticule crosshair. The vehicle is now correctly aligned for thrusting.

When the proper orientation has been achieved, the pilot depresses a button to align the IMU with respect to the new line of sight. Non-axial velocity components are displayed as components along the line between the two reference stars and along the line perpendicular to the reference line. Thus, as long as the roll alignment of the vehicle is such that the line between the two reference stars is parallel to the vehicle yaw plane, the orthogonal velocity components are displayed in the vehicle's yaw and pitch planes.

While the pilot is maneuvering the vehicle to align it for thrusting the copilot dials in the required ΔV and at some even increment of time prior to the thrust onset time, he sets a countdown clock. When the countdown clock reaches zero, the pilot manually initiates thrust. The required ΔV is displayed and the display is driven to zero during thrusting. Thrust is terminated automatically when the correct ΔV is achieved but the copilot monitors the display and is prepared to cut off thrust manually when the display reaches zero as a backup to the automatic system. Throughout the thrust period the pilot controls engine gimbaling to null out orthogonal rates as they develop. The stellar reference viewer display provides pitch and yaw information which serves as lead information to the pilot. To simplify the pilot's control task, vehicle roll is controlled by the copilot. The copilot controls the roll attitude to keep the nonadjustable images of the star on a horizontal line in the stellar reference viewer display.

Since the line between the fixed image of the two stars provides a roll reference, it is necessary that these stars be within the field of view of the stellar reference viewer during thrusting. Because a narrow-angle field of view is used to obtain high pointing accuracy, the reference stars cannot be separated by more than about 5 degrees.

Following the guidance-correction orbit determination, navigation observations are taken again and the data is processed as described above to obtain the parameters of the new orbit. Significant deviations from the nominal orbit, however, would not be acceptable and would require another earth-orbit correction cycle.

7-8. Injection into Cis-Martian Trajectory

7-9. Navigational Observations

The navigational observations performed after the last orbit correction provide all the navigational information necessary for cis-Martian injection guidance. The nominal trajectory on which the mission is based defines the orbit from which the vehicle should inject, the time of injection, the ΔV and celestial attitude which must be held during the injection process. The orbit determination process already completed will enable the crew to determine any changes which are required. Once the earth orbit has been corrected, only two adjustments are likely to be needed: turn-on time and ΔV. The former is most likely and would be used to compensate for the effect of improper orbital altitude. However, minor deviations of the angle of inclination of the orbit from the nominal are compensated for by a slight variation in celestial attitude during thrusting. The guidance information is again obtained by table lookup. Table requirements for determining attitude adjustments will be minimal because orbit corrections will have resulted in an orbital plane very close to nominal.

7-10. Guidance Procedures

The guidance procedures for cis-Martian injection are exactly as described above for earth-orbit correction. However, because of the much greater velocity impulse required and because it is desirable to keep thrust levels relatively low to ensure acceptable manual control, the thrust period will be considerably longer than was the case for earth-orbit correction. Depending on the level of thrust employed, the thrust period will be between 10 and 30 minutes.

In considering thrust levels for injection, there is a tradeoff between thrust duration and thrust level. On the basis of the human-performance literature, it can be anticipated that the ability of a human operator to accurately null the orthogonal rates produced during thrusting will diminish over a 20-minute period. However, the high thrust levels that would be required to produce a relatively short thrust period are undesirable. The higher the thrust level the greater the frequency and amplitude of attitude and orthogonal acceleration noise. Further, in a thrust period as long as twenty or thirty minutes, there could be significant drift in the IMU. Experimental data is needed to resolve these factors and to develop principals for specifying thrust levels in human controlled thrust systems.

7-11. Phase 3. Post and Terminal Adjustments

7-12. Navigational Observations

Summary. Navigational information for post and terminal trajectory adjustments is obtained from photographic techniques, for several reasons: (1) the vehicle stabilization requirements are far less stringent than would be the case for real time sextant observations: (2) the photograph can be measured with extreme care at the leisure of the navigator; (3) background stars provide self-calibration of each photograph; (4) the photographs themselves provide a permanent record of the observations; (5) each pair of background stars can be used to perform independent trajectory calculations; and (6) a film can be selected with spectral sensitivities ideally suited to the phenomenon under observation.

Measurements of photographic images of either the earth or Mars are used. Adjustments of interplanetary trajectories will be performed 1 to 20 days after leaving or before arriving at a planet to provide navigational data for the adjustments. Photographs are taken of the planetary disk, and the distance between known stars and the planet center is measured.

Equipment. To avoid the necessity for enlaring photographs, a camera taking a very large film frame-up to 20 by 24 inches — is utilized. The camera incorporates a number of interchangeable lenses so that at any distance from earth or Mars a large image of the planet can be obtained. The camera is gimbal-mounted and is free to rotate in horizontal and vertical planes, and about the line-of-sight axis of its lens system.

The difference in illumination between the navigation background stars and the planet is sufficient so that serious underexposure of the stars or overexposure of the planet disk is possible. To avoid this problem the film used is a composite, with a center circular section of lower sensitivity than the surrounding film. The film will be available with low-sensitivity patches of different diameters to accommodate any combination of planet size, distance, and camera lens so that the entire planetary disk but none of the navigation stars impinge on the low-sensitivity area.

A transparent overlay with inscribed circles and a microcaliper are used to provide the measurement of the photographic images. A jig with a movable frame is used to hold the overlay and the photograph during the measurement.

Dry-chemical techniques, such as were employed aboard the lunar orbiter spacecraft, are used to develop the exposed images.

Procedure. Thirty-six hours after injection into Cis-Martian orbit, the first navigational measurements are taken. The pilot manually maneuvers the vehicle to bring the earth disk into position for photography and then selects the attitude-hold mode. The navigator images the planetary disk on the ground-glass screen of the camera and then locks the camera in place. The navigator selects the lens that produces the largest image of the planetary disk without losing the images of the navigation background stars.

The image of the disk is centered on the cross hairs inscribed on the ground-glass viewing screen. The camera is then rotated about its own axis until one of the observation stars coincides the with the vertical cross hair. This procedure defines the orientation of the planetary disk in the photographs and permits subsequent corrections for the planet's oblateness. When these adjustments have been made, the camera gimbals are locked. On the basis of the size of the image of the planetary disk, the navigator selects a film frame with an appropriately sized low-sensitivity area. The film frame is inserted into the camera and an exposure is made. When the exposed film is removed from the camera the mission time at which it was taken is noted on the film.

The exposed film is developed immediately after exposure. Dry-chemical processing is used since this technique produces entirely acceptable results and avoids the problem of handling liquids in a zero-G environment. The processed film is then placed in a measurement jig. To determine the center of the planetary disk, a transparent plastic overlay inscribed with concentric outlines of the earth's oblate sphere, as seen from various distances in space, is placed over the photograph. The jig allows the overlay to be rotated and to be moved in X and Y relative to the photograph. Because of the slight eccentricity of the earth's outline, the overlay must be properly oriented with respect to the photograph before the outline of the disk or crescent can be aligned with one of the concentric outlines on the overlay. To accomplish this, the pilot consults a table which he enters with the date and the name of the star aligned with the vertical cross hair in the photograph. The output of the table is in degrees of rotation. The transparent overlay has radial degree lines emanating from the center; the overlay is rotated until the correct degree line intersects the reference star. The overlay is then adjusted until the entire rim of the planet disk or crescent coincides exactly with one of the overlay outlines or lies between two concentric, adjacent overlay outlines. The overlay and the photograph are locked together and the center of the overlay now coincides with the center of the disk or crescent image.

Distances from reference stars to the center of the planetary disk or crescent and between reference stars are made with a microcaliper. Measurements are made from the center of the disk or crescent to the edge along a specific axis to determine the radius of the planetary disk. This radius measurement is used to estimate distance of the vehicle from the planet.

7-13. Data Processing

Summary. A procedure based on a precalculated nominal cis-Martian trajectory is used to determine the required guidance adjustments. The raw navigational data required to determine the corrections are the angle between two known navigation stars and the earth center and the distance of the spacecraft from the earth. The distance from the earth is obtained from integration of the IMU output.

Equipment and Procedure. Distance from the earth is obtained from the linear accelerarometers; however, diameter of the photographic disk is used as a check on the accelerometer data. The guidance information is obtained by a table-lookup procedure in which the navigator enters the table with distance and two star-horizon angles. To obtain correct figures, the star-horizon angles are subjected to a calibration process based on the distance on the photograph between two known stars. The guidance information is given in the form of two celestial angles and a total ΔV. This procedure is repeated several times with different pairs of navigation stars and the resulting guidance data subjected to an averaging process.

7-14. Guidance

The navigation and data-processing procedure described above is repeated every 12 hours. Depending on the size of the navigation errors, guidance correction may or may not be performed. If a guidance correction is performed, the observation cycle is repeated immediately afterward. Results of successive every-12-hour observation cycles are pooled to enhance confidence in the results. The pooling process will

be a weighted averaging which will reflect variations in the seriousness of a given velocity error, accuracy of observation, and confidence in the data with increasing distance from earth (or decreasing distance from Mars) and the number of observations. If the error velocities thus obtained are below a certain threshold value, that is, in the noise region of the phenomena being observed, no guidance correction will be made. The guidance procedure itself is exactly as described for earth-orbit correction. The observation and guidance cycle is repeated every 12 hours until the vehicle is approximately 20 days away from the earth. Until the vehicle approaches to within 20 days of Mars, no near-body navigation is performed.

During the midcourse portion of the earth-to-Mars leg, solar observations are performed. While solar sightings are not as accurate as near-body sightings (an error velocity determined on a basis of one solar sighting, of sufficient magnitude to emerge from phenomenal background noise, would be catestrophically large), the data from many solar sightings will be available fro pooling and smoothing. For nearly 200 days, the spacecraft will be too far from either earth or Mars for useful near-body measurements. Pooling the data of the many solar measurements that will be taken in the midcourse phase may provide velocity error data sufficiently reliable to make relatively small guidance corrections feasible. Solar navigation during the midcourse phase is also important for psychological reasons. Regularly scheduled observation cycles during the midcourse phase will provide the crew with a set of mission-related tasks and an important sense of control over the outcome of the mission.

Solar observation will be performed every 24 hours during the mid course phase, using the photographic technique described above. Successive observations will be pooled to determine the vehicle trajectory. As the number of observations on which the trajectory calculations are based increases, an evaluation of the reliability of the data will be made on the basis of the variance of the obtained parameters. When a sufficient number of observations have been obtained to provide a given

level of confidence in the results, the trajectory parameters will be compared with the parameters of the nominal trajectory via table look-up techniques and a ΔV correction applied as required.

When the vehicle approaches the region of Mars (about 20 days away), near-body measurements are resumed and terminal trajectory adjustments applied as required. The navigation, data processing, and guidance are exactly as described for the post-injection adjustments. Observations are made every 12 hours with guidance adjustments as required until the vehicle is 24 hours from entry into Mars orbit.

7-15. Phase 4. Mars-Orbit Entry

Orbit entry is the most important phase from a human operator's standpoint in a manual navigation system, as this phase is most sensitive to navigation guidance errors and places the geatest demands on the crew.

With the predicted terminal trajectory, established from the terminal adjustment phase, orbit entry is essentially the reverse of the injection process. However, because the plane of the adjusted trajectory will be very close to the plane of the nominal trajectory during the terminal adjustment phase, no out-of-plane velocity corrections will be performed. For this reason, sextant measurements of star-to-Mars horizon angles will be unnecessary. Orbit entry is achieved by applying the correct braking-velocity vector, and at a proper altitude, determined on the basis of the precomputed nominal trajectory. Navigation, data processing, and guidance are not meaningfully separable in this phase and therefore are discussed together.

Equipment. No new equipment is required for this phase.

Procedure. Following the last terminal adjustment to the earth-Mars trajectory, a final cycle of photographic observations is performed.

Because of the time that will have elapsed since injection into the earth-Mars trajectory, range and range-rate data will be obtained from

successive measurements of the radius of the photographic image of the Mars planetary disk rather than from the IMU. The star-horizon angles, range, and range-rate data are used to determine Mars orbit entry guidance requirements. Guidance data is given in the form of two celestial angles relative to two known stars, a required ΔV, and the range or altitude at which thrust is initiated. As before, the necessary calculations are tabled.

As the time for the orbit entry impulse approaches, the pilot performs the maneuver previously described to orient the vehicle properly for thrust. Up to the moment of the guidance impulse, the pilot continuously monitors spacecraft attitude and makes adjustments as required. The correct figure is dialed into the thrust control system. The navigator commences a series of stadimeter sightings. The frequency of the sightings depends on how much time an operator requires to make accurate stadimeter sightings. Within this constraint, sightings are taken as frequently as possible; it is assumed that one accurate observation every 2 minutes is feasible. A plot of the range and time of observation is maintained to establish a range rate.

When, on the basis of the range and range-rate plot, the vehicle is a few minutes from the altitude at which thrust is to be initiated, a last range observation is performed and thrust onset time, relative to the time of the last reading, is computed. The range rate will be sufficiently constant over a period of a few minutes that a calculation of thrust onset time made on this basis will be accurate to within better than 2 minutes; this is a better approach than initiating thrust on the basis of stadimeter readings alone. Using the latter technique, the uncertainty of the thrust onset time would be equivalent to the amount of time required to take a reading. When the thrust onset time has been established, the navigator gives the pilot a verbal countdown and the pilot manually initiates thrust at the proper time. The navigator continues to take stadimeter readings after the injection impuse to determine the size and eccentricity of the orbit and to ensure very quickly that the orbit does not intercept the surface of the planet. A pair of

sightings 15 minutes apart is sufficient to determine the geometrics of the orbit with acceptable accuracy to ensure the safety of the vehicle.

7-16. TIMELINE ANALYSIS

Figure 7-1 shows the timeline task sequence of crew members as they take navigational observations in the earth-orbit determination and collection phase. (The task sequence analysis was performed for this phase because the crew is more heavily loaded than in any other navigation phase.) Three crew members are required, the pilot and two navigators, designated navigator 1 and navigator 2. Approximately 20 minutes is required to obtain two independent stadimeter altitude observations of the nearest horizon and two independent pairs of sextant star horizon readings. In one orbit, a three-man crew could obtain six independent stadimeter sightings and six independent pairs of star-horizon sightings, the two-star horizon sightings within a pair taken simultaneously. The two navigators are fully loaded during this sequence; however, the pilot is not heavily loaded and would have time throughout most of the sequence to monitor ship status.

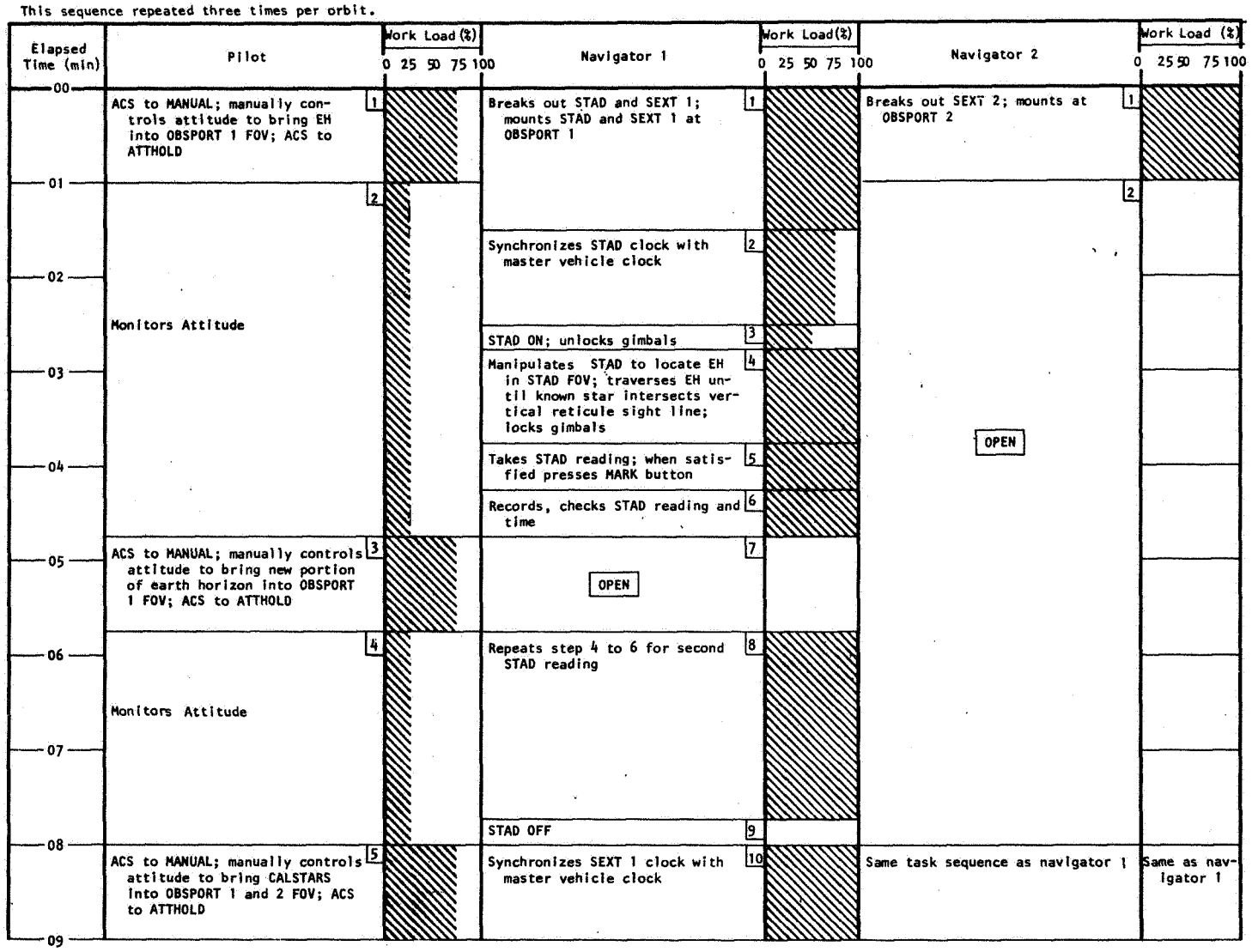

Figure 7-1. Timeline Task Sequence of Crew Members During Earth-Orbit Determination

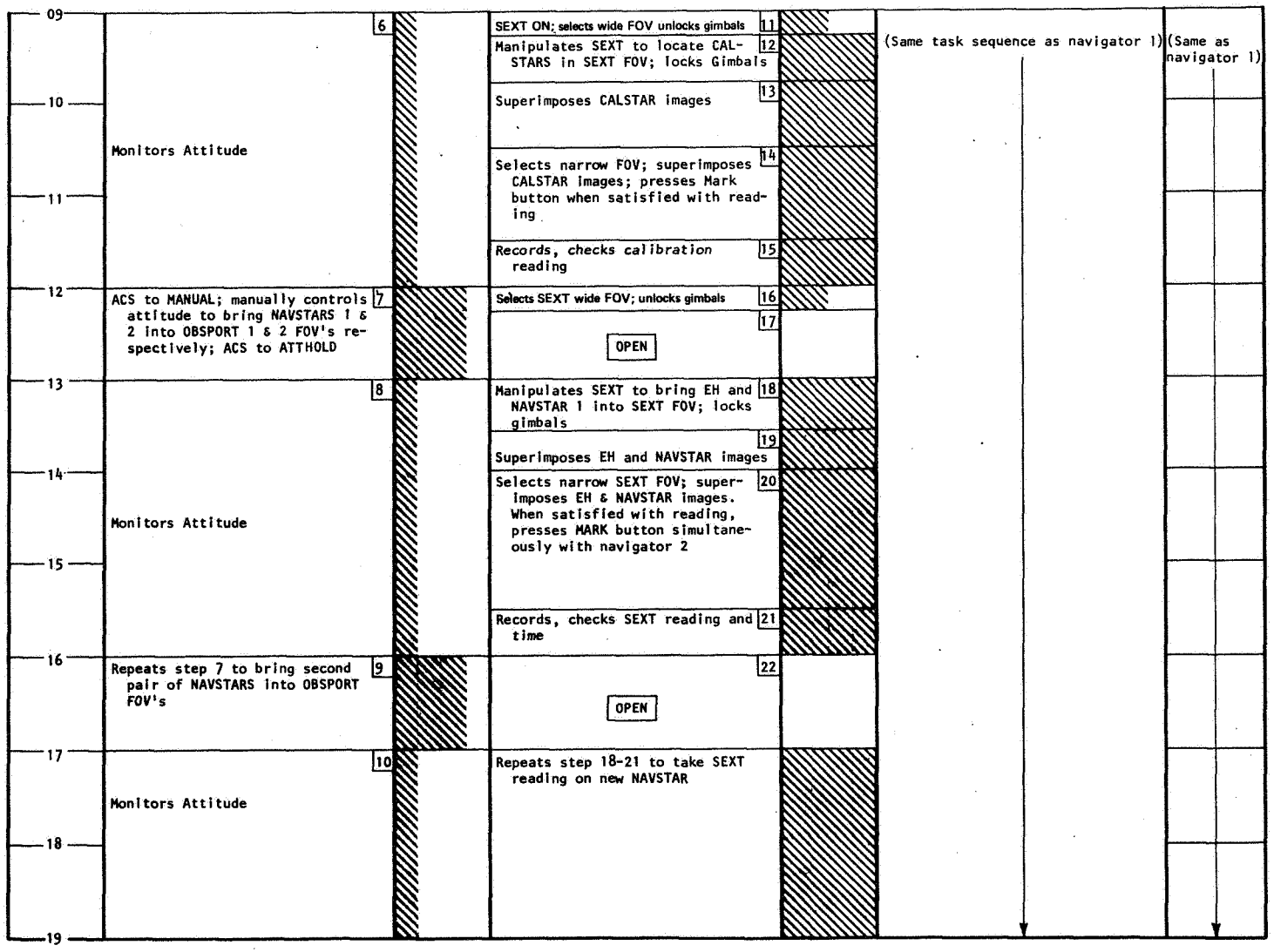

Figure 7-1. Timeline Task Sequence of Crew Members During Earth-Orbit Determination (Continued)

REFERENCES

Acken, R. A., "Navigator Performance Studies for Space Navigation Using the NASA CV-990 Aircraft", NASA Working Paper 219, 1966.

Battin, R. H., *Astronautical Guidance*, McGraw-Hill, 1964.

Bowditch, Nathaniel, *The New American Practical Navigator: being an epitome of navigation; containing all the tables necessary to be used with the nautical almanac in determining the latitude and longitude by lunar observation; and keeping a complete reckoning at sea*, Fourth edition, N.Y.,, published by E. M. Blunt and Samuel A. Burtus, August 1817.

Clark, H. J., *Trajectory Versus Line-of-Sight Space Rendezvous Using Out-of-Window Visual Cues*, AMRL-TR-65-10, Aerospace Medical Research Laboratories, February 1965.

Clarke, V. C. Jr., *et al.*, *Earth-Mars Trajectories*, Jet Propulsion Laboratory, Technical Memorandum 33-100, March 1, 1967.

Duke, C. M., and Jones, M. S., *Human Performance During a Simulated Apollo Midcourse Navigation Sighting*, Massachusetts Institute of Technology, 1964, DDC No. AD 610 526.

Farber, E., *et al.*, *Manned Terminal Rendezvous Simulation Program*, Advanced Manned Systems Engineering, General Electric Company, Missile and Space Division, February 7, 1963.

Foudriat, E. C., and Wingrove, R. C., *Guidance and Control During Direct-Descent Parabolic Re-Entry*, NASA TN D-979, National Aeronautics and Space Administration, Washington, D. C., November 1961.

Havill, D. C., *An Emergency Midcourse Navigation Procedure for a Space Vehicle Returning from the Moon*, NASA-TN D-1765, 1963.

Holleman, E. C., Armstrong, N. A., and Andrews, W. H., "Utilization of the Pilot in the Launch and Injection of a Multi-Stage Orbital Vehicle", paper presented at IAS 28th Annual Meeting, New York, January 26, 1960.

Jorris, T. R., Silva, R. M., and Vallerie, E. M., *Initial Results of the Air Force Space Navigation Experiment on Gemini*, AFAL-TR-66-183, Wright Patterson Air Force Base, 1966.

Jorris, T. R., Silva, R. M., and Vallerie, E. M., *The Air Force Space Navigation Experiment on Gemini*, AFAL-TR-66-289, Wright-Patterson Air Force Base, 1966.

Lampkin, B.A., *Navigator Performance Using a Hand-Held Sextant to Measure the Angle Between a Moving Line of Sight to a Flashing Light and a Simulated Star*, Working Paper 218, Ames Research Center, October 10, 1966

Lampkin, B. A. and Randle, R. J., *Investigation of a Manual Sextant Sighting Task in the Ames Midcourse N & G Simulator*, NASA TN D-2864, 1965.

Levin, E., Ward, J., *Manned Control of Orbital Rendezvous*, AD 616402, The Rand Corporation, Santa Monica, California, October 20, 1959.

Lozins, N., *Spatial Aiming of Reconnaissance Sensor*, AFAL-TR 64-324, 1964.

Miller, A. B., *Pilot Re-Entry Guidance and Control*, NASA CR-331, National Aeronautics and Space Administration, Washington, D. C. November 1965.

Miller, G. K. Jr., Fletcher, H. S., *Simulator Study of Ability of Pilots to Establish Near-Circular Lunar Orbits Using Simplified Guidance Techniques*, National Aeronautics and Space Administration, Washington, D. C. February 1965.

Moul, M. T., Schy, A. A., *A Fixed-Base Simulator Study of Piloted Entry into the Earth's Atmosphere at Parabolic Velocity*, NASA TN D-2707, National Aeronautics and Space Administration, Washington, D. C. March 1965.

Muckler, F. A., and Obermayer, R. W., *The Use of Man in Booster Guidance and Control*, NASA CR-81, National Aeronautics and Space Administration, Washington, D. C., July 1964.

Pennington, J. E., *et al.*, *Visual Aspects of a Full-Size Pilot-Controlled Simulation of the Gemini-Agena Docking*, NASA TN D-2632, National Aeronautics and Space Administration, Washington, D. C., February 1965.

Silva, R.M. (Captain, USAF) and Jorris, T.R. (Captain, USAF), *Initial Results of the Air Force Space Navigation Experiment on Gemini: -Experiment B-9.*

White, K.C., The Effect of Spacecraft Windows on Navigation Sighting Measurements, NASA Working Paper 217, 1966.

Wingrove, R. C., *et al., A Study of the Pilot's Ability to Control an Apollo Type Vehicle During Atmosphere Entry,* NASA TN D-2467, National Aeronautics and Space Administration, Washington, D.C., August 1964.

APPENDIX A

EXPLANATION OF HELIOCENTRIC NOTATION

(Reproduced from Jet Propulsion Laboratories TM 33-100)

Tabular listings of pertinent quantities of the heliocentric and planetocentric trajectories, differential corrections, guidance, and orbit determination parameters are given at 1-day launch date intervals and 2-day flight time intervals over the selected launch period. The launch period is selected to encompass the minimum energy transfer dates.

Each trajectory begins with a header giving launch date, flight time (in days), and arrival date. All the heliocentric transfer trajectories are calculated assuming launch into the heliocentric orbit at 0 hours of the launch date and arrival at 0 hours of the arrival date. Later, however, when the launch-planet ascent trajectories are computed, the actual launch times during the launch day for each launch azimuth are given.

Each page lists four trajectories, each of which is divided into five basic print groups: HELIOCENTRIC CONIC, PLANETOCENTRIC CONIC, DIFFERENTIAL CORRECTIONS, MID-COURSE EXECUTION ACCURACY, and ORBIT DETERMINATION ACCURACY. Each quantity is assigned an identifying alphabetic symbol of no more than three letters. The definitions of the symbols and quantities they represent are given below. All pertinent quantities are referenced to the mean equinox and equator, or ecliptic, of *launch* date.

A. Heliocentric Conic Group

The HELIOCENTRIC CONIC group gives the characteristics of the heliocentric transfer ellipse, such as the position and velocity vectors at launch and arrival, some orbital elements, and other quantities of engineering interest. The printout array is as follows:

HELIOCENTRIC CONIC DISTANCE

RL LAL LOL VL GAL AZL HCA SMA ECC INC V1

RP LAP LOP VP GAP AZP TAL TAP RCA APO V2

RC GL GP ZAL ZAP ETS ZAE ETE ZAC ETC CLP

After the words HELIOCENTRIC CONIC, the heliocentric arc DISTANCE traveled by the spacecraft from launch to arrival is printed. The quantities are defined as follows (all angles are in deg; distances are in millions of km; speeds are in km/sec):

Column 1

RL, $R_L = |\mathbf{R}_L|$ — the heliocentric radius of the launch planet at 0 hours of the launch date.

LAL, β_L — the celestial latitude of the launch planet at 0 hours of the launch date.

LOL, λ_L — the celestial longitude of the launch planet at 0 hours of the launch date.

VL, $V_L = |\mathbf{V}_L|$ — the heliocentric speed of the probe at 0 hours of the launch date.

GAL, Γ_L — the path angle of the probe at 0 hours of the launch date, i.e., the complement of the angle between the position and velocity vectors, $\mathbf{R}_L$ and $\mathbf{V}_L$, defined by

$$\sin\Gamma_L = \frac{\mathbf{R}_L \cdot \mathbf{V}_L}{R_L V_L} \qquad -\frac{\pi}{2} \leq \Gamma_L \leq \frac{\pi}{2}$$

AZL, Σ_L — the azimuth angle of the probe at 0 hours of the launch date, i.e., the angle, measured in a plane perpendicular to the radius vector $\mathbf{R}_L$, between the projection of the ecliptic north and the projection of the velocity vector $\mathbf{V}_L$ on the plane perpendicular to $\mathbf{R}_L$, defined by

$$\cos\Sigma_L = \frac{\mathbf{V}_L \cdot \Psi^1}{V_L \cos\Gamma_L} \qquad 0 \leq \Sigma_L \leq 2\pi$$

$$\sin\Sigma_L = \frac{(\mathbf{R}_L \times \mathbf{V}_L) \cdot \Psi^1}{|\mathbf{R}_L \times \mathbf{V}_L|}$$

where $\Psi^1 = (\mathbf{K}' - \mathbf{R}_L^1 \sin\beta_L)\sec\beta_L$, where the superscript 1 denotes a unit vector.

HCA, Ψ — the heliocentric central angle, or angle between the position vector $\mathbf{R}_L$, of the launch planet at 0 hours of the launch date and the position vector $\mathbf{R}_p$, of the target planet at 0 hours of the arrival date.

SMA, a — the semimajor axis of the heliocentric transfer ellipse.

ECC, e — the eccentricity of the heliocentric transfer ellipse.

INC, i — the inclination of the heliocentric transfer ellipse.

V1, $V_1 = |\mathbf{V}_1|$ — the heliocentric speed of the launch planet at 0 hours of the launch date.

Column 2

RP, $R_p = |\mathbf{R}_p|$ — the heliocentric radius of the target planet at 0 hours of the arrival date.

LAP, β_p — the celestial latitude of the target planet at 0 hours of the arrival date.

LOP, λ_p — the celestial longitude of the target planet at 0 hours of the arrival date.

VP, $V_p = |\mathbf{V}_p|$ — the heliocentric speed of the probe at 0 hours of the arrival date.

GAP, Γ_p — the path angle of the probe at 0 hours of the arrival date, defined the same as Γ_L except that $\mathbf{R}_p$ and $\mathbf{V}_p$ are substituted for $\mathbf{R}_L$ and $\mathbf{V}_L$.

AZP, Σ_p — the azimuth angle of the probe at 0 hours of the arrival date, defined the same as Σ_L except that $\mathbf{R}_p$ and $\mathbf{V}_p$ are substituted for $\mathbf{R}_L$ and $\mathbf{V}_L$.

TAL, v_L — the true anomaly of the probe in the heliocentric transfer ellipse at 0 hours of the launch date.

TAP, v_p — the true anomaly of the probe in the heliocentric transfer ellipse at 0 hours of the arrival date.

RCA, R_{CA} — the perihelion distance of the heliocentric transfer ellipse. This distance is printed even though the probe may not transit perihelion.

APO, R_A — the aphelion distance of the heliocentric transfer ellipse. This distance is printed even though the probe may not transit aphelion.

V2, $V_2 = |\mathbf{V}_2|$ — the heliocentric speed of the target planet at 0 hours of the arrival date.

Column 3

RC, R_C — the communication distance, or distance between the launch and target planets at 0 hours of *the arrival date.*

GL, γ_L — the angle between the launch hyperbolic-excess velocity vector $\mathbf{V}_{hL}$ and its projection on the orbital plane of the launch planet, defined by

$$\sin\gamma_L = \frac{\mathbf{W}_1 \cdot \mathbf{V}_{hL}}{V_{hL}} \qquad -\frac{\pi}{2} \leq \gamma_L \leq \frac{\pi}{2}$$

where $\mathbf{W}_1$ is a unit normal to the launch planet's orbital plane. This angle is useful in describing the direction in which the probe leaves the launch planet.

GP, γ_p — the angle between the incoming arrival hyperbolic-excess velocity vector $\mathbf{V}_{hp}$, and its projection on the target planet's orbital plane, defined by

$$\sin\gamma_p = \frac{\mathbf{W}_2 \cdot \mathbf{V}_{hp}}{V_{hp}} \qquad -\frac{\pi}{2} \leq \gamma_p \leq \frac{\pi}{2}$$

where $\mathbf{W}_2$ is a unit normal to the target planet's orbital plane. This angle is useful in determining whether the probe is approaching from above or below the target planet. If γ_p is positive, the probe approaches from below —if negative, from above.

ZAL, ζ_L — the angle between the outgoing launch asymptote (or hyperbolic-excess velocity vector) and the launch *heliocentric* radius vector $\mathbf{R}_L$ at launch time. This is the Sun–launch-planet–probe angle and is a good approximation to the launch-planet–probe–Sun angle as the probe leaves the launch planet. It is an important quantity in the design of attitude control systems which use the Sun and launch planet as optical references. The quantity ζ_L is defined as follows:

$$\cos\zeta_L = \frac{\mathbf{V}_{hL} \cdot \mathbf{R}_L^1}{V_{hL}} \qquad 0 \leq \zeta_L \leq \pi$$

The next six quantities, all angles, have the same general definition. They are important in the design of the near-target trajectory and are used in determining the aiming point for interplanetary flyby trajectories. Consider the target-centered geometry of Fig. A-1.

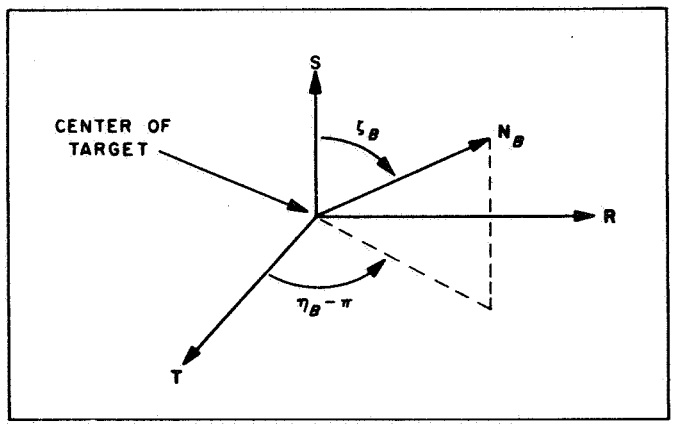

Fig. A-1. Generalized geometry for aiming point angles

In this diagram, the reference coordinate system is the same target **R**, **S**, **T** system defined in Section IIC. A unit vector $\mathbf{N}_B$ (subscript B for body) is directed from the target center to another celestial body. The angular quantity ζ_B is the angle subtended at the target center between the incoming asymptote **S** and the target–celestial body line $\mathbf{N}_B$. Thus

$$\cos \zeta_B = \mathbf{S} \cdot \mathbf{N}_B = \frac{\mathbf{V}_{hp} \cdot \mathbf{N}_B}{V_{hp}} \qquad 0 \leq \zeta_B \leq \pi$$

since

$$\mathbf{S} = \frac{\mathbf{V}_{hv}}{V_{hp}}$$

The angle η_B is the supplement of the angle between the **T** direction and the projection of $\mathbf{N}_B$ on the $\mathbf{R} - \mathbf{T}$ plane, defined by

$$\sin \eta_B = \frac{-\mathbf{R} \cdot \mathbf{N}_B}{\sin \zeta_B} \qquad 0 \leq \eta_B \leq 2\pi$$

$$\cos \eta_B = \frac{-\mathbf{T} \cdot \mathbf{N}_B}{\sin \zeta_B}$$

These quantities are computed for three celestial bodies: the Sun (ζ_S and η_S), the Earth (ζ_E and η_E), and the star Canopus (ζ_C and η_C). Thus,

ZAP, ζ_S (or ζ_p) — the Sun–target–probe angle. Actually, this angle should be symbolized ZAS, but, for historical reasons, is not. This angle is useful in that it indicates the direction of the probe's approach to the target. If $\zeta_S < \pi/2$, the probe approaches from the target planet's dark side. If $\zeta_S > \pi/2$, it approaches from the light side.

ETS, η_S — defined as above.

ZAE, ζ_E — the Earth–target–probe angle. This angle is useful in locating the Earth as the probe approaches the target.

ETE, η_E — defined as above.

ZAC, ζ_C — the Canopus–target–probe angle.

ETC, η_C — defined as above.

CLP, σ_p — the angle between the projection of the incoming asymptote **S** on the target planet's orbital plane and the target–Sun line at arrival time, defined by

$$\cos \sigma_p = -\mathbf{R}'_p \cdot \mathbf{S}_{pr} \qquad -\pi \leq \sigma_p \leq \pi$$

$$\sin \sigma_p = -\mathbf{S}_{pr} \cdot (\mathbf{W}_2 \times \mathbf{R}'_p)$$

where $\mathbf{S}_{pr}$ is the projection of **S** on the target's orbital plane given by

$$\mathbf{S}_{pr} = \frac{\mathbf{S} - \mathbf{W}_2 (\mathbf{S} \cdot \mathbf{W}_2)}{|\mathbf{S} - \mathbf{W}_2 (\mathbf{S} \cdot \mathbf{W}_2)|}$$

Recall that $\mathbf{W}_2$ is the unit normal vector to the target's orbital plane. This angle is illustrated in Fig. A-2.

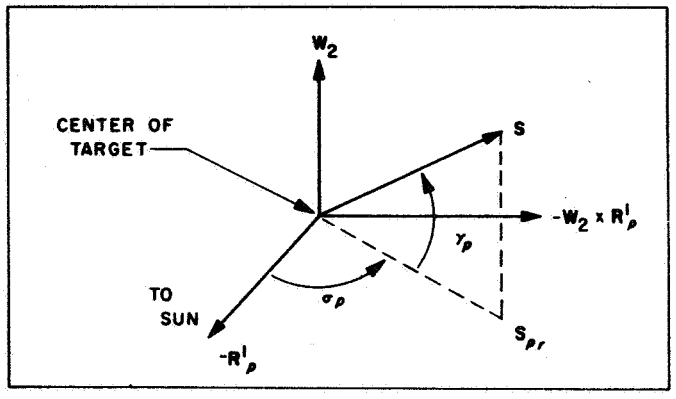

Fig. A-2. Definition of σ_p and γ_p

APPENDIX B

GUIDANCE EQUATIONS

B-1. POSITION DETERMINATION

To navigate in space we must first determine position. In space there are no "landmarks" to give us an idea of our position, nor is there a sense of movement or direction. Only after many days of movement at great speed could a person observe a change in the relative position of a few of the light points on the celestial sphere. The moving points are, of course, the planets and by means of their motion we can determine position within the celestial sphere. The stars alone, being essentially fixed, are not suitable for position location since even large changes within the solar system make no decernable changes in the appearance of the celestial sphere.

In any event a statement of position in the solar system requires a system of co-ordinates and for the solar system the system should have the sun, a "fixed" point, as it's center. Such a system can be built up from the position of the Earth's orbit in the Universe. If the plane of this orbit is extended until it intersects the celestial sphere, the line of intersection is called the ecliptic. The astronomers take as zero-point the vernal equinox of the ecliptic. However, this point is of importance only for terrestrial conditions, because it is the intersection of the equator with the ecliptic. Since this point has the disadvantage that it is not fixed, we can look for another point, which does not have this disadvantage and which is easy to find. We can take as this point a bright fixed star close to the ecliptic. The most convenient star for this purpose is Regulus, α Leonis, the brightest star in the Leo constellation. Regulus is only $+0^{\circ}27'$ away from the ecliptic, its distance from the vernal equinox is 151.6°.

Regulus complies much better with the condition of being a fixed point, and it is advantageous to take as zero-point the intersection of the ecliptic with the meridian through Regulus.

In figure B-1, S represents the Sun, and R Regulus. The position of the star St is determined by the arc RA (the longitude λ), and the arc ASt (the latitude β). The longitude λ is counted from the zero-point in the anti-clockwise direction. The latitude β is counted from the ecliptic towards the poles. These co-ordinates are called the heliocentric co-ordinates, since in this system the Sun is at the center. Thus, the position of a spacecraft in space can be determined by finding its distance from the sun and its heliocentric co-ordinates.

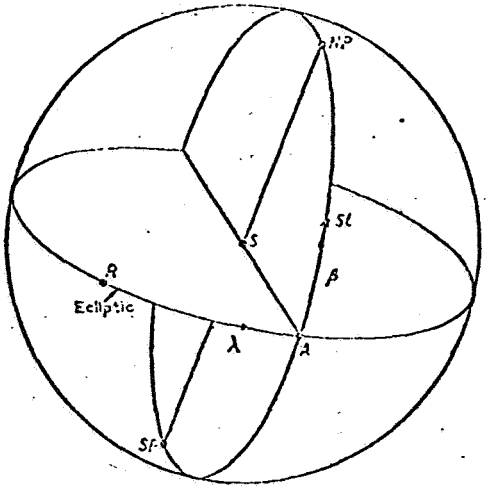

Figure B-1. Heliocentric Longitude and Latitude

These co-ordinates can be calculated by observing the positions of the Sun and of a planet, or of two planets, among the fixed stars, seen from the spaceship. The heliocentric co-ordinates of the planets are known and tables are available and will of course be available on a space vehicle if needed. In this discussion we will use the case of the Sun and a planet based position determination.

Also, for the sake of simplicity we shall deal only with the case when the planet and the spaceship are both in the plane of the ecliptic.

When this is not the case, the calculations are much more intricate, but they are based on the same general principles.

In Figure B-2, R is the position of the spaceship, P a planet, and S the Sun. The stars indicate the direction of Regulus.

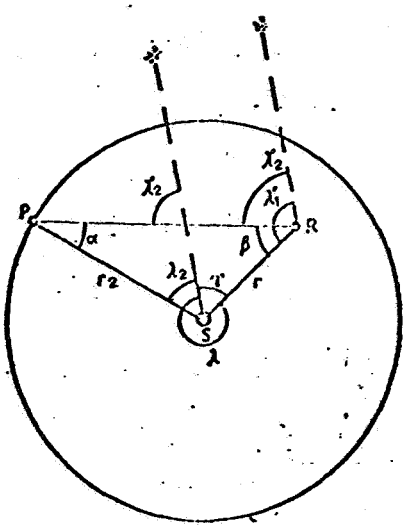

Figure B-2. Determination of Position in Space

We know from observation:

The longitude of the Sun, seen from the spaceship: λ'_1
The longitude of the planet, seen from the spaceship: λ'_2

We have the data for the time at which the readings were taken in cluding:

The heliocentric longitude of the planet: λ_2
The distance of the planet from the Sun: r_2

We can derive from the figure

$$\alpha = \lambda'_2 - \lambda_2$$
$$\beta = \lambda'_1 - \lambda'_2$$

and by the sine rule

$$\frac{r}{r_2} = \frac{\sin \alpha}{\sin \beta} = \frac{\sin (\lambda'_2 - \lambda_2)}{\sin (\lambda'_1 - \lambda'_2)}$$

or

$$r = r_2 \frac{\sin(\lambda'_2 - \lambda_2)}{\sin(\lambda'_1 - \lambda'_2)} \tag{1}$$

Furthermore

$$\begin{aligned} \lambda &= 180^\circ - \lambda'_2 - \beta \\ &= 180^\circ - \lambda'_2 - \lambda'_1 + \lambda'_2 \\ &= 180^\circ - \lambda'_1 \end{aligned}$$

also

$$\lambda = 360^\circ - r = 360^\circ - 180^\circ + \lambda'_1$$

or

$$\lambda = 180^\circ + \lambda'_1 \tag{2}$$

λ and γ determine the position of the spaceship R in space.

The method of determining the angles λ'_1 and λ'_2 the angles between the star Regulus and the Sun and between Regulus and the planet can vary. Optical devices, such as the narrow angle comparitor can be used to determine the angle between the planet or sun and a selected star, and then the star can be referenced back to our zero point, or a photographic technique could be used. In either case, or indeed with star, planet and sun trackers, the conversion to planet-Regulus or Sun-Regulus angles is simple.

If a photographic method or a narrow angle comparator technique were used, the determination of position would proceed as follows. Prior to launch the nominal mission would be prepared. As a result of these data the navigator would know the spacecraft position for appropriate times. He would also know, of course, the positions of the planets at various times.

To determine his heliocentric position at a specific time he could proceed as follows. Figure B-3 shows the nominal mission conditions and the known values. The navigator would take the measurement of the angle betwen the earth and the selected navigation star and would then have the information required to determine a line of possible positions

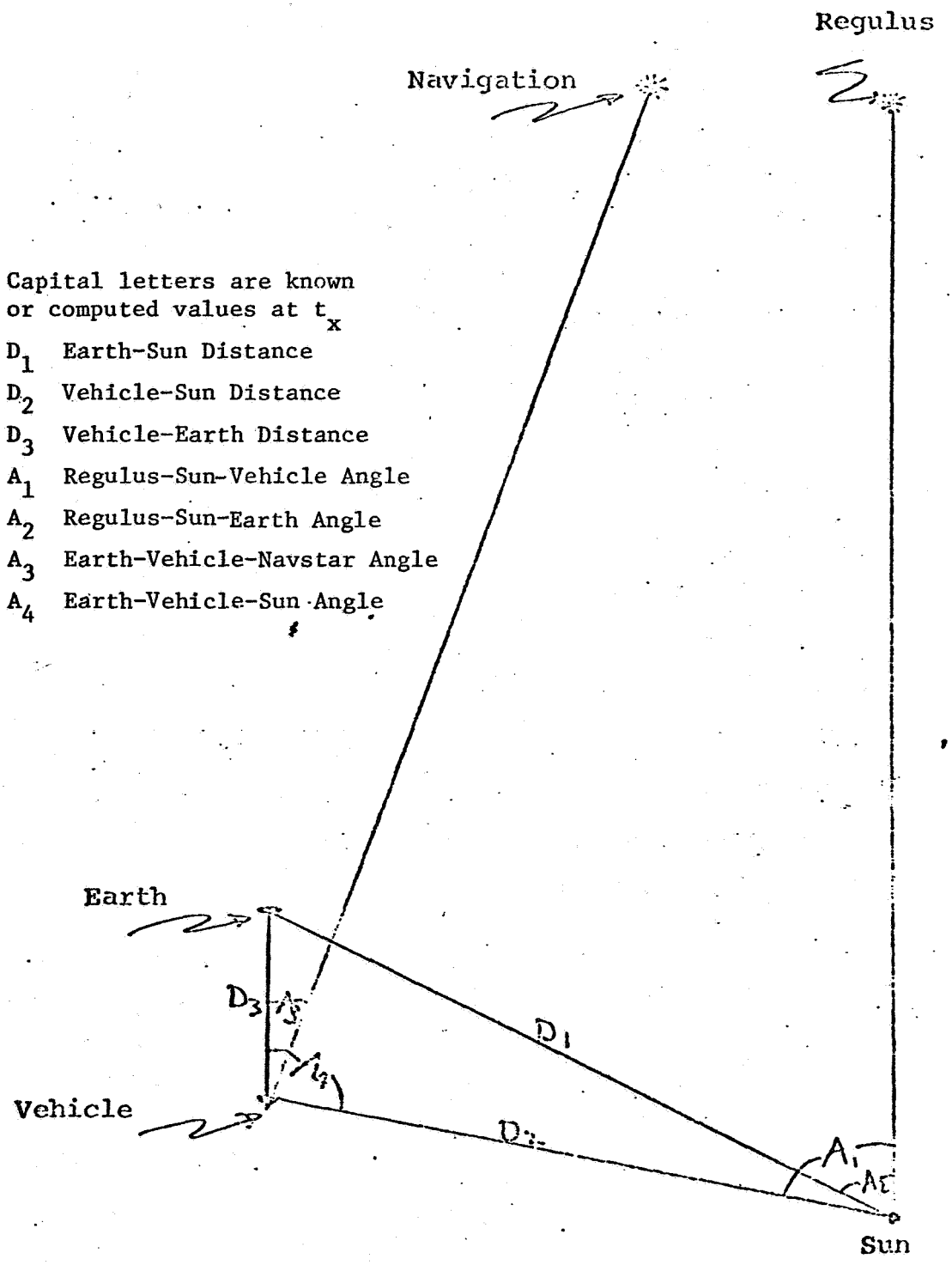

Figure B-3. Known Nominal Distances and Angles

which represent deviations (shown in Figure B-4) for various distances from the earth. Because of the distance to the navigational star the actual vehicle-star line may be considered parallel to the nominal vehicle-star line, hence, when the earth-vehicle-star angle is measured and an earth distance value determined the distance between the nominal star line of sight and the actual star line of sight can be determined. Since the measured angle is the same as angle a, the angle may be used directly to correct the vehicle-earth-sun angle.

The distance from earth may be determined either by dead reckoning (up to say 12 hours) by disc diameter measurement (until about 5 days) or by taking the earth-vehicle-sun angle. If the latter course is used the solution is obvious. Since the vehicle-earth-sun angle has been determined and the earth-vehicle-sun angle has been measured, two of three angles of a triangle are known. The sun to earth distance is also known and, consequently, the earth-vehicle and vehicle-sun distances can be determined and, of course, the two known angles can be summed and subtracted from 180^{o} to give the actual earth-sun-vehicle angle. The latter can then be used to correct the Regulus to vehicle angle.

Selecting a suitable star, or stars, should be no problem since as Vertregt indicates there are many stars within $\pm 10^{o}$ of the ecliptic.

In this strip encompassing 20^{o} north and south of the ecliptic there are seven stars of the first magnitude,

Scorpio	(Antares)	Canis Majoris	(Procyon)
Virginis	(Spica)	Orionis	(Betelguese)
Leonis	(Regulus)	Tauri	(Aldebaran)
Geminorum	(Pollux)		

11 stars of the second, 56 of the third magnitude and about 650 stars of the fourth and fifth magnitudes.

Thus, on the average an area 5^{o} on a side would contain 2.5 stars which could be used to obtain the raw angular data for reference to the zero-point. The proper stars would, of course, be preselected but simple star maps would make it possible to select stars on-board if desired.

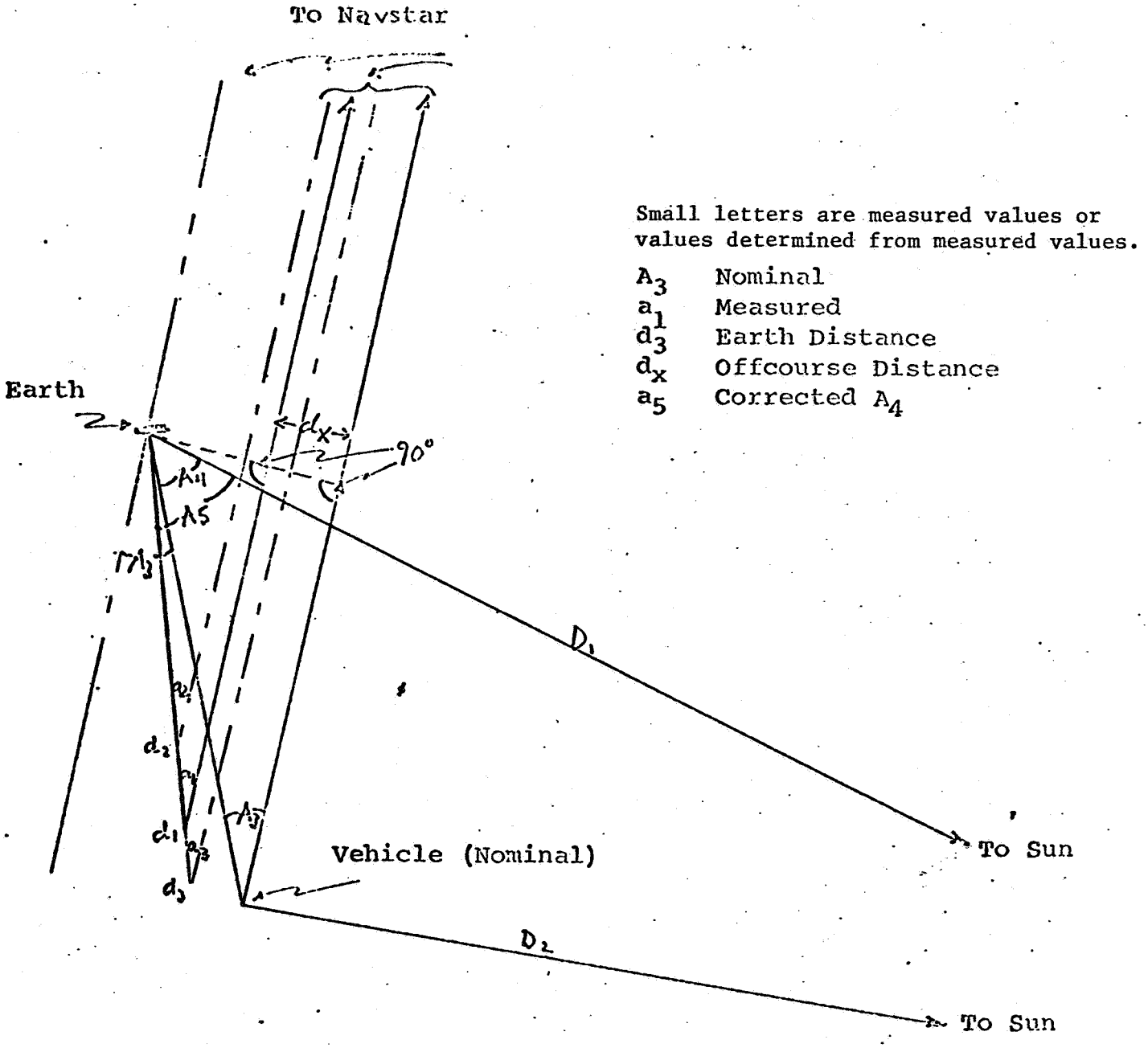

Figure B-4. Correction Distance Determined from Angle Between the Earth and the Navigation Star

B-2. HELIOCENTRIC ORBIT DETERMINATION

The position of a space vehicle in space can be determined from the postion of the sun and a planet among the stars, but in order to find the shape of the orbit, we must determine three consecutive positions.

If we take a simple example, and assume that the path of the spaceship is in the plane of the ecliptic we can proceed to determine the heliocentric orbit in the following manner.

In Figure B-5, S is the Sun, and R_1, R_2, and R_3 are the consecutive observed positions of the spaceship.

The co-ordinates are:

Position	Distance from the Sun	Longitude
R_1	r_1	1
R_2	r_2	2
R_3	r_3	3

For each of these observations we can use the equation

$$r = \frac{p}{1 + \varepsilon \cos \varphi}$$

in which r is the focal radius, p is the parameter of the ecliptic orbit, ε is the eccentricity of the orbit and φ is the angular distance of the perihelion.

Therefore

$$r_1 = \frac{p}{1 + \varepsilon \cos \varphi_1}$$

and if it is that the radius-vector to the perihelion makes an angle with the line Sun-Regulus. We have then

$$\varphi_1 = \lambda_1 - \pi$$

so that

$$r_1 = \frac{p}{1 + \varepsilon \cos(\lambda - \pi)} \qquad (3)$$

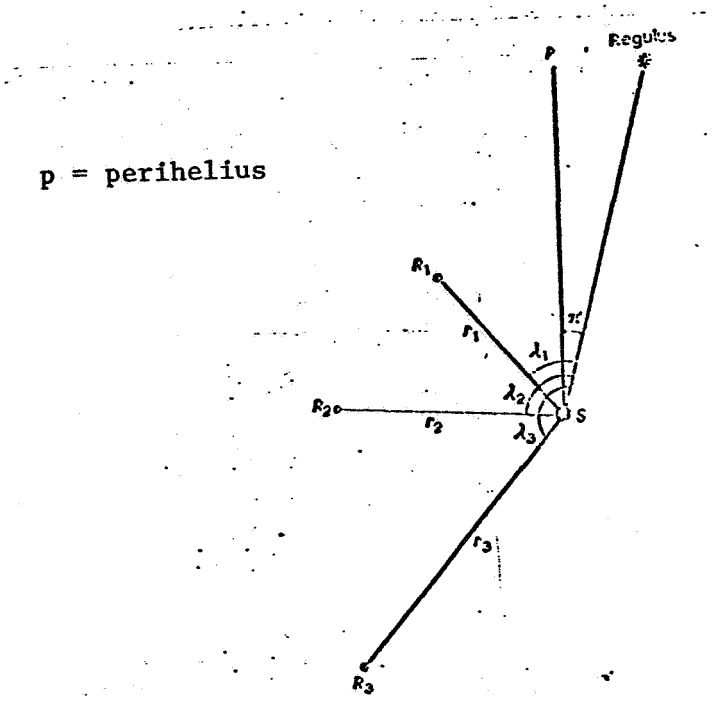

Figure B-5. Three Positions of the Space Ship on Consecutive Dates

In the same way we obtain from the second observation

$$r_2 = \frac{p}{1 + \varepsilon \cos(\lambda_3 - \pi)} \tag{4}$$

and from the third observation

$$r_3 = \frac{p}{1 + \varepsilon \cos(\lambda_3 - \pi)} \tag{5}$$

It is apparent then that

$$p = r_1 + r_2 \varepsilon \cos(\lambda_1 - \pi) = r_2 + r_2 \varepsilon \cos(\lambda_2 - \pi)$$

hence

$$\varepsilon = \frac{r_2 - r_1}{r_1 \cos(\lambda_1 - \pi) - r_2 \cos(\lambda_2 - \pi)} \tag{6}$$

and that

$$p = r_2 + r_2 \varepsilon \cos(\lambda_1 - \pi) = r_3 + r_3 \varepsilon \cos(\lambda_3 - \pi)$$

hence

$$\varepsilon = \frac{r_3 - r_2}{r_2 \cos(\lambda_2 - \tilde{\pi}) - r_3 \cos(\lambda_3 - \tilde{\pi})} \tag{7}$$

From the equations for ε shown above it is clear that

$$\frac{r_2 - r_1}{r_1 \cos(\lambda_1 - \tilde{\pi}) - r_2 \cos(\lambda_2 - \tilde{\pi})} = \frac{r_3 - r_2}{r_2 \cos(\lambda_2 - \tilde{\pi}) - r_3 \cos(\lambda_3 - \tilde{\pi})}$$

and

$$(r_3 - r_1) r_2 \cos(\lambda_2 - \tilde{\pi}) = (r_3 - r_2) r_1 \cos(\lambda_1 - \tilde{\pi}) + (r_2 - r_1) r_3 \cos(\lambda_3 - \tilde{\pi}) \tag{8}$$

since

$$\cos(\lambda_1 - \tilde{\pi}) = \cos\lambda_1 \cos\tilde{\pi} + \sin\lambda_1 \sin\tilde{\pi}$$

We can substitute and by using

$$(r_3 - r_2)\, r_1 = A$$

$$(r_3 - r_1)\, r_2 = B$$

$$(r_2 - r_1)\, r_3 = C$$

we have

$$B(\cos\lambda_2 \cos\tilde{\pi} + \sin\lambda_2 \sin\tilde{\pi}) = A(\cos\lambda_1 \cos\tilde{\pi} + \sin\lambda_1 \sin\tilde{\pi}) + C(\cos\lambda_3 \cos\tilde{\pi} + \sin\lambda_3 \sin\tilde{\pi})$$

Dividing by $\cos\tilde{\pi}$ we have

$$B(\cos\lambda_2 + \tan\tilde{\pi} \sin\lambda_2) = A(\cos\lambda_1 + \tan\tilde{\pi} \sin\lambda_1) + C(\cos\lambda_3 + \tan\tilde{\pi} \sin\lambda_3)$$

so that $\tan\tilde{\pi}$ can be found easily from this equation:

$$\tan\tilde{\pi} \frac{A\cos\lambda_1 - B\cos\lambda_2 + C\cos\lambda_3}{A\sin\lambda_1 - B\sin\lambda_2 + C\sin\lambda_3} \tag{9}$$

With $\tilde{\omega}$ then determined we can calculate and p and since

$$p = a(1 - \varepsilon^2)$$

we can then calculate the major semi-axis of a from p and ε.

B-3. EXAMPLE OF AN ORBITAL CALCULATION

Vertregt gives an example of this type of calculation which procedes as follows.

Suppose that on the 10th of October 2056 at 10 hours Universal Time two photographs are taken on board spaceship X, one of the Sun and one of the Earth. Measurements on the plates produce the following results:

Apparent Regulus - longitude of the Sun, $\lambda'_1 = 92^\circ$
Apparent Regulus - longitude of Earth, $\lambda'_2 = 136^\circ$

The term "apparent longitude" means the longitude seen from the spaceship, and "regulus - longitude" means that the meridian through Regulus is taken as the zero-point of the ecliptic.

We find the following co-ordinates of the Earth in the Astronautical Data for the year 2056, 10th October, 10 hours Universal Time:

Regulus-longitude, $\lambda_2 = 226^\circ$

Distance between the Sun and Earth, $r_2 = 1.49 \times 10^8$ km. We find from Eq (1) that the distance of the spaceship from the Sun is

$$r = r_2 \frac{\sin(\lambda'_2 - \lambda_2)}{\sin(\lambda'_1 - \lambda'_2)} = 1.49 \times 10^8 \frac{\sin(136^\circ - 226^\circ)}{\sin(92^\circ - 136^\circ)} = 2.15 \times 10^8 \text{ km}$$

We have also

$$\lambda = 180^\circ + \lambda'_1 = 180^\circ + 92^\circ = 272^\circ$$

We have thus determined the position of the spaceship in our solar system, since we assumed that the motion took place in the plane of the ecliptic. If this is not the case, we have to take a further co-ordinate into account, viz., the latitude of the spaceship.

We obtain two further positions from two more observations. We have then three data (Table B-1).

We calculate first:

$$A = (r_3 - r_2)r_1 = (1.47 - 1.86)\ 2.15 = 0.9395\ (X\ 10^{16})$$

$$B = (r_3 - r_1)r_2 = (1.47 - 2.15)\ 1.86 = 1.2648\ (X\ 10^{16})$$

$$C = (r_2 - r_1)r_3 = (1.86 - 2.15)\ 1.47 = 0.4263\ (X\ 10^{16})$$

We have then

$$\tan\Pi = \frac{-0.83585 \cos 272^\circ + 1.2648 \cos 289^\circ - 0.4263 \cos 303.5^\circ}{-0.8385 \sin 272^\circ + 1.2648 \sin 289^\circ - 0.4263 \sin 303.5^\circ}$$

$$= \frac{-0.029 + 0.412 - 0.235}{+0.838 - 1.197 + 0.355} = 37$$

so that

$$\Pi = 88.5^\circ$$

We can now calculate the eccentricity

$$t = \frac{r_2 - r_1}{r_1 \cos(\lambda_1 - \Pi) - r_2 \cos(\lambda_2 - \Pi)}$$

$$= \frac{1.86 - 2.15}{2.15 \cos 183.5^\circ - 1.86 \cos 200.5^\circ} = 0.71$$

and

$$p = r\{1 + \varepsilon \cos(\lambda - \Pi)\}$$

$$= 2.15 \times 10^8\ (1 + 0.71 \cos 183.5^\circ)$$

$$= 2.15 \times 10^8\ (1 - 0.708) = 0.63 \times 10^8 \text{ km}$$

so that

$$a = \frac{p}{1 - \varepsilon^2} + \frac{0.63 \times 10^8}{1 - 0.71^2} + 1.27 \times 10^8 \text{ km}$$

We now have all the data necessary to determine the shape of the ellipse, and Π indicates the position of the major axis and of the perihelion.

Table B-1. Coordinates of the Spaceship

Date	r		Regulus - Longitude
	km	miles	
10th October 2056	2.15×10^8	1.34×10^8	272°
29th November 2056	1.86×10^8	1.15×10^8	289°
28th December 2056	1.47×10^8	0.91×10^8	303.5°

B-4. ORBIT CORRECTION

The problems faced on a flight are of course, more difficult than the mere determination of position and claculation of the spacecraft trajectory. The added difficulty arises because the mission requires that the spacecraft arrive at a specific point at a specific time. The basic trajectory, previously selected and computed on the ground, will consider all possible factors and will be determined by algorithms of what ever complexity the problem requires.

On board computation requirements will naturally be held to a minimum or, at any rate, to a level significantly below that required to perform the basic mission trajectory selection and nominal mission trajectory calculations.

However, no matter how accurately the orbit has been specified, deviations will occur, since there are limits to the accuracy of equipment.

These small deviations will prevent absolute adherance to the prescribed path, and will require some course corrections if the arrival point and time are to be held constant.

Vertregt also addresses this problem and shows a solution based on using a Maclaurin's series. However, an evaluation of Vertregt's proposed solution performed at RSD suggests that it would not be adequate. The following solution was therefore developed to illustrate a method that could be used to solve the problem.

(NOTE: We are no longer using Vertregt's symbols)

An optimal track will comprise a number of arcs of free orbit meeting at junctions at which sufficient fuel is expended to transfer the rocket from one orbit into another. Suppose J is the next jundtion point on the optimal track when an error is observed. The procedure is to alter the velocity at P in such a way that it moves into an orbit passing through J, the instant of arrival at J being arranged to be the same as that at which it would have arrived at this point by the optimal route.

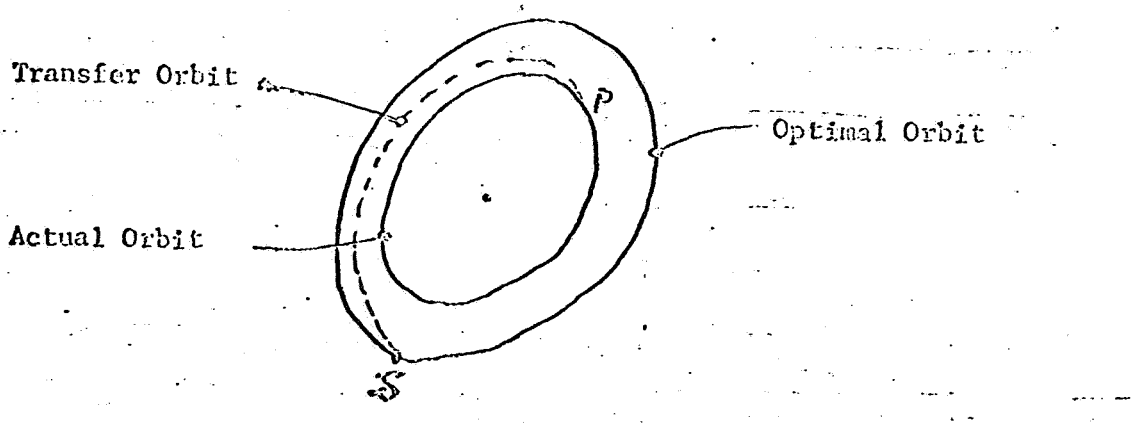

Since the required trajectory PJ will not diverge greatly, either from the optimal track, or from the trajectory the rocket was actually following prior to its arrival at P several simplifying assumptions can be made: First the planes of the orbits will be assumed to be the same. (There is no difference in latitude between the orbit.) Secondly, the position of the rocket at J (x_1, y_1, z_1) may be written:

$$x_1 = x\ (t_1, x_o, y_o, z_o, u_o, v_o, w_o) \quad (1)$$

$$y_1 = y\ (t_1, x_o, y_o, z_o, u_o, v_o, w_o) \quad (2)$$

$$z_1 = z\ (t_1, x_o, y_o, z_o, u_o, v_o, w_o) \quad (3)$$

where (x_o, y_o, z_o) is the position of the rocket at t_o at the outset of its transfer and (u_o, v_o, w_o) is its velocity at that point. Also, we write the approximation

$$u_o = u + Su$$

$$v_o = v + Sv$$

$$w_o = w + Sw$$

where (u, v, w) are the velocity components with which the rocket arrives at P and (Su, Sv, Sw) are the components of the velocity increment necessary to get to J at the right time. Substituting the approximations into our relations (1), (2), (3) obtains

$$\lambda_1 - \lambda_1' = \frac{\partial x}{\partial u} \delta u + \frac{\partial x}{\partial v} \delta v + \frac{\partial x}{\partial w} \delta w$$

$$\gamma_1 - \gamma_1' = \frac{\partial y}{\partial u} \delta u + \frac{\partial y}{\partial v} \delta v + \frac{\partial y}{\partial w} \delta w$$

$$z_1 - z_1' = \frac{\partial z}{\partial u} \delta u + \frac{\partial z}{\partial v} \delta v + \frac{\partial z}{\partial w} \delta w$$

where $x_i = x\,(t_1, x_o, y_o, z_o, u, v, w)$. (x_i', y_i', z_i') is the point J' at which the rocket will arrive at time t, if no connection is made. Depending on the functional values of the parameters, these equations may be easy or impossible to solve.

In the case of an inverse square attractive force these equations can be solved. If (r_o, θ_o), (r_1, θ_1) are the coordinates of P and J, a the semimajor axis of the elliptic orbit, e its eccentricity, and w the longitude of perihelion.

$$r_o = a\,(1 - e \cos E_o)$$

$$r_1 = a\,(1 - e \cos E_1)$$

$$\tan \tfrac{1}{2}(\theta_o - w) = \sqrt{\frac{1+e}{1-e}}\, \tan \tfrac{1}{2} E_o$$

$$\tan \tfrac{1}{2}(\theta_1 - w) = \sqrt{\frac{1+e}{1-e}}\, \tan \tfrac{1}{2} E_1$$

where E_o and E_1 are the eccentric anomalies defined by

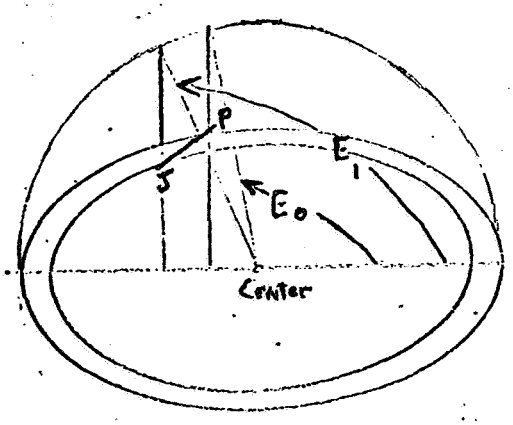

Reference Circle

If $\frac{\mu}{r^2}$ is the attraction per unit mass on the rocket, we also have from Kepler's equation

$$E_1 - E_o \quad e\,(\sin E_1 - \sin E_o) = \frac{\mu^{1/2} T}{a^{3/2}}$$

These five equations will determine a, e, w, E_o, E_1 where r_o, θ_o, r_1, are given

Approximate values can be obtained from our equations (4), (5), (6).

$$S a\,(1 - e \cos E_o) - a\,S e \cos E_o + a\,e\,S E_o \sin E_o = r_o - a\,(1 - e \cos E_o)$$

$$S a\,(1 - e \cos E_1) - a\,S e \cos E_1 + a\,e\,S E_1 \sin E_1 = r_1 - a\,(1 - e \cos E_1)$$

$$S\omega \sec^2 \tfrac{1}{2}(\theta_o - \omega) + \frac{2\,S e}{(1-e)\sqrt{1-e^2}} \tan \tfrac{1}{2} E_o + S E_o \sqrt{\frac{1+e}{1-e}} \sec^2 \tfrac{1}{2} E_o = 2 \tan \tfrac{1}{2}(\theta_o - \omega) - 2\sqrt{\frac{1+e}{1-e}} \tan \tfrac{1}{2} E_o$$

$$S\omega \sec^2 \tfrac{1}{2}(\theta_1 - \omega) + \left(\frac{2\,Se}{1-e\sqrt{1-e^2}}\right) \tan \tfrac{1}{2} E_1 + SE_1 \sqrt{\frac{1+e}{1-e}} \sec^2 \tfrac{1}{2} E_1$$

$$2 \tan \tfrac{1}{2}(\theta_1 - \omega) - 2\sqrt{\frac{1+e}{1-e}} \tan \tfrac{1}{2} E_1$$

$$\frac{3T\mu^{1/2}}{2a^{5/2}} Sa + Se(\sin E_0 - \sin E_1) - SE_0(1 - e\cos E_0) -$$

$$SE_1(1 - e\cos E_1) = \frac{t\mu^{1/2}}{a^{3/2}} - (E_1 - E_0) +$$

$$e(\sin E_1 - \sin E_0)$$

Since E_0 is the eccentric anomaly of the point P on the orbit (a, e, w) we have

$$r_0 = a(1 - e\cos E_0)$$

$$\tan \tfrac{1}{2}(\theta_0 - \omega) = \sqrt{\frac{1+e}{1-e}} \tan \tfrac{1}{2} E_0$$

the right hand sides of the first and third equations are zero. Also

$$\tan \tfrac{1}{2}(\theta_1 - \omega) = \sqrt{\frac{1+e}{1-e}} \tan \tfrac{1}{2} E_1$$

and the right hand side of the fourth equation is zero.

In actually computing the values we first substitute our values into a computer program and solve the five linear equations for the five unknowns. Then the results

$a' = a + Sa$
$w' = w + Sw$
$e' = e + Se$
$E_0' = E_0 + SE_0$
$E_1' = E_1 + SE_1$

are substituted back into the relation and the new values obtained. This second re-calculation reduces the errors inherent in the assumption very significantly.

Suppose (a, e, w) are the elements of the rockets trajectory before correction and (a + Sa, + S , w + Sw) are the same elements after correction. We can easily show that the velocities in the O and r directions in the uncorrected orbit will be

$$V_r = \frac{\mu^{1/2} e}{a^{1/2}(1-e^2)^{1/2}} \sin(\theta_0 - \omega)$$

$$V_\theta = \frac{\mu^{1/2} a^{1/2} (1-e^2)^{1/2}}{r_0}$$

To first order, the corrections necessary in our velocity to achieve successful results in reaching point J are:

$$SV_r = \frac{-\mu^{1/2} e Sa}{2a^{3/2}(1-e^2)^{1/2}} \sin(\theta_0 - \omega) + \frac{\mu^{1/2} Se}{a^{1/2}(1-e^2)^{3/2}} \sin(\theta_0 - \omega)$$

$$- \frac{\mu^{1/2} e Sw}{a^{1/2}(1-e^2)^{1/2}} \cos(\theta_0 - \omega)$$

$$SV_0 \frac{\mu^{1/2} Sa (1-e^2)^{1/2}}{2 r_0 a^{1/2}} - \frac{\mu^{1/2} a^{1/2} e Se}{r_0 (1-e^2)^{1/2}}$$

The total time taken by GE-235 deskside computer in the calculation of from the orbital inputs would be about 2-3 minutes. This computer has a microsecond memory cycle and 16K work storage capacity. The Disc Storage Unit (DS-20) is a large capacity, fast random access storage

device which serves as the main path of the data and information transfer in both directions. Either central processor has access to the 18,000,000 character Unit. Since the computer capacity required for this problem is far less than the amount available in a GE-235 a much smaller computer could be used. Indeed, the smallest desk size computors could solve the problem in the same time. However, if one were to attempt solution by hand it would take a significantly longer time.

Our assumption that the orbital planes are coincidental is probably a very good one. Current guidance systems guarantee an error in predetermined latitude of less than 20 sec of arc. However, to include an analysis of this out of plane turn would complicate our equations considerably, by a factor of at least 2.

B-5. TYPICAL SEQUENCE OF NAVIGATION AND GUIDANCE EVENTS

The following events would occur in a typical sequence:

a. Take planet (earth) - star angle measurement to determine deviation in the plane.
b. Take planet-sun angle.
c. Solve for position.
d. Repeat a, b and c at a later time.
e. Repeat a, b and c again at a later time.
f. Use position Pa, Pb, and Pc to solve for actual course.
g. Calculate corrected course.
h. Solve for V corrections and vectors.
i. Point spacecraft in proper direction.
j. Burn

B-6. ESTIMATE OF THE DELTA V ERROR IN EACH PHASE OF THE MARS MISSION

B-7. Injection

If an automatic system is assumed for the injection phase, errors such as those shown in the following table would be expected. These

error estimates are based on the assumption that an inertial navigation system of the Centaur accuracy class with a velocity accuracy of 3M/sec. and a path angle accuracy of 1 milliradian is used.

CROSS-COURSE INJECTION
VELOCITY ERRORS-DELTA V_N

			Delta V_N (M/sec)
Injection Velocity	8Vi	3 M/sec	3
Flight Path Angle	8	1 m	10
Altitude Error	8h	5 KM	5
Position in Orbit	8X	5 KM	5
		$\leq V_N$	13 M/sec

ALONG-COURSE INJECTION
VELOCITY ERROR-DELTA V_T

Injection Velocity	8Vi	3 M/sec	5
Altitude Error	8h	5 KM	5
		$\leq V_T$	7 M/sec

B-8. Post-Earth Correction

The results of the injection errors show up as a variation in the post earth trajectory from the pre-computed baseline trajectory. A post-earth correction must be applied to the space vehicle to correct the position and velocity error introduced at injection.

If the first correction is made several days after injection, the earth-star measurements on which the correction is based should have an accuracy significantly better than the correction. For example, for 1 milliradian path angle error a 20 arcsec or better sighting accuracy is required. This level of sighting would permit a corrective computation within $\pm$10% of the actual required Delta V correction.

The second error computation maybe applied between the 10th to 16th day and should be based on planet sighting accuracies in the 5 arc sec range. This would permit a computation of a new correction to an accuracy of 25% (see Table B-2).

Table B-2. Calculated Correction Errors

POST-EARTH CORRECTION

			Delta V_N
1st Correction	Path angle error (at 1-2 days out) (desired sighting accuracy 20 sec)	1 MR	8M/sec
2nd Correction	(at 10-16 days out) (sighting accuracy 5 sec)		1M/sec

B-9. Midcourse Corrections

If a midcourse correction were attempted at the midpoint angle measurement accuracies of approximately 2 to 20 arcsec would result in errors of 1000 to 10,000 miles. Since the planet positions are not perfectly known, the computed corrections would be further in error due to planet position errors upon which the measurement errors were superimposed.

If our navigation measurements were taken to 2 arcsec accuracies the resulting error added to the calculation errors due to position errors of the planets would exceed our expected Delta V error at that point by a signficant amount. Hence we would not make a correction, unless, of course, some strange perterbation had caused us to have the post earth correction phase far out of our expected path.

B-10. Mars Terminal Adjustment

The instrumentation for the MARS terminal adjustment is essentially the same as for the Post Earth Correction instrumentation. Based on the stated navigation and guidance accuracy of the spacecraft if should make its approach toward Mars with positional accuracy of approximately $\pm$10,000 KM. The range to Mars at the start of the approach phase is approximately 6,640,000 KM so that the positional error at worst reflects itself as an angular error approximately 1.5 mr. At this range the planet appears as a disc 1 mr in diameter, ranging at this distance

is obtained optically by measuring the planet diameter. Range estimating accuracy under these conditions is 0.1 to 0.5%, depending on the techniques used. Automatic devices do not appear to offer significant advantages over manual approaches.

The angle between MARS and near by stars is an effective indication of the approach trajectory. For example, a change of 100 arc sec in the adjusted MARS star angle will occur over an 8 day time interval from the start of the approach if the trajectory is on a tangent line with the surface of the planet. A change of approximately 4 mr or 832 arcsec occurs during the last 24 hours prior to the day of entry. The desired accuracy of sighting in order to calculate correction 8 days prior to entry would be 10 arc sec.

A 30 arcsec error at 1 day from the planet entry point would result in a 120 KM path error and would require a corrective thrust of less than 1 M/sec.

When we begin the Terminal Approach Phase we will be in a position where measurement accuracy is best and the Delta V required to correct an existing path error is the least. However, the angles we measure are not changing rapidly and since the course correction calcuations are primarily based on the angular change the measurements are of limited value. As we get closer to the planet the angles change more rapidly and although the measurements are less accurate the larger changes make the data more meaningful.

Larger Delta V corrections are required, however, to correct a given path error if the error is permitted to exist late into the approach. Therefore, we have two correction accuracy problems, which can be considered as (1) an initial correction error and (2) a final correction error.

An initial correction made at day 8, the approach phase would be based on calculations performed upon our deviations from the nominal angular changes. Our nominal course has a change of about 100 arc sec over this period (16th to 8th day) and if our measurements are accurate

to 5 arcsec we could then have a measured angular change that could be 10 arcsec in error. The error in measurement could result in a correction that left our trajectory offset 30 KM for each arcsec, or 300 KM. At eight days this represents a Delta V error of about 1.8 meters per sec.

If we assume the 10,000 KM error which could result from the uncorrected Post Earth Correction error and sphemeros error we would be making a correction at this point of about 18 meters per second. A velocity impulse error fo $\pm$5% could also exist and this would result in a further error of about 1 meter per second of a total uncorrected error of approximately 2.8 meters per second. The effects of this error would have to be corrected in the "final" correction. If no intervening corrections are made this could represent an off nominal trajectory error of about 1700 KM.

From two days prior to entry to the day before entry there would be a 4 mr (832 sec) nominal effective angular change. The angles involved could be measured to an accuracy of about $\pm$32 arcsecs. This is primarily due to inaccuracy in sighting the center of the planet. Since the change is so large, however, we can compute the required correction quite closely and would expect an erronious determination of only about 4 KM per arcsec. Thus, at the time of correction we would expect to be correcting from a computed trajectory which could have a displacement error of about 130 KM from the actual trajectory.

Since we have carried forward an uncorrected 1700 KM error we again have two possible error sources; the navigation accuracy and the errors or the thrust control system accuracy. The latter error have been given as $\pm$5% the same accuracy can be assumed here. The 1700 KM correction would then require a correction of about 20 meter per second with a possible error, therefore, of 1 meter per second. The uncorrectable 130 KM error due to data inaccuracies would also contribute an uncorrected Delta V error. This would represent a Delta V of about 1.5 meters per second. The total estimated Delta V, therefore, is about 2.5 meters per second.

B-11. Orbit Entry

Our nominal entry altitude over Mars was considered to be about 1000 KM. Thus, an entry made with the carried over errors from the last terminal adjust could involve an altitude -over Mars- error of about 200 KM. If this error represented a too high approach it would require correction of 25 meters per second Delta V more than nominal plus additional fuel expenditures to circularize the orbit.

If we consider that this correction would, if necessary, be performed with the previously mentioned Centau class guidance system we would have to consider the following uncorrected error as the burn was completed.

A method of firing the engines can be shown which would permit the orbit entry thrust to be based on altitude measurement. If 1% is taken as the altitude measurement accuracy the after thrust error would be 1 meter per second. Thus, the thrust as calculated would require 25 meters per second to reduce the velocity from the interplanetary rate, to the Mars orbital rate. With a Centaur class guidance system the additional thrust Delta V error, based on the 10,000 meter per second correction, would be 2 to 3 meters per second. This would create an out of circular orbit error of 24 to 32 KM at the 180^{o} point.

B-12. Venus Flyby

The Venus Flyby instrument action is quite similar to the MARS approach. The principle requirement is to properly steer the offset path as with the MARS approach.

Assuming a position error of approximately 10,000 KM, a 1 mr level correction could readily be made at 10,000,000 KM from Venus. A 5 meter per second correction could adjust the path angle error and reduce the offset trajectory error (Delta b) to about 500 KM. An attempt should be made to further reduce the Delta b error to say 50 to 100 KM. This might readily be done when the vehicle is within several days of planet encounter using a 2 meter per second correction.

After passing Venus the requisite Delta V to hold the turn angle on course would be about 14 meters per second. This Delta V would be applied when the spacecraft was at a sufficient distance to insure reasonable high planet sighting accuracy, say 12,322,000 KM range or a 1 mr planet diameter.

INSTRUMENT ACCURACIES

Planet Trackers..... Phenomena limit 1% of Planet Disc.
Image scan Disc - 8 arc sec (Mars @ 2,000,000 miles).
Image Orthicon G.E. 20 sec.

Horizon Scanners ..... Phenomena limit $.1^{o}$ or 6 arc min.
Accuracy highly dependent on planet characteristic.

Sun Trackers ..... Phonema limit @ arc second level.
Devices designed to date have 3-6 arc minute accuracies.

Star Trackers ..... Phenomena limit at arc second level.
Star tracker accuracy is a function of; brightness, collecting aperature, detector, signal to noise ratio and spectral characteristics, and the inverse of the servo loop bandwidth.

Radar Altimeters..... Range accuracy - 0.1% - 1%
The range accuracy for a bandwidth-limited, pulsed radar may be determined from the following relationship.

$$\text{Range accuracy } (3\sigma) = - \frac{C}{4BR \quad S/N}$$

where

C = speed of light
B = power bandwidth
S/N = signal power to noise power ratio
R = Range

i.e. at a 1000 KM - R
20 db - S/N
1200 cps - B
Range accuracy = 1%

Sextants Manual ..... Phenomena limits. Combination of horizon scanner and star tracker phenomena limitations. Accuracy is highly dependant on general planet characteristics and specific region sighted.

Under specific test conditions using a 28X and 40X power optical system the following accuracies were obtained with a hand held device;

Random (1σ) error 1.5 - 3.0 arc sec.
Mean error 3.0 - 6.0 arc sec.

Gimbaling the instrument provided for a slight improvement.

Planet-Star Comparator.. Phenomena limitations are basically those of the planet tracker and the star tracker individually. The use of a small angle approach may be very desirable as it reduces the angle readout portion of the error to a second order value.

There is a photographic study by Havrill that claims planet-star center to center measurements of 0.25%.

Stadimeter ..... Phenomena limits highly dependent on both general and specific planet characteristics. Probable 1σ accuracy of 1/4 - 1% in range.

Resolution 1 part in 7000.

There is a photographic study by Havrill 1963 that claims disc diameter measurement to 0.035%.

Delta V Measurement..... Accuracies to one part in 10^5 can be obtained with inertial grade equipment. Open loop manual techniques should be in the percent class.

Gyro Performance..... 0.02^o/hr. to $.002^o$/hr for high performance conventional single degree of freedom gyros. Electrically suspended gyro @0.0001^o/hr level. Lasers 0.2^o/hr.

Strapdown Inertial Measuring Unit Performance..... 6 arc min/hr in a moderate environment. Degrades rapidly under high dynamic environment.